

Electronic Thesis and Dissertation Repository

6-6-2013 12:00 AM

Novel Thiophene Supported N,N'-Chelating Ligands and Their Main Group Compounds

Jacquelyn T. Price, *The University of Western Ontario*

Supervisor: Professor Paul J. Ragogna, *The University of Western Ontario*

A thesis submitted in partial fulfillment of the requirements for the Doctor of Philosophy degree in Chemistry

© Jacquelyn T. Price 2013

Follow this and additional works at: <https://ir.lib.uwo.ca/etd>

 Part of the [Inorganic Chemistry Commons](#), and the [Materials Chemistry Commons](#)

Recommended Citation

Price, Jacquelyn T., "Novel Thiophene Supported N,N'-Chelating Ligands and Their Main Group Compounds" (2013). *Electronic Thesis and Dissertation Repository*. 1304.
<https://ir.lib.uwo.ca/etd/1304>

This Dissertation/Thesis is brought to you for free and open access by Scholarship@Western. It has been accepted for inclusion in Electronic Thesis and Dissertation Repository by an authorized administrator of Scholarship@Western. For more information, please contact wlsadmin@uwo.ca.

Novel Thiophene Supported *N,N'*-Chelating Ligands and Their Main Group
Compounds
(Thesis format: Integrated Article)

by

Jacquelyn T. Price

Graduate Program in Chemistry

A thesis submitted in partial fulfillment
of the requirements for the degree of
Doctor of Philosophy

The School of Graduate and Postdoctoral Studies
The University of Western Ontario
London, Ontario, Canada

© Jacquelyn T. Price 2013

Abstract

Main group chemistry has advanced from studying fundamental curiosities, including low oxidation state, low-valent, p-block elements to tailoring these unique, reactive species for specific functional applications. This thesis examines the structure, bonding and reactivity of select group 13, 14 and 15 elements supported by *N,N'*-chelating ligands decorated with either thiophene, benzo[1,2-b:5,6-b']dithiophene or bis(2,5-dimethylthienyl)ethene substituents and allowing for subsequent reactivity and photophysical properties to be determined.

The synthesis of a new diamino ligand containing a thiophene ring in the backbone was used to support a 7-membered phosphonium cation. The 1:1 stoichiometric reaction between the amine:chlorophosphine was dependant on the substitution at nitrogen. A 1:1 stoichiometric reaction between PCl_3 and diamine ($\text{R} = 2,4,6\text{-trimethylphenyl}$), yielded the acyclic bis(aminodichlorophosphine), while with diisopropylphenyl groups on nitrogen both the 1:1 cyclic aminochlorophosphine and 1:2 acyclic bis(aminodichlorophosphine) were observed in a 4:1 ratio. To amend the poor selectivity, a new diamine was designed with benzo[1,2-b:5,6-b']dithiophene in the backbone as this ligand generates a rigid five-membered ring upon coordination to main group elements. The detailed synthesis of this ligand, its pnictenium cations ($\text{Pn} = \text{P}, \text{As}$ and Sb) and their metal complexes were discussed, along with the spectroscopic properties. The synthesis of an N-heterocyclic carbene (NHC) with the benzo[1,2-b:5,6-b']dithiophene in the backbone, silver(I) transfer reagent and the BPh_3 adduct were also synthesized. The donor strength of the NHC was measured from the carbonyl IR stretching frequencies of the isolated $\text{NHC-Rh(CO)}_2\text{Cl}$ complex along with the resulting photophysical properties.

The synthesis of a versatile diimine ligand containing adjacent 2,5-dimethyl(thienyl) rings in the backbone and its coordination to main group atoms was also achieved. This diazabutadiene acts as a precursor to a novel photochromic ligand that has been used to coordinate to both boron and phosphorus elements, along with the synthesis of a phosphorane side chain functionalized polymer. A study of the resulting photochromic properties of these compounds was completed and the following was observed: (i) The UV-visible absorption spectra of the ring closed isomer was dependent of the element present in the *N,N'*-chelating

pocket; and (ii) incorporating the dithienylethene into a side functionalized phosphorane polymer greatly increased the ring closed/open reversibility and decreased the formation of by-products.

Keywords

Thiophene, photochromic, dithienylethene, pnictogen, N-heterocyclic carbene, N-heterocyclic phosphonium, low coordinate, main group chemistry.

Co-Authorship Statement

This thesis includes material from 4 previously published manuscripts presented in Chapters 2, 3, 4 and 5. The material presented in Chapter 2 was co-authored by J. T. Price, N. D. Jones and P. J. Ragona (*Can. J. Chem.*, **2013**, DOI: 10.1139/cjc-2013-0015). All of the experimental was performed by JTP. All of the diffraction data was collected and solved by JTP. This work was started under the supervision of NDJ and then continued under the supervision of PJR. JTP was responsible for writing the manuscript, which was edited by PJR.

The work described in Chapter 3 was accepted for publication and was authored by J. T. Price, M. Lui, N. D. Jones and P. J. Ragona (*Inorg. Chem.*, **2011**, *50*, 12810). JTP synthesized the phosphorus containing compounds while ML is credited with the initial synthesis of the compounds containing arsenic and antimony, which were then fully characterized by JTP. All X-ray crystallography was done by JTP. The manuscript was written by JTP and PJR.

The material outlined in Chapter 4 was published as a full paper and co-authored by J. T. Price and P. J. Ragona (*Inorg. Chem.*, **2012**, *51*, 6776). All experimental and X-ray crystallography was performed by JTP. The manuscript was written by JTP and edited by PJR.

The work presented in Chapter 5 was authored by J.T. Price and P. J. Ragona published as a full paper in *Chem. Eur. J.*, **2013**, DOI: 10.1002/chem.201301086. All experimental details and X-ray crystallography were carried out by JTP. The manuscript was written by JTP and edited by PJR.

Acknowledgments

I would first like to express my greatest gratitude to my supervisor Professor Paul Ragona for his support throughout my doctoral studies. I am grateful for his guidance and constant encouragement and I am certain without his support I would not have been as successful in my graduate career.

I would also like to thank all the staff members of the Chemistry department. In particular I would like to thank Dr. Mathew Willans for help with NMR spectroscopy, Doug Hairsine for mass spectrometry, Yves Rambour for fixing our broken glassware, Darlene McDonald for answering all my questions pertaining to various deadlines and ChemBio Stores staff, specifically Sherrie McPhee, Don Yakobchuk, Monica Chirigel and Marylou Hart. I would especially like to thank John Vanstone and Jon Aukema for their ability to fix everything including our dry box and the X-ray diffractometer. I would also like to thank Dr. Nick Payne, Dr. Jason Dutton, Dr. Benjamin Cooper and Dr. Paul Boyle for all of their help with X-ray crystallography. I would also like to show my gratitude to Dr. Nathan Jones for his guidance during the first year of my PhD, Professor Mark S. Workentin, Professor Martin Stillman for their useful discussions and Professor Robert H.E. Hudson and Dr. Mojmir Suchy for allowing me to use their UV-vis spectrometer and fluorometer on multiple occasions.

I would like to thank my committee members Professor Michael A. Kerr, Professor Richard J. Puddephatt, Professor Michael O. Wolf and Professor Paul A. Charpentier for taking the time to read my thesis and for their useful feedback.

I owe sincere thankfulness to all the past Ragona group members including Dr. Jason Dutton, Dr. Jocelyn Tindale and Dr. Preeti Chadha for initially welcoming me into their group and a great source of information and help in the beginning stages of my PhD.

My current lab mates Eleanor Magdzinski, Ryan Guterman, Mahboubeh Hadadpour, Yuqing Liu and Tyler Cuthbert and especially Dr. Bradley Berven, Jonathan Dube, Dr. Allison Brazeau and Dr. Christine Caputo who assisted in editing my thesis.

I thank Western University and NSERC for generous funding over the last 4.5 years and finally I would like to thank my family and my partner Craig Stephenson for their encouragement and support during the entire course of my educational career.

Table of Contents

Abstract.....	ii
Co-Authorship Statement	iv
Acknowledgments.....	v
Table of Contents	vi
List of Tables	x
List of Figures.....	xi
List of Schemes.....	xv
List of Symbols and Abbreviations.....	xvii
Chapter 1.....	1
1 Introduction	1
1.1 Thiophene.....	1
1.2 Advances in main group chemistry	2
1.3 N-Heterocyclic carbenes and their group 15 analogues.....	2
1.3.1 Synthesis.....	3
1.3.2 Reactivity.....	6
1.4 Group 14 and 15 elements in functional materials	8
1.5 Photochromic dithienylethenes	11
1.5.1 Photochromism	11
1.5.2 Dithienylethenes.....	12
1.5.3 Thermal stability and fatigue resistance	14
1.5.4 Versatility	15
1.6 Scope of thesis.....	17
1.7 References	18
Chapter 2.....	24

2	Phosphenium cation in a seven membered ring supported by thiophene	24
2.1	Introduction	24
2.2	Results and Discussion.....	26
2.2.1	Synthesis	26
2.2.2	Photophysical properties.....	29
2.2.3	X-ray crystallography.....	31
2.2.4	Conclusions.....	34
2.3	Experimental.....	34
2.3.1	General experimental	34
2.3.2	Synthetic procedures	34
2.4	References	40
	Chapter 3.....	42
3	Group 15 cations supported by a benzo[1,2-b:5,6-b']dithiophene core.....	42
3.1	Introduction	42
3.2	Results and Discussion.....	43
3.2.1	Synthesis	43
3.2.2	Photophysical properties.....	48
3.2.3	X-ray crystallography.....	51
3.2.4	Conclusion	58
3.3	Experimental.....	59
3.3.1	General experimental	59
3.3.2	Synthetic procedures	59
3.4	References	66
	Chapter 4.....	69
4	An N-Heterocyclic carbene containing a benzo[1,2-b:5,6-b']dithiophene backbone: Synthesis and coordination chemistry	69

4.1 Introduction	69
4.2 Results and Discussion.....	71
4.2.1 Synthesis	71
4.2.2 Photophysical properties.....	77
4.2.3 X-ray crystallography.....	80
4.2.4 Conclusions.....	82
4.3 Experimental.....	83
4.3.1 General experimental	83
4.3.2 Synthetic procedures	83
4.4 References	87
Chapter 5.....	90
5 A versatile dithienylethene functionalized Ph-DAB ligand: From photoswitchable main group molecules to photochromic polymers	90
5.1 Introduction	90
5.2 Results and Discussion.....	92
5.2.1 Synthesis	92
5.2.2 X-ray crystallography.....	98
5.2.3 Photophysical properties.....	101
5.2.4 Conclusions.....	108
5.3 Experimental.....	108
5.3.1 General experimental	108
5.3.2 Synthetic procedures	109
5.4 References	114
Chapter 6.....	116
6 Conclusions and future work.....	116
6.1 Conclusions	116

6.2 Future work	118
6.3 References	120
Appendices.....	121
Appendix 1: General considerations	121
A.1 General experimental considerations.....	121
A1.2 General crystallography considerations.....	122
A1.3 References	122
Appendix 2: Copyright permission	123
A2.1: American Chemical Society's policy on theses and dissertation.....	123
A.2.3: National Research Council of Canada Rights Retained by Journal Authors.....	125
Appendix 3: Supplementary information	126
Curriculum Vitae.....	129

List of Tables

Table 2.1: UV-visible absorption and extinction coefficients of compounds 2.2 - 2.9	30
Table 2.2: Crystal data for compounds 2.2^{Mes}, 2.5^{Dipp}, 2.6, 2.8 and 2.9	31
Table 2.3: Selected bond lengths (Å) and angles (°).....	32
Table 3.1. Optical properties of compounds 3.3 - 3.12	50
Table 3.2. Crystal data for compounds 3.4 - 3.8	53
Table 3.3: Crystal data for compounds 3.9 - 3.12	54
Table 3.4: Selected bond lengths [Å] and angles [°] for compounds 3.4 - 3.12	55
Table 4.1: Average CO stretching frequencies (ν_{avg}) of various (carbene)Rh(CO) ₂ Cl Complexes.....	76
Table 4.2: Photophysical properties of the bithiophene NHC	78
Table 4.3: Crystal data for compounds 4.1, 4.3, 4.4 and 4.5	81
Table 5.1: X-ray details for compounds 5.2, 5.3, 5.4 and 5.7	100

List of Figures

Figure 1.1: Thiophene (1.1) and Poly(thiophene) (1.2).....	2
Figure 1.2: Resonance structures of the N-heterocyclic carbene.....	3
Figure 1.3: Frontier orbitals of two coordinate carbene and phosphonium cation.	3
Figure 1.4: The frontier molecular orbitals of a diaminophosphenium (left) and diaminocarbene (right).	6
Figure 1.5: The phosphonium cation can adopt either a planar or pyramidal geometry similar to that of NO^+	7
Figure 1.6: Main group elements incorporated into extended π -conjugated molecules and polymers.	10
Figure 1.7: Examples of organic switchable photochromic molecules.....	12
Figure 1.8: The ring closed and ring open isomers of DTEs.....	13
Figure 1.9: The structural changes and stabilization energies of the generated closed-ring isomers.....	14
Figure 1.10: Areas of functionalization on the DTE framework.....	16
Figure 1.11: Main group elements incorporated into DTE core.....	17
Figure 1.12: Novel <i>N,N'</i> -chelating ligands used to coordinate p-block elements.....	18
Figure 2.1: Previously synthesized NHCs and NHPns (Pn = Pnictogen) containing pendant thiophene rings.....	25
Figure 2.2: UV-Visible spectrum of compounds 2.2 - 2.9 in a 5×10^{-5} M CH_2Cl_2 solution. ...	30
Figure 2.3: Solid-state structures of compounds 2.2 ^{Mes} , 2.5 ^{Dipp} , 2.6 , 2.8 and 2.9 . Thermal ellipsoids are drawn to 50% probability and hydrogen atoms have been omitted for clarity.	

Compound 2.9 , the triflate anion has been omitted for clarity and a side on view of the molecule is shown in 2.9b in which the Dipp groups have been omitted.	33
Figure 3.1: Previously reported phosphonium cation with the triiodide counter ion and the reported new pnictenium cations (3.1).	43
Figure 3.2: Stacked plot of the ¹ H NMR spectra of A) the proligand, compound 3.4 ; B) Compound 3.5 , Pn = P; C) Compound 3.6 , Pn = As; and D) Compound 3.7 , Pn = Sb.	45
Figure 3.3: UV-absorption spectra of compounds 3.4 - 3.12 in CH ₂ Cl ₂	49
Figure 3.4: Fluorescence spectra of compounds 3.4, 3.5, 3.8, 3.9 and 3.10 in CH ₂ Cl ₂	49
Figure 3.5: Solid-state structures of 3.4 to 3.12 . Ellipsoids are drawn to 50% probability. The triflate anions for compounds 3.8 - 3.12 and hydrogen atoms are removed except on the nitrogen atoms for compound 3.4 and the phenyl rings on compounds 3.11 and 3.12 for clarity.	57
Figure 3.6: Crystal packing of 3.9	58
Figure 4.1: (i) bis(imino)acenaphthene, (ii) NHC orthogonal to the thiophene rings, quinoidal structure of tert-thiophene (iii) and our NHC (4.2).	71
Figure 4.2: UV-visible spectra of compounds 4.1, 4.4, 4.5, 4.7 and 4.8 in CH ₂ Cl ₂ and compound 4.3 in toluene.	79
Figure 4.3: Solid state structures of compounds 4.1, 4.3, 4.4 and 4.5 . Ellipsoids are drawn to 50% probability and hydrogen atoms have been removed for clarity.	82
Figure 5.1: The anti-parallel and parallel ring open isomers and the photo-switching to the ring closed-isomer.	90
Figure 5.2: Variable temperature ¹ H NMR of compound 5.4 (top left); Simulated variable temperature ¹ H NMR of compound 5.4 (top right); Arrhenius plot of the rate of conversion between parallel and anti-parallel states vs. 1/T and the calculated activation energy required for the conversion between parallel and anti-parallel states for compound 5.4	95

Figure 5.3: Variable temperature ^1H NMR of compound 5.5 (top left); Simulated variable temperature ^1H NMR of compound 5.5 (top right); Arrhenius plot of the rate of conversion between parallel and anti-parallel states vs. $1/T$ and the calculated activation energy required for the conversion between parallel and anti-parallel states for compound 5.5	96
Figure 5.4: Variable temperature ^1H NMR of compound 5.6 (top left); Simulated variable temperature ^1H NMR of compound 5.6 (top right); Arrhenius plot of the rate of conversion between parallel and anti-parallel states vs. $1/T$ and the calculated activation energy required for the conversion between parallel and anti-parallel states for compound 5.6	97
Figure 5.5: Polymerization of monomer 5.7 ; a) AIBN; C_6H_6 ; $80\text{ }^\circ\text{C}$; 8 h; 42 %; Proton NMR spectra of monomer (bottom) and polymer (top) in CDCl_3	98
Figure 5.6: Solid state structures of compounds 5.2 , 5.3 , 5.4 and 5.7 . Thermal ellipsoids are drawn to 50 %. Hydrogen atoms and solvent were removed for clarity.	101
Figure 5.7: Left) Changes in the UV-vis absorption spectra (5.4) when a <i>n</i> -pentane solution ($5 \times 10^{-5}\text{M}$) is irradiated with 254 nm light as a function of time; Right) Changes in the fluorescence spectra (5.4) when a <i>n</i> -pentane solution ($5 \times 10^{-5}\text{M}$) is irradiated with 254 nm light as a function of time.	103
Figure 5.8: Stacked ^1H spectra of compound 5.4 , where o = open, c = closed and IR = irreversible rearrangement product. A) the ring open isomer before irradiation. B) after irradiation for 90 min with 254 nm light and C) after being left out in ambient light for 8 h.	104
Figure 5.9: Left) Changes in the UV-vis absorption spectra of 5.7 when a pentane ($1 \times 10^{-5}\text{M}$) solution is irradiated with 254 nm light and its decomposition after 5 cycles; Right) Changes in the UV-vis absorption spectra of 5.8 when a toluene ($1 \times 10^{-5}\text{M}$) solution is irradiated with 254 nm light and its decomposition after 5 cycles.....	105
Figure 5.10: Left) Decay trace of the closed ring isomer by thermal cycloreversion at various temperatures in deoxygenated hexanes (5.4 and 5.7) and deoxygenated toluene (5.8) at 498 nm (5.4) and 448 nm (5.7 and 5.8); Right) Arrhenius plot of the thermal backward reaction of the closed ring isomer.....	107

Figure 6.1: DTE lanthanide complexes (6.6) and a DTE diamine (6.7).	119
Figure A. 1: ^1H NMR spectrum of compound 4.7	126
Figure A. 2: TGA of polymer 5.8	127
Figure A. 3: GPC trace of polymer 5.8	127
Figure A. 4: A linear plot of the amount of polymer/monomer vs. time for compound 5.8	128

List of Schemes

Scheme 1.1: Synthesis of NHC by deprotonation of the imidazolium salt (i) , reduction (ii) and <i>in situ</i> using Ag ₂ O and onward transfer to a different metal (iii)	4
Scheme 1.2: General synthesis of a phosphonium cation (E = element, A = anion and X = halide).....	5
Scheme 1.3: Synthesis of a phosphonium cation by using internal or external reducing agents.....	5
Scheme 1.4: The reversible photochromic conversion of compound A to compound B	11
Scheme 1.5: DTE in equilibrium between the parallel (1.16) and anti-parallel (1.17) conformations and conversion to the ring-closed isomer from the anti-parallel form.....	13
Scheme 1.6: Decomposition of the DTE from singlet oxygen to an irreversible ring-closed conformer; (top) the formation of endoperoxides; (bottom) six-membered ring product.....	15
Scheme 2.1: Synthesis of (2.2^{Mes}) and (2.3^{Dipp}) diimines.....	26
Scheme 2.2: Synthesis of compound 2.4^{Mes} and 2.5^{Dipp} diamines.	27
Scheme 2.3: Synthesis of compounds 2.6 , 2.7 , 2.8 and 2.9 ; (a) NMM, PCl ₃ , -78°C - rt.; (b) Me ₃ SiOTf, CH ₂ Cl ₂ , rt.....	29
Scheme 3.1: Synthesis of 3.4 . (a) <i>p</i> -OMe-C ₆ H ₄ NH ₂ , EtOH, reflux 4 h, 82%; (b) NaCN, DMF, rt. 48 h, 80 %.....	43
Scheme 3.2: Synthesis of 3.5 , 3.6 and 3.7 then subsequent halide abstraction yielding compounds 3.8 and 3.9	46
Scheme 3.3: Synthesis of 3.10	47
Scheme 3.4: Synthesis of pnictenium metal complexes.....	48

Scheme 4.1: Synthesis of the imidazolium salt 4.1; a) DMF, NaCN, r.t., 48 h; b) 4M HCl, HC(OEt) ₃ , 145°C, 2 min.	72
Scheme 4.2: Synthetic scheme of the bithiophene substituted NHCs.	73
Scheme 5.1: Synthesis of B(III) substituted DTE; a) TiCl ₄ , CH ₂ Cl ₂ , 12 h, 76 %; b) Li _(s) , Et ₂ O, 2 d, rt.; NEt ₃ ·HCl, 2 h; b) CH ₂ Cl ₂ , BBr ₃ or BCl ₂ Ph, 12 h, rt.; c) Et(ⁱ Pr) ₂ N, 2 h, (X = Br, 32 %, X = Ph, 48 %).	92
Scheme 5.2: Synthesis of compounds 5.5, 5.6 and 5.7; a) CH ₂ Cl ₂ , PI ₃ , 12 h, 95 %; b) CH ₂ Cl ₂ , PBr ₃ , 12 h, 92 %; c) THF, NEt ₃ , HEA, S ₈ , 65 %.....	94
Scheme 6.1: Synthesis of thiophene polymers containing either main group or transition metal elements.....	118
Scheme 6.2: Synthesis of CpCoCb side chain functionalized polymers with photochromic DTEs (6.11).....	120
Scheme 6.3: Dimerization of compound 6.9 using ZrCp ₂ Cl ₂ and the exchange of ZrCp ₂ with either main group elements or transition metals.	120

List of Symbols and Abbreviations

Abbreviation	Definition
AIBN	azobisisobutyronitrile
br.	broad
avg.	average
Calcd	calculated
Cb	cyclobutadiene
cf.	<i>confer</i> (compare)
cm	centimeter
Cp	cyclopentadiene
d	doublet
d.p.	decomposition point
dd	doublet of doublets
Dipp	2,6-diisopropylphenyl
DMF	dimethylformamide
DSC	differential scanning calorimetry
DTE	dithienylethene
e.g.	<i>exempli gratia</i> (for example)
Et	ethyl
<i>et al.</i>	<i>et alii</i> (and others)
FT	fourier transform
g	grams
GPC	gel permeation chromatography
h	hours
HEA	hydroxyethylacrylate
HMDS	Bis(trimethylsilyl)amine
h ν	energy of the photon
HOMO	highest occupied molecular orbital
HRMS	high resolution mass spectrometry
Hz	Hertz
<i>in vacuo</i>	in a vacuum
ⁱ Pr	isopropyl
IR	Infrared
<i>J</i>	coupling constant
K	Kelvin
kcal	kilocalories
kJ	kilojoules
KO ^t Bu	potassium tert-butoxide
LEC	light emitting electrochemical cell

LED	light emitting diode
LUMO	lowest unoccupied molecular orbital
M	Molar
m	multiplet
m.p.	melting point
Me	methyl
MeOH	methanol
Mes	2,4,6-trimethylphenyl; mesityl
min	minute(s)
mL	milliliter
mmol	millimole
Mn	molecular weight
mol	mole
nBuLi	n-butyllithium
NHC	N-heterocyclic carbene
NHP	N-heterocyclic phosphonium
NHPn	N-heterocyclic pnictene
nm	nanometer
NMM	n-methylmorpholine
NMR	nuclear magnetic resonance
OFET	organic field effect transistor
OLED	organic light emitting diode
OTf	triflate
<i>p</i> -	para
PDI	polydispersity index
Pn	pnictogen
ppm	parts per million
RAFT	reverse addition-fragmentation chain-transfer
rt.	room temperature
s	singlet
sept	septet
t	triplet
<i>t</i> Bu	tert-butyl
<i>t</i> BuLi	tert-butyllithium
Tc	coalescence temperature
Tg	glass transition
TGA	thermogravimetric analysis
THF	tetrahydrofuran
UV	ultra violet
vdW	van der Waals
vs.	versus
{ ¹ H}	proton decoupled
Å	angstrom

δ	chemical shift
δ_B	chemical shift boron (ppm)
δ_C	chemical shift carbon (ppm)
δ_F	chemical shift fluorine (ppm)
δ_H	chemical shift proton (ppm)
δ_P	chemical shift phosphorus (ppm)
$\Delta\delta$	change in chemical shift (ppm)
ϵ	extinction coefficient
Φ	quantum yield
λ	wavelength
μL	microliter
$^\circ$	degree
$^\circ\text{C}$	Degrees Celsius
σ	sigma
Σ	sum

Chapter 1

1 Introduction

1.1 Thiophene

Lecturer Victor Meyer serendipitously discovered thiophene (**1.1**, Figure 1.1) in 1882. It has since become one of the most extensively studied heterocyclic ring compounds because of its abundant availability and synthetic versatility.¹ The driving force behind the continuous development of new thiophene based materials is because through the functionalization of the thiophene ring, one can fine-tune the HOMO/LUMO band gap.² The ability to tailor the photophysical properties of thiophene and its resilience to a vast range of different chemistries has made it a staple in materials science, where it is used in many different fields, from dye chemistry,³ electronic and optoelectronic devices,⁴⁻⁶ and conductivity based sensors.⁷⁻⁹

The polymerization of acetylene was first initiated in the 1970's when Heeger and MacDiarmid discovered that poly(acetylene) upon partial oxidation or reduction the conductivity could be increased more than a billion fold (100 S cm^{-1}).¹⁰ These polymers however, were difficult to process and unstable in the presence of oxygen and water. Conjugated polymers with increased stability were gradually investigated and this led to the development of poly(thiophene), (**1.2**, Figure 1.1), which was superior to its counterparts because of its high stability in the doped and undoped states, and structural versatility. In parallel to the discovery of poly(thiophene), Garnier and Fichou discovered that smaller conjugated systems, oligothiophenes, could be used as organic field effect transistors (OFETs), organic light emitting diodes (OLEDs) and solar cells. Poly(thiophene) and oligothiophenes are unique in that they are able to combine the electrical and optical properties of metals while maintaining the processing advantages and mechanical properties of organic polymers.¹⁰

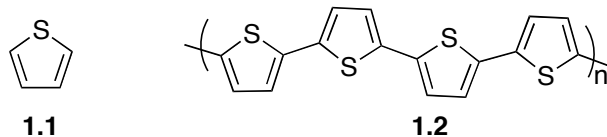


Figure 1.1: Thiophene (1.1) and Poly(thiophene) (1.2).

1.2 Advances in main group chemistry

The main group elements with the exception of hydrogen can be found in groups 1 and 2 (s-block) and 13-18 (p-block) in the periodic table. They are the most abundant elements on earth and can be considered to be the representative elements. An area of active research in main group chemistry has been the isolation of highly reactive low-valent, low-oxidation state s- and p-block atoms, which has resulted in many breakthroughs centering on new structure, bonding and reactivity. Chemistry of the p-block elements is currently evolving, and research is moving beyond studying the fundamental chemistries of these unique elements to incorporating them into the design and synthesis of novel materials, which include hydrogen storage,¹¹⁻¹³ sensors,¹⁴ functional polymers¹⁵⁻¹⁷ and semiconductors.¹⁸ As new synthetic methods are developed; our understanding of their structure and reactivity will expand and bring about significant advances in the design of novel small molecules, closing the gap between fundamental, curiosity driven research and applied research.¹⁹

1.3 N-Heterocyclic carbenes and their group 15 analogues

N-heterocyclic carbenes (NHCs), once only thought of as an alternative to phosphine ligands, have established themselves as superior ligands in metal-mediated catalysis and also find utility in functional materials, which include dynamic polymers, sensors, and electronically active molecules.²⁰ Bertrand and co-workers were the first to synthesize a free carbene in 1988,²¹ however, it was not until 1991 when Arduengo isolated the N-heterocyclic carbene that its full potential was realized.²² NHCs typically consist of a five membered ring with a C₃N₂ framework with the two nitrogen atoms adjacent to the carbenic carbon. The stability of this singlet carbene arises from the interaction of the π

electrons on the nitrogen atoms with the empty p_π orbital on the carbenic carbon forming a stable three-center four electron π system and a complete octet (Figure 1.2).²³

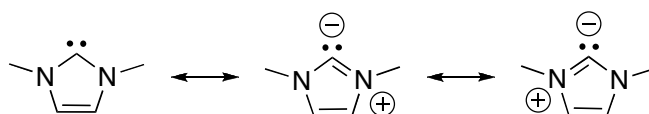


Figure 1.2: Resonance structures of the N-heterocyclic carbene.

NHCs share many similarities with their heavier group 15 counterparts, the N-Heterocyclic phosphonium cation (NHP) (Figure 1.3). Although the NHC and NHP are isovalent and isolobal to each other, they are the electronic inverse. Similar to the carbenic carbon in NHCs, the phosphorus atom in NHPs is also dicoordinate, possesses a lone pair of electrons and an empty π orbital. They differ in the fact that the NHP is cationic and exists in the +3 oxidation state. These combined components dominate the NHP chemistry and make NHPs weak σ donors and strong π acceptors, whereas NHCs are strong σ donors and poor π acceptors. Both NHCs and NHPs have unique diagnostic downfield resonances in their corresponding ^{13}C and ^{31}P NMR spectrum appearing between $\delta_{\text{C}} = 210 - 220$ and $\delta_{\text{P}} = 200 - 500$ respectively.^{23,24}

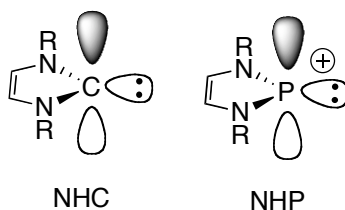
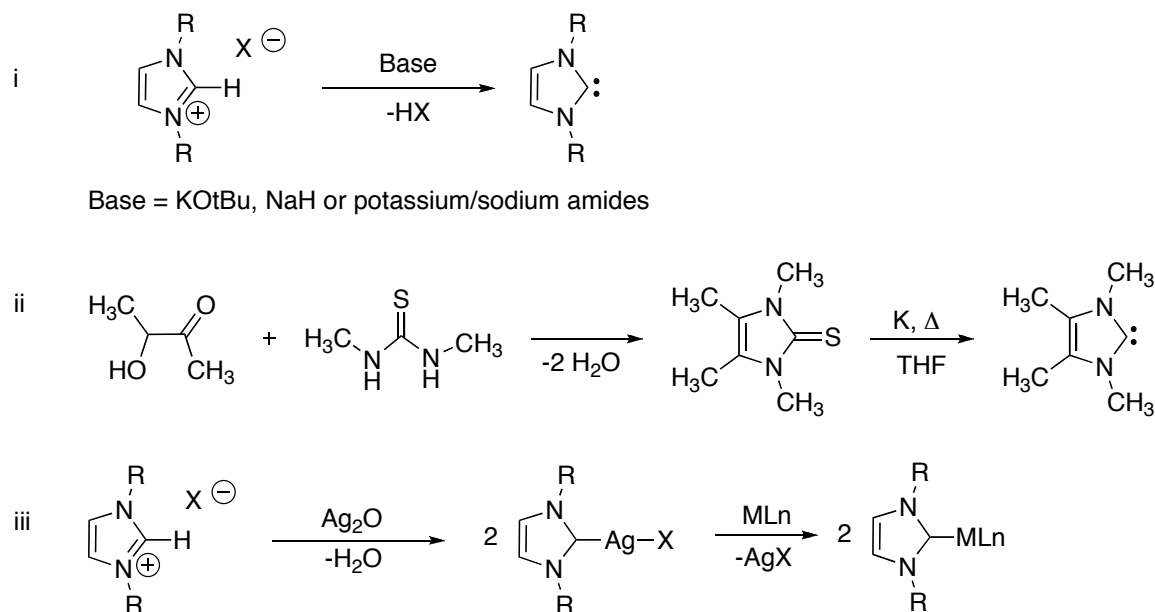


Figure 1.3: Frontier orbitals of two-coordinate carbene and phosphonium cation.

1.3.1 Synthesis

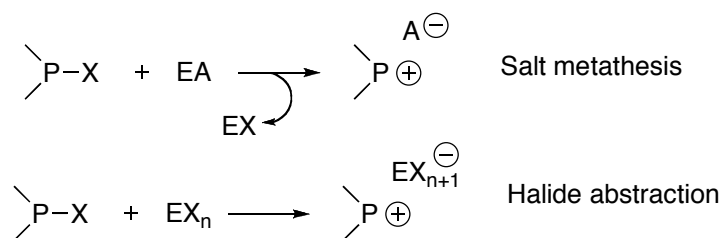
N-Heterocyclic carbenes can be synthesized in a variety of ways. The most common synthetic route is the deprotonation of an imidazolium salt precursor using either NaH, KOtBu or potassium/sodium amides (i, Scheme 1.1). A second approach involves a condensation reaction of *N,N'*-dialkylthiourea with 3-hydroxy-2-butanone yielding the 1,3,4,5-tetramethylimidazole-2-thione which can then be reduced using potassium in THF (ii, Scheme 1.1).²³ The isolation of the free carbene is not always possible and in

1997 Bertrand,²⁵ followed by Lin and Wang,²⁶ found they could generate the silver-NHC directly from the imidazolium salt *in situ* using silver bases. These silver-NHC complexes could then be used as transfer reagents to other metal centers (iii, Scheme 1.1).



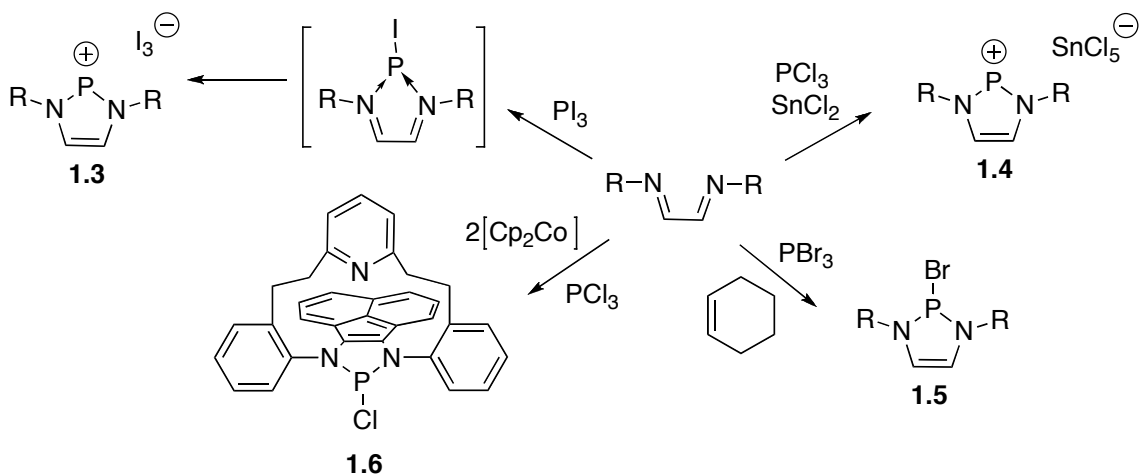
Scheme 1.1: Synthesis of NHC by deprotonation of the imidazolium salt (i), reduction (ii) and *in situ* using Ag₂O and onward transfer to a different metal (iii).

Contrary to the synthesis of NHCs where Bronsted bases are routinely used, NHPs can be generated a number of different ways. This includes protic,²⁷ electrophilic attack,^{28,29} internal^{30,31} and external redox^{32,33} routes as well as halide abstraction. The most common method of generating a phosphonium cation is through the halide abstraction of chlorine from the chlorophosphine precursor.²⁴ This can be done two ways, either through salt metathesis (eg. (Me₃SiOTf (OTf = CF₃SO₃), KPF₆, AgOTf, AgBF₄, TIBAr_F (BAR_F = tetrakis(3,5-bis(trifluoromethyl)phenyl)borate))^{31,34-37} or abstraction of the halide using Lewis acids (e.g. GaCl₃, FeCl₃, PCl₅ and Al₂Cl₆) (Scheme 1.2).³⁸⁻⁴⁰



Scheme 1.2: General synthesis of a phosphonium cation (E = element, A = anion and X = halide).

A second method of generating NHPs is through either internal or external redox routes. The research groups of Cowley and Macdonald have demonstrated that the use of a P(I) synthon in the presence of an α -diimine yields the phosphonium cation with either a triiodide (**1.3**) or chlorostanate anion (**1.4**). Unfortunately, these highly reactive anions can somewhat diminish their utility.^{30,41-43} An alternative route also developed by Macdonald adopted a similar method of generating a P(I) synthon using PBr_3 and cyclohexene. This synthesis yielded the diaminobromophosphine (**1.5**) which is an excellent precursor to NHPs and avoid reactive counter anions.³¹ Ragogna and co-workers utilized cobaltacene as an external one-electron reductant to generate the halophosphine precursor in the presence of the "clamshell" ligand (**1.6**, Scheme 1.3).³²



Scheme 1.3: Synthesis of a phosphonium cation (**1.3** and **1.4**) or the halophosphine precursor (**1.5** and **1.6**) by using internal or external reducing agents.

1.3.2 Reactivity

The reactivity of the NHP is dominated by their cationic charge, empty p_π orbital and coordinative unsaturation at the phosphorus atom. Examination of the frontier molecular orbitals in Figure 1.4 reveal that the LUMO is represented by the empty anti-bonding π orbital on phosphorus making the NHP Lewis acidic whereas the lone pair of the NHP is found in the HOMO-1. In contrast to their heavier phosphorus group 15 analogues, NHCs are strong σ donors and poor π acceptors. The strong σ donating ability of the NHC is due to their stability in the 1A_1 ground state with both electrons occupying the sp^2 orbital on carbon. Their stability in the singlet state is also attributed to the inductive effects of the σ -withdrawing amine substituents stabilizing the σ orbital on the carbenic carbon increasing the singlet-triplet energy gap. Further stabilization is provided by p_π donation from the N atoms into the empty p_π orbital on carbon. This is supported by the frontier molecular orbitals, where the HOMO corresponds to the σ lone pair on the carbenic carbon (Figure 1.4).

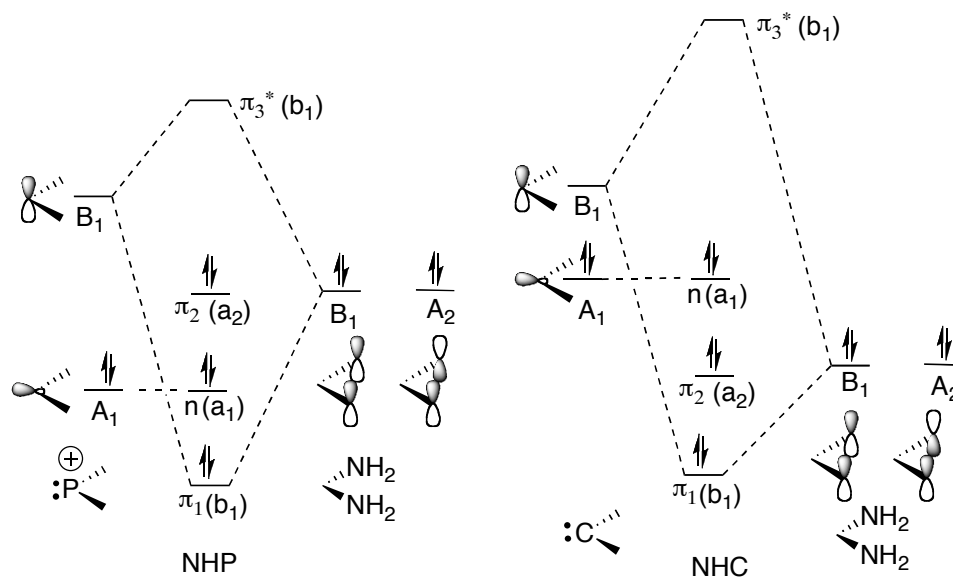


Figure 1.4: The frontier molecular orbitals of a diaminophosphenium (left) and diaminocarbene (right).

The empty p_π orbital and coordinative unsaturation at the phosphorus atom of NHPs enable them to undergo cycloadditions, form Lewis acid - Lewis base adducts and act as

ligands to late transition metals.²⁴ The Lewis acidic nature of phosphonium cations can be observed by their ability to form adducts with Lewis bases including carbenes,⁴⁴ amines,⁴⁵ imines⁴⁶ and phosphines.^{35,47} A number of studies have also focused on cycloaddition reactions between both acyclic and cyclic phosphonium cations with 1,3-butadienes yielding spirocyclic phospholenium cations.^{34,48,49}

The presence of a lone pair and an empty π orbital make NHPs suitable ligands for low valent late transition metals ranging from groups 6 -10.^{35,50-55} NHPs have been described to have similar coordination chemistry to NO^+ because both ligands not only have a positive charge but can also adopt either a pyramidal or planar transition metal binding mode (Figure 1.5). The reactivity of NHP metal complexes has been limited to ligand exchange and reaction with nucleophiles.⁵⁰ Their use as catalysis has also been proposed because of their π accepting ability, however work in this area is limited.⁵⁶⁻⁶⁰

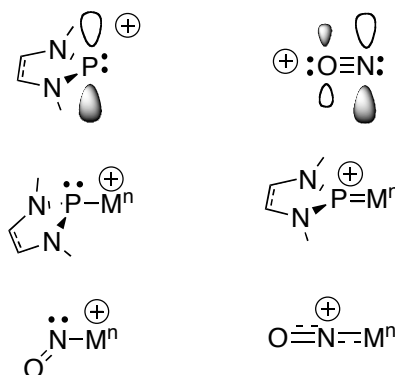


Figure 1.5: The phosphonium cation can adopt either a planar or pyramidal geometry similar to that of NO^+ .

In contrast to NHPs, N-heterocyclic carbene metal complexes are known with almost all transition metals and main group elements. Their ability to act as strong σ donors and weak π acceptors has made them ideal ligands in transition metal chemistry and has led to significant advances in olefin metathesis and Pd-catalyzed cross coupling reactions.⁶¹ In addition, NHCs have been used extensively in main group chemistry to stabilize highly reactive diatomic allotropes of group 14 and 15 elements,⁶² main group hydrides⁶³⁻⁶⁶ and polycationic p-block atoms.⁶⁷

The stabilization of NHCs from the p_x orbitals on nitrogen and the presence of the lone pair in the HOMO give NHCs their strong nucleophilic and Lewis basic properties. These properties have enabled NHCs not only to act as excellent ligands to transition metals but also be used as a catalyst in many organic transformation which include benzoin condensations, generation of homoenolates, amidations, *trans*-esterifications and ring opening polymerizations. Because of their strong nucleophilicity, NHCs can also form dimers. This can hinder their catalytic utility, particularly those derived from the saturated imidazolin-2-ylidene. The dimerizations of NHCs are based on a fine balance of both steric and electronic properties. NHCs that possess a large singlet-triplet energy gap and increased steric bulk on the N atoms are more likely to exist as a monomeric species. Denk *et. al* found an increase in the stability of the monomeric NHC for R = Me, Et, ⁱPr, *t*Bu was due to increased electron donation and a progressive destabilization of the enetetraamine.⁶⁸ The substitution of the nitrogen atoms with S, P and O can also lead to cyclic carbenes with a much higher tendency to form dimers.

1.4 Group 14 and 15 elements in functional materials

The synthesis of NHC polymers, specifically where the NHC is incorporated into the main polymer chain have shown potential utility in functional materials. This is because they have the advantage of combining both the desired properties of organometallic complexes with organic polymers.²⁰ Bielawski and co-workers have exploited the inherent reactivity of NHCs and their ability to form dimers, act as nucleophiles, and bind to transition metals to synthesize structurally dynamic polymers based on bis(NHCs) (Figure 1.6). The homopolymer (**1.7**) displayed extended conjugation whereas the alternating bis(NHCs) with bis(isothiocyanates) (**1.8**) and bis(azides) (**1.9**) resulted in increased stability to moisture and air, with the later being structurally reversible. Semi-conducting properties were also observed when group 10 metals were incorporated into the bis(NHC) system (**1.10**).⁶⁹ Along these lines, Cowley and co-workers have developed an α -diimine ligand with bis(bithiophene) rings in the backbone. Silver, gold and iridium NHC complexes (**1.11**) were synthesized and subsequently polymerized by oxidative electropolymerization of the thiophene rings. This represents the first polymer where the main group element was positioned orthogonal to the main polymer chain.^{70,71}

The bis(bithiophene) diimine was also utilized as a redox active ligand to generate phosphonium cations (**1.12**), however there has yet to be any further work done with this compound possibly because of the reactive I_3^- counter ion.⁴²

The integration of phosphorus into conjugated systems has also become an important building block in the synthesis of tunable π -conjugated materials. Baumgartner and Réau have thoroughly investigated the functionalization of phosphorus in phosphole ring systems and have developed a series of phosphole-based conjugated molecules (Figure 1.6). They were able to finely tune the band gap of these conjugated systems by altering the oxidation state and functionality at phosphorus (**1.13** and **1.14**, Figure 1.6).^{17,72} Baumgartner and co-workers were also able to change the band gap of tetracenes through the oxidation state of sulfur and the fluorescence quantum yield by substitution on phosphorus.⁷³ Dyer and co-workers have taken advantage of phosphonium salts as an oxidant and homo-coupled an equilibrium mixture of pyridal-N-phosphinoimine/ $\sigma^4-1\lambda^5$ -[1,3,2]diazaphosphole in a Scholl type reaction (**1.15**). The salt possessed a 4,4'-dihydropyridine core that resulted in an extended π -conjugated material that emits in the near IR region.⁷⁴ These simple modifications of the phosphorus atom allow for easy access to a wide range of different derivatives with varying structure and electronic properties.⁷² In summary, not only have main group atoms found utility in conjugated organic frameworks but are now also emerging into other areas of materials science.

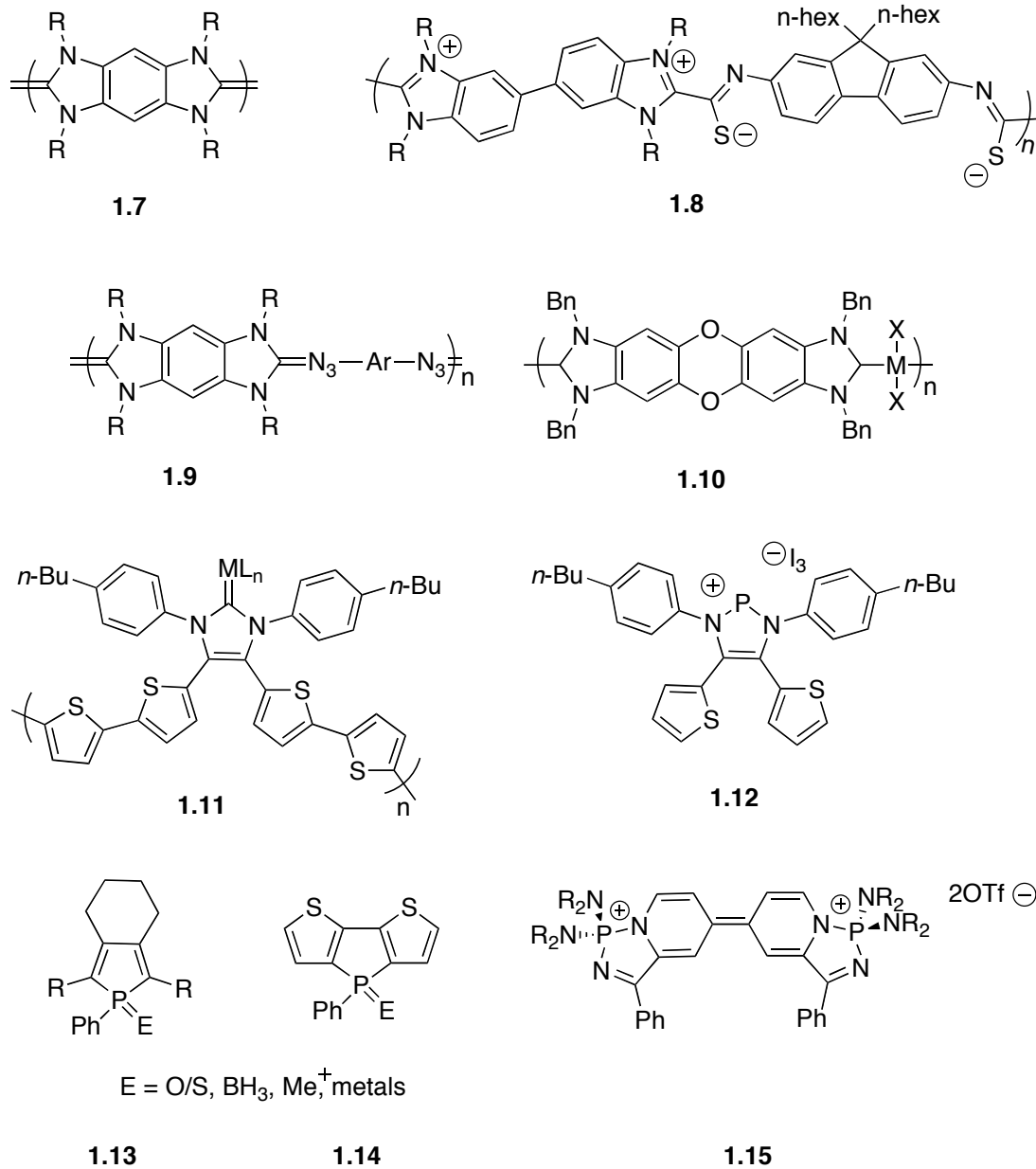
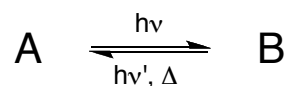


Figure 1.6: Main group elements incorporated into extended π -conjugated molecules and polymers.

1.5 Photochromic dithienylethenes

1.5.1 Photochromism

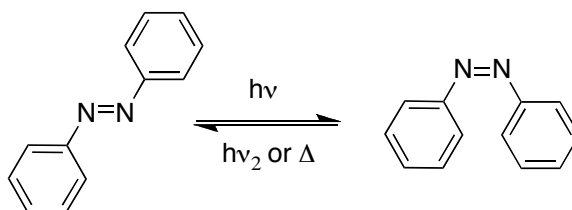
Photochromism is defined as a reversible transformation of a chemical species induced in one or both directions by absorption of electromagnetic radiation between two forms, **A** and **B**, that have two different absorption spectra.⁷⁵ During the photo-isomerization process the absorption spectra not only changes but also the various photophysical properties including the refractive index, dielectric constant, oxidation/reduction potential and the geometric structure. These changes can be induced using either UV, visible or IR radiation.⁷⁵ The reversible back reaction can occur through two different pathways: thermally (T-type photochromism) or photochemically (P-type photochromism)⁷⁵ and are shown in Scheme 1.4.



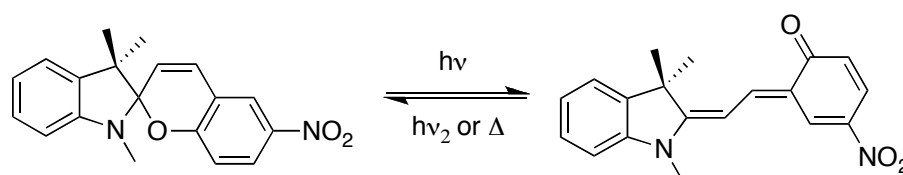
Scheme 1.4: The reversible photochromic conversion of compound **A** to compound **B**.

The most prevalent system is positive photochromism, which involves a unimolecular reaction where **A** is most often colorless or pale yellow, while **B** is colored. The most commonly used classes of photochromic molecules are: stilbenes and azo compounds which undergo cis-trans (E/Z) isomerization; and the pericyclic reactions, which include spiropyrans, fulgides and dithienylethens⁷⁵ (Figure 1.7).

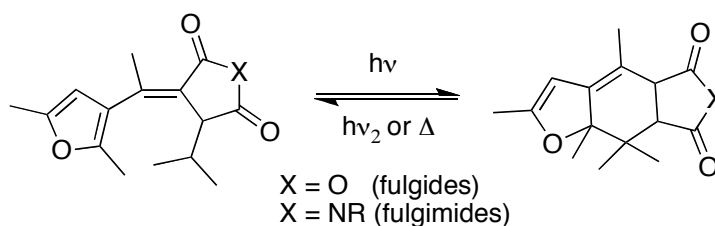
Azo Compounds



Spiropyrans



Fulgides and Fulgimides



Dithienylethenes

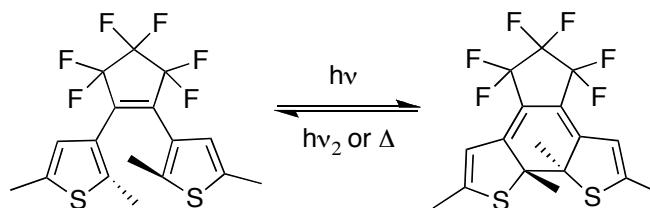


Figure 1.7: Examples of organic switchable photochromic molecules.

1.5.2 Dithienylethenes

Molecular switches that reversibly change colour when exposed to light have shown potential for various applications, including information storage systems, imaging devices, displays and sensors.⁷⁶ For a photochromic molecule to be successfully incorporated into either memory devices or sensors they must have high fatigue resistance and be thermally irreversible.⁷⁶ Among the many different categories of photochromic compounds, those possessing the 1,2 dithienylhexatriene (DTE) framework have shown significantly more potential amongst the other classes (Figure 1.8). This is

because they possess these desirable properties, while maintaining their ability to be highly functionalized.⁷⁶

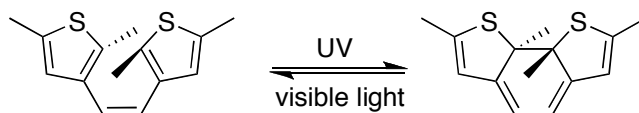
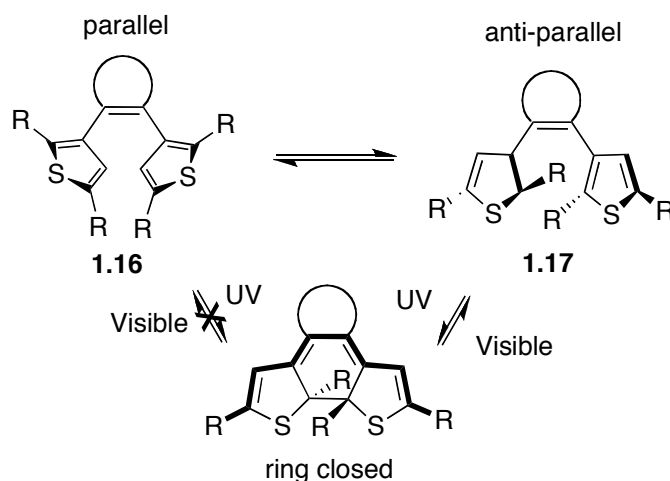


Figure 1.8: The ring closed and ring open isomers of DTEs.

Radiation of UV light onto the DTE framework generates the formation of a ring-closed, coloured, rigid π -conjugated system, from the flexible, colourless, ring-open isomer. The ring-open DTE exist in equilibrium between two different conformations with the thiophene rings being parallel (**1.16**) or anti-parallel (**1.17**) with respect to each other. This is important because the ring closing cyclization can only occur when the molecule is in the anti-parallel conformation (**1.16**, Scheme 1.5).⁷⁶ These alterations in the DTE framework upon switching from the ring-open to the ring-closed conformations are what dictates how the open and closed isomers absorb, emit and refract light, and their ability to act as chemical switches.⁷⁷



Scheme 1.5: DTE in equilibrium between the parallel (**1.16**) and anti-parallel (**1.17**) conformations and conversion to the ring-closed isomer from the anti-parallel form.

1.5.3 Thermal stability and fatigue resistance

In order for photochromic molecules to be potential candidates for both optical memory devices and optical switches they must have a high thermal stability of both ring-closed and ring-open forms. The DTE closed isomer has a high thermal stability and will not revert back to the open conformation in the absence of light. The ring closing reaction follows the Woodward-Hoffmann rules based on the π -orbital symmetry. A large energy barrier prohibits the symmetry allowed thermal disrotatory cyclization, however no such energy barrier exists for the photoexcited state and the DTEs thus undergo a conrotatory cyclization in the presence of UV light.⁷⁸ A second component to consider is the stability of the photo-generated closed-ring isomer due to the change in aromaticity going from the ring-open to ring-closed states. The height of the thermal energy barrier required to undergo cycloreversion is inversely related to the difference in the aromatic stabilization energy of the aryl groups in the open and closed form. The structural changes of the aryl groups in the reaction from ring-open to ring-closed are shown in Figure 1.9, along with the differences in energy between both isomers. From the series of heterocycles studied, thienyl substituents have the smallest energy difference in aromatic stabilization and therefore the largest thermal energy barrier for cycloreversion making them the most thermally stable systems.⁷⁸

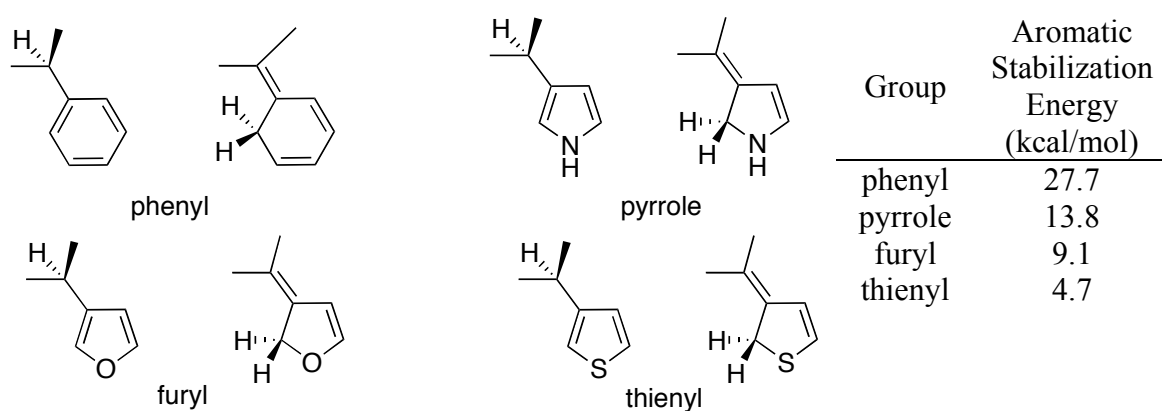
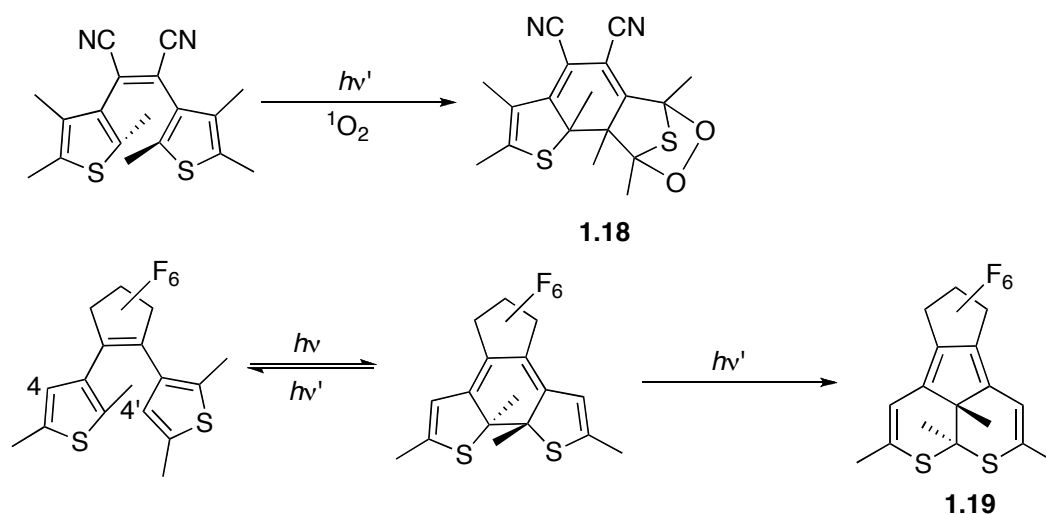


Figure 1.9: The structural changes and stabilization energies of the generated closed-ring isomers.

Fatigue resistance is another important property because during the course of the cyclization reaction undesirable side reactions can take place, which then limits the number of cycles. Although fatigue resistant DTEs exist, designing these compounds can be quite challenging. For example, if an undesirable side reaction has a quantum yield of 0.001, after only 1000 cycles 63% of the initial concentration of the DTE will have decomposed.⁷⁶ Irie and co-workers have isolated two of the main by-products from irradiation. Some compounds were found to decompose in less than 80 cycles in the presence of air due to the formation of endoperoxides (**1.18**).⁷⁹ Six-membered ring formation (**1.19**) was also observed when there was no substitution in the 4, 4' positions of the thiophene ring (Scheme 1.6). When the thiophene rings were replaced with benzothiophene the cycle number increased dramatically because of its lower reactivity to singlet oxygen, inhibiting the formation of the oxidized product.^{80,81}



Scheme 1.6: Decomposition of the DTE from singlet oxygen to an irreversible ring-closed conformer; (top) the formation of endoperoxides; (bottom) six-membered ring product.

1.5.4 Versatility

The DTE framework can undergo a vast range of different chemistries and has a high tolerance to a wide variety of different functional groups.^{2,75-77,82,83} The most common sites of modification to the DTE framework are the 2,2' and 5,5' positions on the

thiophene and the central ring (Figure 1.10). The synthetic manipulation of the DTE framework in which different functional groups are installed can result in different steric and electronic effects upon ring-closing and ring-opening events. These changes can then translate to other photophysical properties including, but not limited to fluorescence emission, UV-absorption spectra, conjugation, dipole interaction, magnetic properties, geometrical structures, electrochemical properties and gated reactivity.⁸³

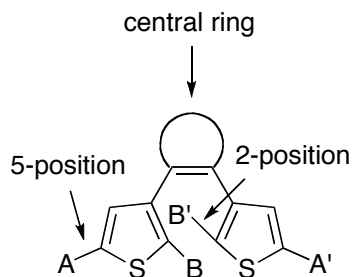


Figure 1.10: Areas of functionalization on the DTE framework.

Yam and co-workers have successfully incorporated tricoordinate boron into DTE systems by appending both a β -diketonate ligand (**1.21**) and a *C,N*-chelated DTE functionalized thienylpyridine core (**1.22**). The coordination of these DTEs to a tetrahedral B(III) center afforded a near IR shift in the ring-closed isomer and have potential utility in both Lewis acid catalysis and π -electronic materials.^{84,85} Branda *et al.* were able to modulate the Lewis acidity of compound **1.20** using the appropriate wavelength of light switching between the open and closed DTE conformations.⁸⁶ Ionic liquids containing a DTE group into the core of an imidazolium salt (**1.23**) has also been successfully synthesized and a series of photoswitchable DTEs containing NHC complexes of Au(I), Ag(I) and Pd(II) (**1.24** and **1.25**) open up new opportunities for photoswitchable catalyst.⁸⁷ Bielawski and co-workers further pursued this idea and developed an NHC functionalized DTE with attenuated catalytic activity in the ring closed conformation for *trans*-esterification and amidation reactions (**1.26**). The catalytic activity of the corresponding organocatalyst could be remotely tuned by exposure to visible and UV light.^{88,89} In addition DTEs with bis(phosphine) ligands in the 5, 5' position on the thiophene rings have also been used in the base stabilization of both Au(I) and selenium atoms (**1.27** and **1.28**).⁹⁰

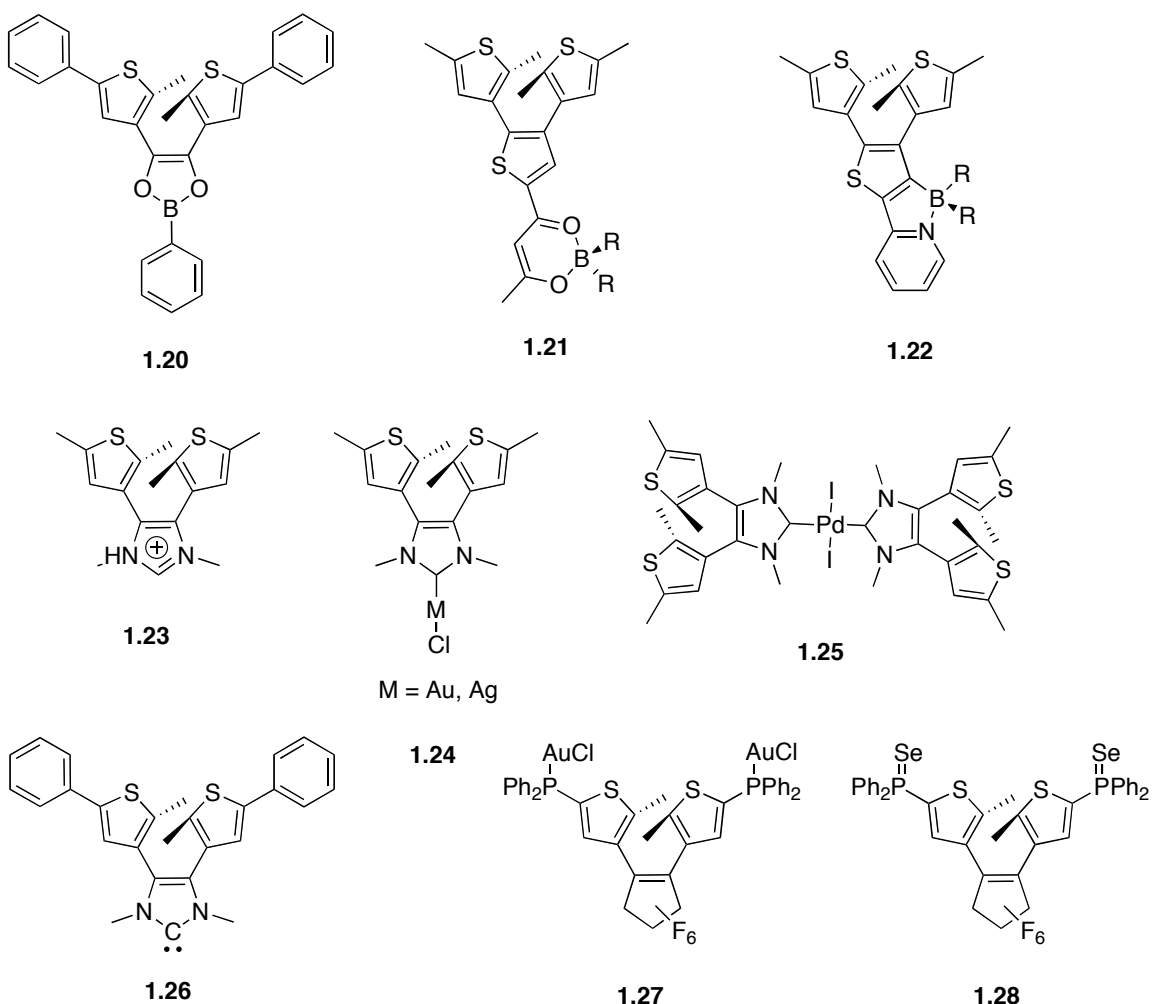


Figure 1.11: Main group elements incorporated into DTE core.

1.6 Scope of thesis

In light of the above discussion, the body of work that follows focuses on the incorporation of main group elements into novel *N,N'*-chelating frameworks containing thiophene rings and studying their photophysical properties. This was accomplished by detailing the design and synthesis of new *N,N'*-chelating frameworks with thiophene rings in the backbone and the coordination of these new molecules to p-block atoms. These studies were aimed at exploring the novel structure and bonding of three distinct ligand sets (**2.4^{Mes}**, **2.5^{Dipp}**, **3.4**, and **5.2**) and their main group compounds along with their respective spectroscopic properties (Figure 1.12).

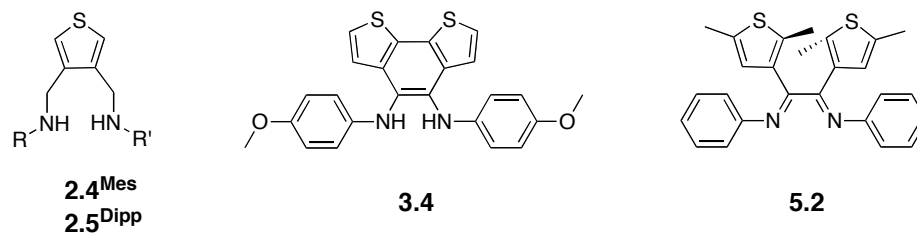


Figure 1.12: Novel N,N' -chelating ligands used to coordinate p-block elements.

Chapter 2 focused on the design and synthesis of a chelating diamino ligand (**2.4^{Mes}** and **2.5^{Dipp}**) with thiophene in the backbone and its coordination to phosphorus. Chapter 3 is concentrated on the synthesis of a new chelating N,N' -diamino ligand (**3.4**), functionalized with benzo[1,2-b:5,6-b']dithiophene and its coordination to phosphorus, arsenic and antimony. This chapter also explores their reactivity and examines the spectroscopic properties of the resulting compounds. Chapter 4 details the synthesis of an NHC and its metal complexes along with a description of the donor strength and spectroscopic properties. Chapter 5 examines the synthesis of a new photochromic DTE diimine (**5.2**) and its coordination to boron and phosphorus, as well its incorporation into side chain functionalized acrylate polymer. The reversible photochromic ring-closing and ring-opening quantum yields and thermal stabilities were also studied along with a complete characterization of all new compounds. Chapter 6 comprises of a summary and conclusions of the work presented in this thesis along with possible directions and projects that can transpire in the future.

1.7 References

- (1) Joule, J. A.; Mills, K. *Heterocyclic Chemistry*; 5 ed.; John Wiley and Sons Ltd, 2010.
- (2) Barbarella, G.; Melucci, M.; Sotgiu, G. *Adv. Mater.* **2005**, *17*, 1581-1593.
- (3) King, W. J.; Nord, F. F. *J. Org. Chem.* **1949**, *14*, 638-642.
- (4) Halik, M.; Klauk, H.; Zschieschang, U.; Schmid, G.; Ponomarenko, S.; Kirchmeyer, S.; Weber, W. *Adv. Mater.* **2003**, *15*, 917-922.

- (5) Rost, C.; Karg, S.; Riess, W.; Loi, M. A.; Murgia, M.; Muccini, M. *Appl. Phys. Lett.* **2004**, *85*, 1613-1615.
- (6) Moorlag, C.; Sih, B. C.; Stott, T. L.; Wolf, M. O. *J. Mater. Chem.* **2005**, *15*, 2433-2436.
- (7) Vriezema, D. M.; Hoogboom, J.; Velonia, K.; Takazawa, K.; Christianen, P. C. M.; Maan, J. C.; Rowan, A. E.; Nolte, R. J. M. *Angew. Chem. Int. Ed.* **2003**, *42*, 772-776.
- (8) Yu, H.-h.; Pullen, A. E.; Büschel, M. G.; Swager, T. M. *Angew. Chem. Int. Ed.* **2004**, *43*, 3700-3703.
- (9) Clot, O.; Wolf, M. O.; Patrick, B. O. *J. Am. Chem. Soc.* **2001**, *123*, 9963-9973.
- (10) Roncali, J. *Chem. Rev.* **1992**, *92*, 711-738.
- (11) Langmi, H. W.; McGrady, G. S. *Coord. Chem. Rev.* **2007**, *251*, 925-935.
- (12) Staubitz, A.; Robertson, A. P. M.; Manners, I. *Chem. Rev.* **2010**, *110*, 4079-4124.
- (13) Stephens, F. H.; Pons, V.; Baker, R. T. *Dalton Trans.* **2007**, 2613-2626.
- (14) Wade, C. R.; Broomsgrove, A. E. J.; Aldridge, S.; Gabbai, F. P. *Chem. Rev.* **2010**, *110*, 3958-3984.
- (15) Blackstone, V.; Presa, S. A.; Manners, I. *Dalton Trans.* **2008**, 4363-4371.
- (16) Manners, I. *J. Polym. Sci., Part A: Polym. Chem.* **2001**, *40*, 179-191.
- (17) Ren, Y.; Baumgartner, T. *Dalton Trans.* **2012**, *41*, 7792-7800.
- (18) Malik, M. A.; Afzaal, M.; O'Brien, P. *Chem. Rev.* **2010**, *110*, 4417-4446.
- (19) Chivers, T.; Konu, J. *Comments on Inorganic Chemistry* **2009**, *30*, 131-176.
- (20) Mercs, L.; Albrecht, M. *Chem. Soc. Rev.* **2010**, *39*, 1903-1912.
- (21) Igau, A.; Grutzmacher, H.; Baceiredo, A.; Bertrand, G. *J. Am. Chem. Soc.* **1988**, *110*, 6463-6466.
- (22) Arduengo, A. J.; Harlow, R. L.; Kline, M. J. *Am. Chem. Soc.* **1991**, *113*, 361-363.
- (23) Herrmann, W. A.; Köcher, C. *Angew. Chem. Int. Ed.* **1997**, *36*, 2162-2187.

- (24) Cowley, A. H.; Kemp, R. A. *Chem. Rev.* **1985**, *85*, 367-382.
- (25) Guerret, O.; Solé, S.; Gornitzka, H.; Teichert, M.; Trinquier, G.; Bertrand, G. *J. Am. Chem. Soc.* **1997**, *119*, 6668-6669.
- (26) Wang, H. M. J.; Lin, I. J. B. *Organometallics* **1998**, *17*, 972-975.
- (27) Dahl, O. *Tetrahedron Lett.* **1982**, *23*, 1493-1496.
- (28) Niecke, E.; Kröher, R. *Angew. Chem., Int. Ed.* **1976**, *15*, 692-693.
- (29) Cowley, A. H.; Kilduff, J. E.; Norman, N. C.; Atwood, J. L.; Pakulski, M.; Hunter, W. E. *J. Am. Chem. Soc.* **1983**, *105*, 4845-4846.
- (30) Reeske, G.; Cowley, A. H. *Inorg. Chem.* **2007**, *46*, 1426-1430.
- (31) Dube, J. W.; Farrar, G. J.; Norton, E. L.; Szekely, K. L. S.; Cooper, B. F. T.; MacDonald, C. L. B. *Organometallics* **2009**, *28*, 4377-4384.
- (32) Brazeau, A. L.; Jones, N. D.; Ragogna, P. J. *Dalton Trans.* **2012**, *41*, 7890-7896.
- (33) Schmidpeter, A. *Heteroat. Chem.* **1999**, *10*, 529-537.
- (34) Caputo, C. A.; Price, J. T.; Jennings, M. C.; McDonald, R.; Jones, N. D. *Dalton Trans.* **2008**, 3461-3469.
- (35) Abrams, M. B.; Scott, B. L.; Baker, R. T. *Organometallics* **2000**, *19*, 4944-4956.
- (36) Reed, R.; Réau, R.; Dahan, F.; Bertrand, G. *Angew. Chem., Int. Ed.* **1993**, *32*, 399-401.
- (37) Brazeau, A. L.; Caputo, C. A.; Martin, C. D.; Jones, N. D.; Ragogna, P. J. *Dalton Trans.* **2010**, *39*, 11069-11073.
- (38) Spinney, H. A.; Korobkov, I.; DiLabio, G. A.; Yap, G. P. A.; Richeson, D. S. *Organometallics* **2007**, *26*, 4972-4982.
- (39) Maryanoff, B. E.; Hutchins, R. O. *J. Org. Chem.* **1972**, *37*, 3475-3480.
- (40) Thomas, M. G.; Schultz, C. W.; Parry, R. W. *Inorg. Chem.* **1977**, *16*, 994-1001.
- (41) Ellis, B. D.; Macdonald, C. L. B. *Inorg. Chim. Acta* **2007**, *360*, 329-344.
- (42) Powell, A. B.; Brown, J. R.; Vasudevan, K. V.; Cowley, A. H. *Dalton Trans.* **2009**, 2521-2527.

- (43) Reeske, G.; Hoberg, C. R.; Hill, N. J.; Cowley, A. H. *J. Am. Chem. Soc.* **2006**, *128*, 2800-2801.
- (44) Hardman, N. J.; Abrams, M. B.; Pribisko, M. A.; Gilbert, T. M.; Martin, R. L.; Kubas, G. J.; Baker, R. T. *Angew. Chem., Int. Ed.* **2004**, *43*, 1955-1958.
- (45) Kaukorat, T.; Neda, I.; Schmutzler, R. *Coord. Chem. Rev.* **1994**, *137*, 53-107.
- (46) Reed, R.; Réau, R.; Dahan, F.; Bertrand, G. *Angew. Chem., Int. Ed.* **1993**, *32*, 399-401.
- (47) Ellis, B. D.; Ragogna, P. J.; Macdonald, C. L. B. *Inorg. Chem.* **2004**, *43*, 7857-7867.
- (48) Marciacq, F.; Sauvaigo, S.; Issartel, J.-P.; Mouret, J.-F. O.; Molko, D. *Tetrahedron Lett.* **1999**, *40*, 4673-4676.
- (49) Boyd, R. J.; Burford, N.; Macdonald, C. L. B. *Organometallics* **1998**, *17*, 4014-4029.
- (50) Caputo, C. A.; Jennings, M. C.; Tuononen, H. M.; Jones, N. D. *Organometallics* **2009**, *28*, 990-1000.
- (51) Pan, B.; Xu, Z.; Bezpalko, M. W.; Foxman, B. M.; Thomas, C. M. *Inorg. Chem.* **2012**, *51*, 4170-4179.
- (52) Montemayor, R. G.; Sauer, D. T.; Fleming, S.; Bennett, D. W.; Thomas, M. G.; Parry, R. W. *J. Am. Chem. Soc.* **1978**, *100*, 2231-2233.
- (53) Spinney, H. A.; Yap, G. P. A.; Korobkov, I.; DiLabio, G.; Richeson, D. S. *Organometallics* **2006**, *25*, 3541-3543.
- (54) Nakazawa, H.; Yamaguchi, Y.; Mizuta, T.; Miyoshi, K. *Organometallics* **1995**, *14*, 4173-4182.
- (55) Nakazawa, H. *Journal of Organometallic Chemistry* **2000**, *611*, 349-363.
- (56) Breit, B. *J. Mol. Catal. A: Chem.* **1999**, *143*, 143-154.
- (57) Caputo, C. A.; Brazeau, A. L.; Hynes, Z.; Price, J. T.; Tuononen, H. M.; Jones, N. D. *Organometallics* **2009**, *28*, 5261-5265.
- (58) Petuskova, J.; Bruns, H.; Alcarazo, M. *Angew. Chem., Int. Ed.* **2011**, *50*, 3799-3802.
- (59) Sakakibara, K.; Yamashita, M.; Nozaki, K. *Tetrahedron Lett.* **2005**, *46*, 959-962.

- (60) Saleh, S.; Fayad, E.; Azouri, M.; Hierso, J.-C.; Andrieu, J.; Picquet, M. *Adv. Synth. Catal.* **2009**, *351*, 1621-1628.
- (61) Crudden, C. M.; Allen, D. P. *Coordination Chemistry Reviews* **2004**, *248*, 2247-2273.
- (62) Wang, Y.; Robinson, G. H. *Dalton Trans.* **2012**, *41*, 337-345.
- (63) Al-Rafia, S. M. I.; Malcolm, A. C.; Liew, S. K.; Ferguson, M. J.; Rivard, E. *J. Am. Chem. Soc.* **2011**, *133*, 777-779.
- (64) Al-Rafia, S. M. I.; Malcolm, A. C.; McDonald, R.; Ferguson, M. J.; Rivard, E. *Angew. Chem., Int. Ed.* **2011**, *50*, 8354-8357.
- (65) Al-Rafia, S. M. I.; Malcolm, A. C.; McDonald, R.; Ferguson, M. J.; Rivard, E. *Chem. Commun.* **2012**, *48*, 1308-1310.
- (66) Thimer, K. C.; Al-Rafia, S. M. I.; Ferguson, M. J.; McDonald, R.; Rivard, E. *Chem. Commun.* **2009**, 7119-7121.
- (67) Dutton, J. L.; Tuononen, H. M.; Ragogna, P. J. *Angew. Chem., Int. Ed.* **2009**, *48*, 4409-4413.
- (68) Denk, M. K.; Hezarkhani, A.; Zheng, F.-L. *Eur. J. Inorg. Chem.* **2007**, 3527-3534.
- (69) Neilson, B. M.; Tennyson, A. G.; Bielawski, C. W. *J. Phys. Org. Chem.* **2012**, *25*, 531-543.
- (70) Powell, A. B.; Bielawski, C. W.; Cowley, A. H. *J. Am. Chem. Soc.* **2009**, *131*, 18232-18233.
- (71) Powell, A. B.; Bielawski, C. W.; Cowley, A. H. *J. Am. Chem. Soc.* **2010**, *132*, 10184-10194.
- (72) Crassous, J.; Reau, R. *Dalton Trans.* **2008**, 6865-6876.
- (73) Ren, Y.; Baumgartner, T. *J. Am. Chem. Soc.* **2011**, *133*, 1328-1340.
- (74) Smith, D. A.; Batsanov, A. S.; Fox, M. A.; Beeby, A.; Apperley, D. C.; Howard, J. A. K.; Dyer, P. W. *Angew. Chem., Int. Ed.* **2009**, *48*, 9109-9113.
- (75) Düre, H.; Bouas-Laurent, H. *Photochromism: molecules and systems*; Elsevier: Amsterdam, 2003.
- (76) Irie, M. *Chem. Rev.* **2000**, *100*, 1683-1684.
- (77) Perepichka, I. F. *Handbook of Thiophene-Based Materials: Applications in Organic Electronics and Photonics, 2 Volume Set*; Wiley, 2009.

- (78) Nakamura, S.; Irie, M. *J. Org. Chem.* **1988**, *53*, 6136-6138.
- (79) Taniguchi, H.; Shinpo, A.; Okazaki, T.; Matsui, F.; Irie, M. *Nippon Kagaku Kaishi* **1992**, *1992*, 1138-1140.
- (80) Irie, M.; Lifka, T.; Uchida, K.; Kobatake, S.; Shindo, Y. *Chem. Commun.* **1999**, 747-750.
- (81) Irie, M.; Mohri, M. *J. Org. Chem.* **1988**, *53*, 803-808.
- (82) Natali, M.; Giordani, S. *Chem. Soc. Rev.* **2012**, *41*, 4010-4029.
- (83) Zhang, J.; Zou, Q.; Tian, H. *Adv. Mater.* **2012**, n/a-n/a.
- (84) Poon, C.-T.; Lam, W. H.; Wong, H.-L.; Yam, V. W.-W. *J. Am. Chem. Soc.* **2010**, *132*, 13992-13993.
- (85) Wong, H.-L.; Wong, W.-T.; Yam, V. W.-W. *Org. Lett.* **2012**, *14*, 1862-1865.
- (86) Lemieux, V.; Spantulescu, M. D.; Baldrige, K. K.; Branda, N. R. *Angew. Chem. Int. Ed.* **2008**, *47*, 5034-5037.
- (87) Yam, V. W.-W.; Lee, J. K.-W.; Ko, C.-C.; Zhu, N. *J. Am. Chem. Soc.* **2009**, *131*, 912-913.
- (88) Neilson, B. M.; Bielawski, C. W. *J. Am. Chem. Soc.* **2012**, *134*, 12693-12699.
- (89) Neilson, B. M.; Lynch, V. M.; Bielawski, C. W. *Angew. Chem. Int. Ed.* **2011**, *50*, 10322 - 10326.
- (90) Sud, D.; McDonald, R.; Branda, N. R. *Inorg. Chem.* **2005**, *44*, 5960-5962.

Chapter 2

2 Phosphenium cation in a seven membered ring supported by thiophene^Ω

2.1 Introduction

The utility of N-heterocyclic carbenes (NHCs) has given rise to a wide range of chemistries, from functional and structurally diverse metal coordination complexes, to enhancing catalytic properties within transition metal catalysis, and in some cases defining new directions in materials chemistry.¹⁻⁵ The NHCs share many similarities with their heavier group 15 analogue the N-heterocyclic phosphenium cation (NHP), as they are isovalent and isolobal to each other, however NHPs are the electronic inverse of the NHC.^{6,7} The phosphorus atom in an NHP is dicoordinate, cationic, formally possesses a lone pair of electrons, an empty π orbital and the central phosphorus is in the +3 oxidation state. The cationic charge at the phosphorus center is normally stabilized by two flanking amino substituents, and it is these combined components that dominate the chemistry of the NHP. These cations are weak σ donors and strong π acceptors, thus enabling NHPs to be good Lewis acidic ligands for electron rich transition metals.⁸⁻¹⁰

The NHP framework typically consists of four, five or six membered rings with phosphorus being the lone reactive site. The main focus in this field has been to harness the chemistry of the P^+ centre, however a shifting philosophy within main group chemistry as a whole (which includes phosphenium chemistry), has moved from studying purely the fundamental structure, bonding and reactivity of these species, to their potential for applications in broader arenas. Examples have surfaced within the past few years in utilizing main group elements in the construction of OLEDs and within catalysis/small molecule activation, by taking advantage of the unique properties that these main group centers possess.¹¹⁻¹⁵ Efforts in these fields by ourselves and other

^Ω A version of this chapter has been published in Price, J. T., Jones, N. D. and Ragogna P. J., *Can. J. Chem.*, **2013**, DOI: 10.1139/cjc-2013-0015 and has been published with permission.

research groups have centered on designing new ligand sets containing thiophene, a ubiquitous building block in the area of redox active and fluorescent materials.^{16,17} Ultimately such architectures target the photoluminescent and polymerizable properties of thiophene, yet look to tune the photophysics of the overall construct by varying the main group element centre. We have previously designed a diamine, which contains a benzo[1,2-b:5,6-b']dithiophene backbone and have demonstrated its ability to stabilize pnictenium cations (Pn = P, As and Sb) and NHCs (compound **i**, Figure 2.1) which will be further discussed in Chapters 3 and 4.^{18,19} Cowley *et al.* have developed a novel redox active α -diimine with pendent thiophene rings in the 2 and 3 position and have used this ligand to coordinate a phosphonium cation with a triiodide counter ion.²⁰ Furthermore, Cowley and Bielawski have used that same α -diimine to synthesize polymers containing NHCs orthogonal to the polymer backbone (compound **ii**, Figure 2.1).^{21,22} Although there are many different ligands able to support main group elements, there is a void in those that can combine the unique reactivity of the members of the p-block with the desired photophysical and polymerizable properties that are required for the design of new materials. A need exists to develop ligands that can meet these requirements, while continuing to push main group chemistry into the applied research fields. In this context, we have synthesized two new chelating diimino- (**2.2^{Mes}** and **2.3^{Dipp}**) and diamino- (**2.4^{Mes}** and **2.5^{Dipp}**) ligands with a thiophene unit in the backbone, where **2.5^{Dipp}** is able to support a phosphonium cation (**2.9**). This is the first synthesis and complete characterization of a seven-membered phosphonium cation, and aids in identifying new opportunities in the unique structure, bonding and reactivity of phosphorus.

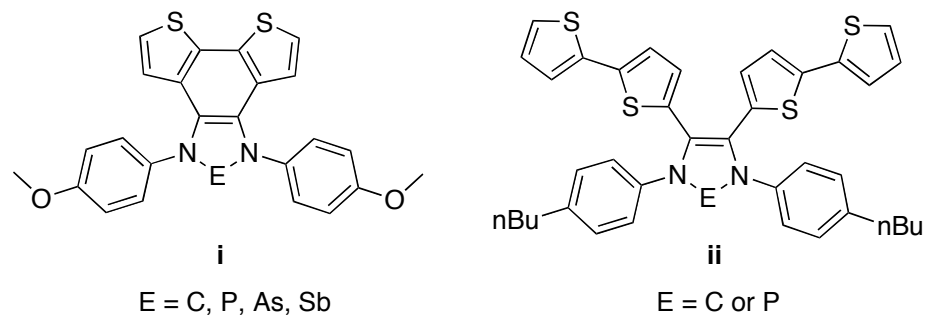
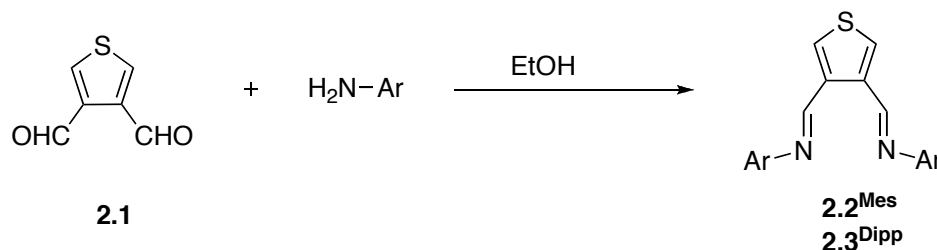


Figure 2.1: Previously synthesized NHCs and NHPns (Pn = Pnictogen) containing pendant thiophene rings.

2.2 Results and Discussion

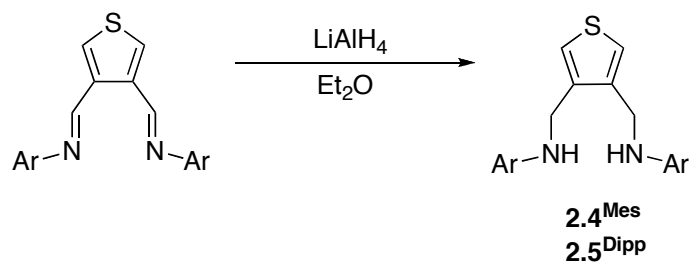
2.2.1 Synthesis

The thiophene substituted aryldiimines, (**2.2^{Mes}** and **2.3^{Dipp}**) were synthesized *via* a condensation reaction between 3,4-diformylthiophene (**2.1**) and the appropriate arylamine in EtOH. The reaction mixtures were stirred overnight at rt. and the yellow precipitates were isolated by filtration and washed with cold EtOH (Scheme 2.1). Upon examination of the ¹H NMR spectrum of the redissolved powders, the proton signal from the aldehyde ($\delta_{\text{H}} = 10.30$) was no longer present and a resonance consistent with an imine appears ($\delta_{\text{H}} = 8.72$). Compounds **2.2^{Mes}** and **2.3^{Dipp}** were isolated in 76 % and 80 % yields, respectively. Single crystals of **2.2^{Mes}** suitable for X-ray diffraction studies were grown from a concentrated solution of CH₂Cl₂ confirming the targeted connectivity (Figure 2.3).



Scheme 2.1: Synthesis of (**2.2^{Mes}**) and (**2.3^{Dipp}**) diimines.

Compounds **2.2^{Mes}** and **2.3^{Dipp}** were then reduced to the diamines **2.4^{Mes}** and **2.5^{Dipp}** using 3 stoichiometric equivalents of LiAlH₄ in Et₂O (Scheme 2.2).²³ The reaction mixture was stirred overnight at rt. and then quenched with a 10% KOH_(aq) solution. The filtrate was collected and concentrated under reduced pressure yielding a white solid. The bulk powders were redissolved in CDCl₃ and the corresponding ¹H NMR spectrum revealed that the aldimine proton was no longer present and a new singlet ($\delta_{\text{H}} = 4.0$) appeared, indicative of the methylene protons adjacent to the thiophene ring. X-ray quality single crystals of **2.5^{Dipp}** were grown from a concentrated solution of CH₂Cl₂ confirming the synthesis of **2.5^{Dipp}**. Compounds **2.4^{Mes}** and **2.5^{Dipp}** were isolated in 85% and 80% yields, respectively (Scheme 2.2).

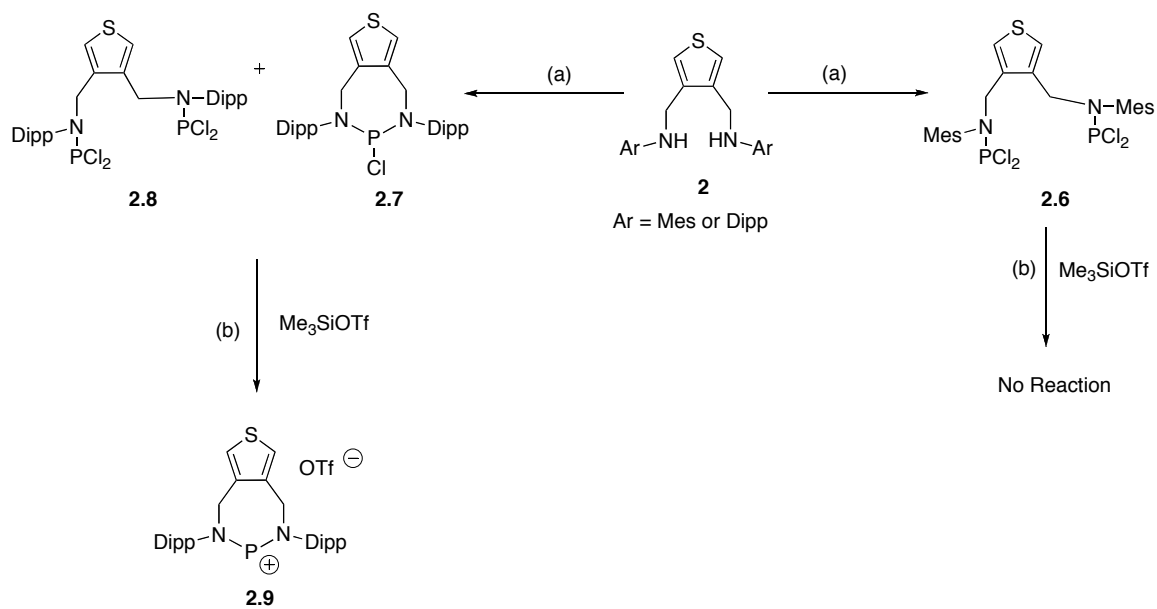


Scheme 2.2: Synthesis of compound **2.4^{Mes}** and **2.5^{Dipp}** diamines.

The chlorophosphine **2.6** was synthesized using a 3:1:1 stoichiometric reaction between N-methylmorpholine, PCl_3 and **2.4^{Mes}** in THF, which resulted in an immediate formation of a white precipitate. Reaction progress was monitored by obtaining $^{31}\text{P}\{^1\text{H}\}$ NMR spectra of aliquots of the reaction mixture that indicated the reaction was complete after 15 h, marked by the disappearance of PCl_3 ($\delta_{\text{p}} = 220$) and the appearance of a new single resonance at $\delta_{\text{p}} = 153$. In the ^1H NMR spectrum, the methylene protons in the 3 and 4 position of the thiophene ring appear as a doublet because of coupling to phosphorus ($^3J_{\text{H-}^{31}\text{P}} = 2.8 \text{ Hz}$) and the methyl protons on the aryl rings were no longer identical, as distinct signals were observed. Subsequent halide abstraction using trimethylsilyl-trifluoromethanesulfonate (Me_3SiOTf) surprisingly resulted in no shift of the phosphorus signal in the $^{31}\text{P}\{^1\text{H}\}$ NMR spectrum. X-ray quality crystals of **2.6** were grown from a concentrated CH_2Cl_2 solution of **2.6** layered with CH_3CN , and subsequent diffraction experiments revealed the 1:2 stoichiometric reaction of diamine:phosphine occurred and explained the apparent lack of reactivity upon the addition of the halide-abstracting agent (Scheme 2.3, Figure 2.3).

Utilizing the ligand **2.5^{Dipp}** yielded differing results from that of **2.4^{Mes}**, where a 3:1:1 stoichiometric amount of NMM, PCl_3 and **2.5^{Dipp}** was stirred for 3 h at -78°C and then warmed to rt. and stirring was continued for 48 h. The reaction progress was monitored by $^{31}\text{P}\{^1\text{H}\}$ NMR spectroscopy, where two separate singlets emerged as the reaction proceeded ($\delta_{\text{p}} = 152$ and $\delta_{\text{p}} = 155$). The signal slightly upfield ($\delta_{\text{p}} = 152$) was tentatively assigned to the 1:1 stoichiometric reaction of PCl_3 with the diamine (**2.5^{Dipp}**), ultimately yielding the cyclic diaminochlorophosphine (**2.7**) in 80 % yield. The more downfield

signal ($\delta_p = 155$), was assigned to the 2:1 reaction between PCl_3 and the diamine(**2.5^{Dipp}**), giving the bis(amino)dichlorophosphine (**2.8**), which was later confirmed by single crystal X-ray diffraction experiments and isolated in 20% yield. Compounds **2.7** and **2.8** had similar solubilities and the separation of compound **2.7** from **2.8** proved to be very difficult. However, by changing the solvent to toluene and slowing the addition of a 0.043 M toluene solution of PCl_3 (1 ml/h over 10 h), the selective synthesis of the cyclic diaminochlorophosphine, (**2.7**) was achieved in 90% isolated yield. Subsequent dehalogenation of **2.7** proceeded when an excess of Me_3SiOTf was added. An aliquot from the reaction solution was examined by $^{31}\text{P}\{^1\text{H}\}$ NMR spectroscopy where the original phosphorus signal ($\delta_p = 152$) was no longer present, and a new peak appeared further downfield ($\delta_p = 257$), which was tentatively assigned to the phosphonium cation (**2.9**). The reaction mixture was then concentrated and washed with Et_2O leaving behind a white powder. A sample of the bulk powder was redissolved and examined by multinuclear NMR spectroscopy. The $^{31}\text{P}\{^1\text{H}\}$ spectrum revealed a single peak ($\delta_p = 257$) consistent with the *in situ* formation of the phosphonium cation (Scheme 2.3, Figure 2.3).



Scheme 2.3: Synthesis of compounds **2.6**, **2.7**, **2.8** and **2.9**; (a) NMM, PCl_3 , -78°C - rt.; (b) Me_3SiOTf , CH_2Cl_2 , rt.

2.2.2 Photophysical properties

The UV-visible absorption spectra of compounds **2.2** - **2.9** are shown in Figure 2.2, with the λ_{max} and the extinction coefficients listed in Table 2.1. Compounds **2.2** - **2.9** were all white to light yellow in colour and had λ_{max} values in the range of 220 - 240 nm, attributed to both $\pi - \pi^*$ and $n - \pi^*$ transitions. There was little variation in the UV-vis absorption spectra between the different compounds and the photophysical properties were dominated by the thiophene functionality in the backbone with no considerable influence from the phosphorus atom.

Table 2.1: UV-visible absorption and extinction coefficients of compounds **2.2** - **2.9**.

Compound	λ nm (ϵ M ⁻¹ cm ⁻¹)	Compound	λ nm (ϵ M ⁻¹ cm ⁻¹)
2.2^{Mes}	240 nm (2.5×10^4) 332 nm (2.8×10^3)	2.6	226 nm (2.5×10^4)
2.3^{Dipp}	242 nm (2.8×10^4) 333 nm (2.1×10^3)	2.7	240 nm (1.8×10^4) 270 nm (7.9×10^2)
2.4^{Mes}	223 nm (1.6×10^4) 242 nm (1.6×10^4) 289 nm (2.4×10^3)	2.8	226 (1.9×10^4)
2.5^{Dipp}	241 nm (1.0×10^4) 281 nm (2.0×10^3)	2.9	226 nm (7.1×10^3) 241 nm (4.1×10^3)

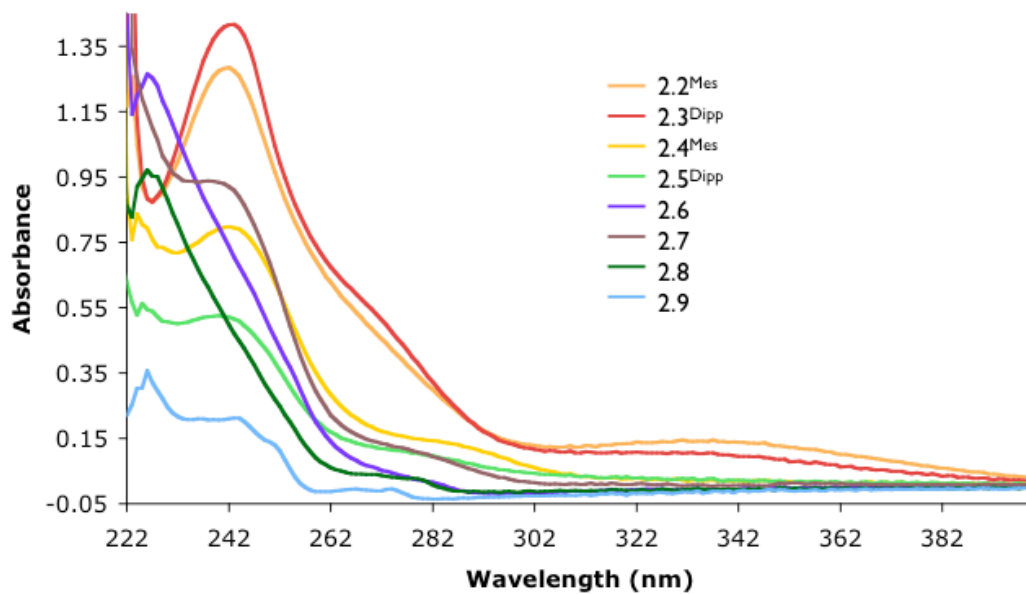


Figure 2.2: UV-Visible spectrum of compounds **2.2** - **2.9** in a 5×10^{-5} M CH_2Cl_2 solution.

2.2.3 X-ray crystallography

Single crystals of compounds **2.2^{Mes}**, **2.5^{Dipp}**, **2.6**, **2.8** and **2.9** were grown by either vapor diffusion using various solvent combination or from concentrated solutions of CH₂Cl₂ layered with either CH₃CN or hexanes. Their solid-state structures were determined by X-ray diffraction studies and the relevant crystallographic data and metrical parameters are detailed in Table 2.2, Table 2.3 and Figure 2.3.

Table 2.2: Crystal data for compounds **2.2^{Mes}**, **2.5^{Dipp}**, **2.6**, **2.8** and **2.9**.

	2.2^{Mes}	2.5^{Dipp}	2.6	2.8	2.9
Empirical formula	C ₂₄ H ₂₆ N ₂ S ₁	C ₃₀ H ₃₈ N ₂ S ₁	C ₂₄ H ₂₈ N ₂ S ₁ Cl ₄ P ₂	C ₃₀ H ₄₀ N ₂ S ₁ Cl ₄ P ₂	C ₃₁ H ₄₀ N ₂ S ₂ F ₃ O ₃ P ₁
FW (g/mol)	374.53	462.72	580.28	664.44	640.74
Crystal system	Monoclinic	Monoclinic	Triclinic	Triclinic	Triclinic
Space group	P2 ₁ /c	C2/c	P $\bar{1}$	P $\bar{1}$	P $\bar{1}$
a (Å)	8.1158(16)	26.1861(19)	9.5478(19)	9.983(2)	10.227(3)
b (Å)	15.946(3)	13.3921(7)	10.435(2)	13.907(3)	10.949(4)
c (Å)	16.190(3)	16.4080(9)	14.707(3)	25.630(5)	15.625(5)
α (deg)	90	90	84.69(3)	75.91(3)	75.021(9)
β (deg)	91.76(3)	106.997(5)	80.09(3)	84.28(3)	75.056(9)
γ (deg)	90	90	75.51(3)	83.86(3)	85.202(9)
V (Å ³)	2094.2(7)	5502.7(6)	1395.6(5)	3421.3(12)	1632.8(9)
Z	4	8	2	4	2
D _c (mg m ⁻³)	1.188	1.107	1.361	1.290	1.303
R _{int}	0.0631	0.0469	0.0490	0.0546	0.0419
R1[I > 2σI] ^a	0.0882	0.0774	0.0884	0.0957	0.0618
wR2(F ²) ^a	0.1959	0.1532	0.1934	0.1627	0.0908
GOF(S) ^a	1.069	0.868	1.060	0.974	1.023

^aR1(I > 2σI) = $\sum ||F_o| - |F_c|| / \sum |F_o|$; ^awR2(F² [all data]) = $[w(F_o^2 - F_c^2)^2]^{1/2}$; S(all data) = $[w(F_o^2 - F_c^2)^2 / (n - p)]^{1/2}$ (n = no. of data; p = no. of parameters varied; w = 1/[σ²(F_o²) + (aP)² + bP] where P = (F_o² + 2F_c²)/3 and a and b are constants suggested by the refinement.

Examination of the solid-state structure of compound **2.2^{Mes}** shows that the C - N bond is consistent with a double bond (1.270(4) Å) corresponding to the diimine, and upon reduction to **2.5^{Dipp}**, the C - N bond is reduced to a single bond and an increase in bond length (1.464(3) Å avg.) is observed in comparison to **2.2^{Mes}**. A comparison of the metrical parameters for compound **2.6** and **2.8** reveal that the P - Cl bond lengths range from 2.0725(13) - 2.1047(14) Å, which are similar to other dichlorophosphines, however much shorter compared to previously synthesized cyclic diaminochlorophosphines, where the P - Cl bonds can range from 2.2 - 2.7 Å.²⁴ These short P - Cl bonds can explain the lack of reactivity with halide abstracting agents observed in both compounds **2.6** and **2.8**.²⁵

The solid-state structure of compound **2.9** revealed a well separated cation-anion pair with the distance between the oxygen and phosphorus being 3.8 Å, well outside the van der Waals radii for P - O ($\sum_{vdw} = 3.3$ Å). The P(1) - N(1) bond is 1.645(2) Å which is slightly shorter than compounds **2.6** and **2.7**, however is consistent with other NHPs reported in the literature. The bond angle between the N(1) - P(1) - N(2) is 111.28(8)° and is much larger than those reported for 5-membered and 6-membered NHPs, which are approximately 90° and 105°. In the solid-state the thiophene ring sits at a 110.80(5)° angle from the C₂N₂P ring in an open book conformation.

Table 2.3: Selected bond lengths (Å) and angles (°).

Bond	Compound				
	2.2^{Mes}	2.5^{Dipp}	2.6	2.8[§]	2.9
N(1) - C(8)	1.270(4)	1.463(2)	1.486(4)	1.493(3)	1.514(2)
N(2) - C(5)	1.270(4)	1.466(2)	1.487(3)	1.493(3)	1.508(2)
P - Cl (avg.)	-	-	2.095(2)	2.090(3)	-
N(1) - P(1)	-	-	1.645(2)	1.651(2)	1.6260(16)
N(2) - P(1)	-	-	1.647(3)	1.645(2)	1.6228(16)
N - P - Cl (avg.)	-	-	103.07(18)	103.1(2)	-
N(1) - P(1) - N(2)	-	-	-	-	111.28(8)

§Metrical parameters for only one of two molecules present in the asymmetric unit.

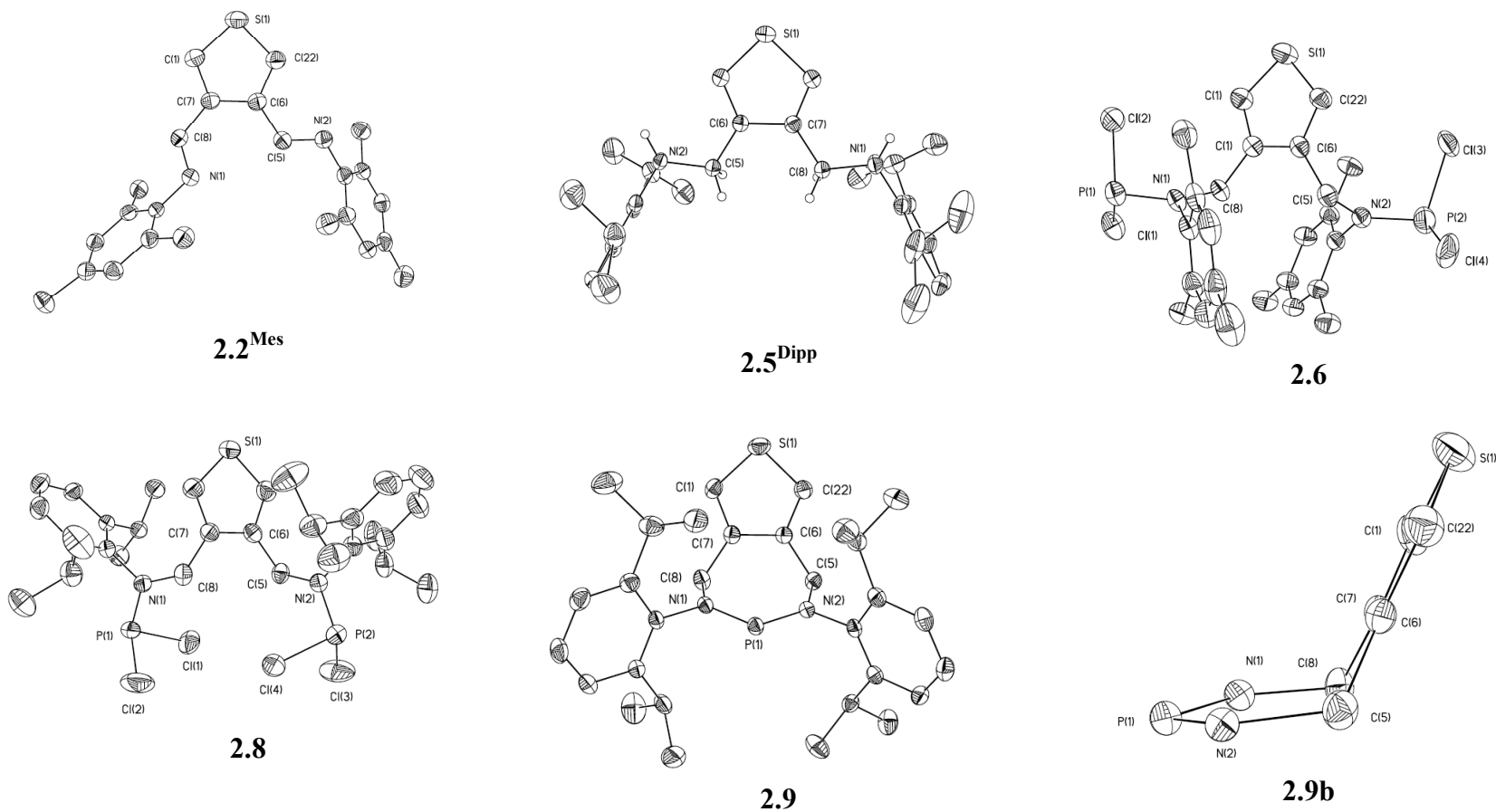


Figure 2.3: Solid-state structures of compounds **2.2^{Mes}**, **2.5^{Dipp}**, **2.6**, **2.8** and **2.9**. Thermal ellipsoids are drawn to 50% probability and hydrogen atoms have been omitted for clarity. Compound **2.9**, the triflate anion has been omitted for clarity and a side on view of the molecule is shown in **2.9b** in which the Dipp groups have been omitted.

2.2.4 Conclusions

A new class of thiophene substituted diimine (**2.2**^{Mes} and **2.3**^{Dipp}) and diamine (**2.4**^{Mes} and **2.5**^{Dipp}) ligands have been synthesized and their reactivity with PCl₃ was explored. Due to the inherent flexibility of the seven-membered ring system there were difficulties controlling the degree of substitution at phosphorus. When Ar = Mes a 1:2 stoichiometry of diamine:phosphine was observed (i.e. compound **2.6**), however when Ar = Dipp both the 1:1 (**2.7**) and 1:2 (**2.8**) products were isolated. When the solvent was changed from THF to toluene and the rate of addition of PCl₃ to **2.2**^{Dipp} was decreased, the cyclic diaminochlorophosphine (**2.7**) was successfully isolated. Compound **2.7** can be converted to the NHP using the halide abstraction/metathesis reagent Me₃SiOTf, where the isolation and solid-state structure of a seven-membered NHP (**2.9**) was achieved. The thiophene ring in the backbone dominated the photophysical properties of these compounds and there was very little variation in the UV-visible spectrum.

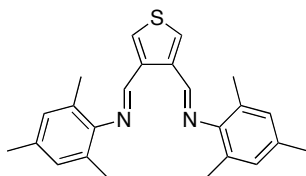
2.3 Experimental

2.3.1 General experimental

General synthetic and crystallography experimental details can be found in Appendix 1.

2.3.2 Synthetic procedures

Compound **2.2**^{Mes}



To a 20 mL EtOH solution of 3,4-diformylthiophene (1.00 g, 7.24 mmol), 2, 4, 6-trimethylaniline (1.93 g, 14.28 mmol) was added. The solution turned dark orange and a yellow solid precipitated from the reaction mixture. The reaction was stirred overnight at rt. and the yellow powder isolated by filtration. The product was washed with 5 x 5 mL of cold EtOH.

Yield: 76 % (2.51 g, 5.46 mmol);

m.p.: 192 - 194 °C;

¹H NMR (CDCl₃ δ (ppm)): δ 8.72 (s, 2H), 8.00 (s, 2H, thienyl), 6.86 (s, 4H, aryl), 2.26 (s, 6H, methyl), 2.12 ppm (s, 12H, methyl);

$^{13}\text{C}\{^1\text{H}\}$ NMR (CDCl_3 δ (ppm)): 158.0, 148.6, 138.5, 132.9, 130.6, 128.6, 126.9, 20.7, 18.3 ppm;

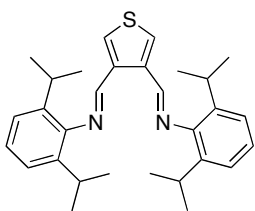
FT-IR (ranked intensity (cm^{-1})): 733(13), 819(2), 859(8), 878(12), 1138(9), 1174(5), 1212(6), 1448(15), 1476(3), 1513(10), 1629(1), 2859(4), 2916(11), 3078(7), 3100(14);

FT-Raman (ranked intensity (cm^{-1})): 124(4), 573(6), 1139(7), 1174(5), 1213(15), 1297(10), 1354(8), 1379(14), 1405(11), 1449(12), 1513(3), 1604(2), 1628(2), 2918(9), 3078(13);

HRMS: ($\text{C}_{24}\text{H}_{26}\text{N}_2\text{S}$) Calcd (found) 374.1817 (374.1824);

λ_{max} : 242 nm ($2.8 \times 10^4 \text{ M}^{-1}\text{cm}^{-1}$), 269 (sh) nm ($1.1 \times 10^4 \text{ M}^{-1}\text{cm}^{-1}$) 333 (sh) nm ($1.1 \times 10^3 \text{ M}^{-1}\text{cm}^{-1}$).

Compound 2.3^{Dipp}



To a 20 mL EtOH solution of 3,4-diformylthiophene (1.00 g, 7.24 mmol), 2, 6-diisopropylaniline (2.65 g, 14.28 mmol) was added. The solution turned dark orange and a yellow solid precipitated from the reaction mixture. The reaction was stirred overnight at rt. and the yellow powder isolated by filtration. The product was then washed with 5 x 5 mL of cold EtOH.

Yield: 80 % (2.13 g, 5.60 mmol);

m.p.: 139-141 °C;

^1H NMR (CDCl_3 δ (ppm)): 8.72 (s, 2H), 8.04 (s, 2H, thienyl), 7.08 (m, 6H, aryl), 2.94 (sept, 4H, $^3J_{\text{HH}} = 6.8$ Hz), 1.10 (d, 24H, $^3J_{\text{HH}} = 6.8$ Hz);

$^{13}\text{C}\{^1\text{H}\}$ NMR (CDCl_3 δ (ppm)): 157.8, 149.5, 138.8, 137.9, 131.7, 124.6, 123.4, 28.4, 23.9;

FT-IR (ranked intensity (cm^{-1})): 758(7), 796(11), 822(3), 851(3), 876(12), 933(16), 1166(5), 1323(9), 1384(10), 1435(4), 1470(15), 1513(8), 1634(1), 2962(2), 3074(14);

FT-Raman (ranked intensity (cm^{-1})): 169(13), 273(2), 528(6), 799(3), 857(11), 957(1), 1042(12), 1110(8), 1159(4), 1247(14), 2861(9), 2905(7), 2937(5), 2961(15), 3089(10);

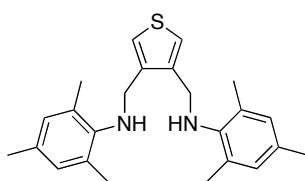
HRMS: ($\text{C}_{30}\text{H}_{28}\text{N}_2\text{S}$) Calcd (found) 458.2756 (458.2764);

λ_{max} : 240 nm ($2.5 \times 10^4 \text{ M}^{-1}\text{cm}^{-1}$), 273 (sh) nm ($8.7 \times 10^3 \text{ M}^{-1}\text{cm}^{-1}$) 332 (sh) nm ($2.8 \times 10^3 \text{ M}^{-1}\text{cm}^{-1}$).

General synthesis for compounds **2.4^{Mes}** and **2.5^{Dipp}**

Solid LiAlH₄ (0.25 g, 6.55 mmol) was added portion wise to a 50 mL Et₂O solution of diimine, 1.00 g (2.18 mmol). The suspension was stirred overnight at rt. Excess LiAlH₄ was quenched with 10 mL of a 10% KOH_(aq) solution. The salts were removed by filtration and the colourless filtrate was dried over MgSO₄ and concentrated under reduced pressure to obtain the diamine.

Compound **2.4^{Mes}**



Yield: 85 % (0.86 g, 2.26 mmol);

m.p.: 104-105 °C;

¹H NMR (CDCl₃ δ (ppm)): 7.23 (s, 2H, thienyl), 7.83 (s, 4H, aryl), 4.03 (s, 4H, alkyl), 2.24 (s, 6H, methyl), 2.22 (s,

12H, methyl);

¹³C NMR (CDCl₃ δ (ppm)): 143.1, 139.9, 131.7, 130.2, 129.4, 123.4, 46.7, 20.5, 18.2;

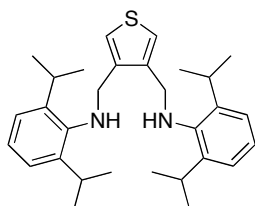
FT-IR (ranked intensity (cm⁻¹)): 569(8), 698(13), 756(15), 804(2), 856(7), 1025(14), 1065(5), 1154(9), 1226(3), 1300(10), 1329(12), 1480(1), 2910(4), 3108(11), 3348(6);

FT-Raman (ranked intensity (cm⁻¹)): 139(15), 492(12), 576(1), 841(14), 957(9), 1066(11), 1155(13), 1228(8), 1301(3), 1379(5), 1446(7), 1608(4), 2912(2), 30109(10);

HRMS: (C₂₄H₂₈N₂S) Calcd (found): 378.2130 (378.2139);

λ_{max}: 223 nm (1.6 x 10⁴ M⁻¹cm⁻¹) 242 nm (1.6 x 10⁴ M⁻¹cm⁻¹), 289 (sh) nm (2.4 x 10⁻³ M⁻¹cm⁻¹).

Compound **2.5^{Dipp}**



Yield: 80 % (0.81 g, 1.75 mmol)

m.p.: 109 - 110 °C.

¹H NMR (CDCl₃ δ (ppm)): 7.34 (s, 2H, thienyl), 7.10 (m, 6H, aryl), 4.03 (s, 4H, alkyl), 3.26 (sept., 4H, ³J_{HH} = 6.8 Hz), 1.23 (d, 24H, ³J_{HH} = 6.8 Hz);

¹³C{¹H} NMR (CDCl₃ δ (ppm)): 143.6, 143.1, 139.8, 124.4, 123.8, 123.2, 50.3, 28.0, 24.5;

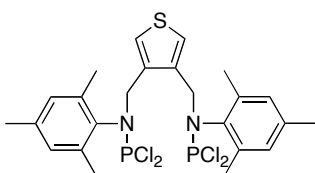
FT-IR (ranked intensity (cm⁻¹)): 527(9), 573(11), 732(1), 803(5), 856(8), 932(7), 1055(4), 1114(13), 1195(6), 1258(14), 1302(10), 1382(12), 1459(3), 2961(2), 3090(15);

FT-Raman (ranked intensity (cm⁻¹)): 150(4), 170(5), 222(10), 273(14), 677(9), 857(13), 889(8), 1043(12), 1248(11), 1448(6), 1590(7), 2908(2), 2936(1), 2960(3);

HRMS: (C₃₀H₃₂N₂S) Calcd (found) 462.3069 (462.3065).

λ_{max}: 241 nm (1.0 x 10⁴ M⁻¹cm⁻¹) 281 (2.0 x 10³ M⁻¹cm⁻¹).

Compound 2.6



A 20 mL THF solution of PCl₃ (0.11 mL, 1.33 mmol) was cooled to -78 °C. A 10 mL THF solution of **3^{Mes}** (0.50 g, 1.33 mmol) was then added dropwise *via* cannula and a white precipitate formed immediately. The reaction mixture stirred at -78 °C for 2 h, then warmed to rt. and then stirred at rt. for 15 h. The white precipitate was removed by centrifuge and the resulting colorless solution was concentrated. The resulting oil was then triturated with CH₃CN resulting in the formation of a white precipitate. The CH₃CN was decanted and the resulting product dried under vacuum.

Yield: 34 % (0.23 g, 0.45 mmol);

m. p.: 125 - 128 °C;

¹H NMR (CDCl₃ δ (ppm)): 6.99 (s, 2H, thienyl), 6.83 (s, 4H, aryl), 4.04 (d, 4H, ³J_{HP} = 2.8 Hz alkyl), 2.27 (s, 3H, methyl), 2.26 (s, 3H, methyl), 1.87 (s, 6H, methyl), 1.86 (s, 6H, methyl);

¹³C{¹H} NMR (CDCl₃ δ (ppm)): 138.7, 136.0, 135.5, 129.8, 128.7, 127.5, 44.4 (d, ²J_{C-P} = 28.0 Hz), 20.9, 18.6;

³¹P{¹H} NMR (CDCl₃ δ (ppm)): 153.8;

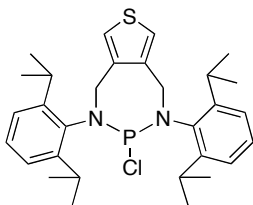
FT-IR (ranked intensity (cm⁻¹)): 434(10), 481(5), 508(12), 525(4), 568(2), 683(8), 808(3), 855(11), 883(6), 1061(1), 1120(13), 1207(7), 1346(15), 1474(9), 2917(14);

FT-Raman (ranked intensity (cm⁻¹)): 191(5), 240(1), 418(12), 456(3), 513(2), 560(15), 574(6), 633(9), 859(14), 1178(11), 1307(4), 1379(10), 1606(8), 2917(7), 3112(3);

λ_{max}: 224 nm (2.5 x 10⁴ M⁻¹cm⁻¹).

Elemental Analysis (%) Calcd for C₂₄H₂₈N₂S₁Cl₄P₂: C 49.67, H 4.86, N 4.83, S 5.53
found C 50.11, H 5.12, N 4.84, S 5.72.

Compound 2.7



A 10 mL toluene solution of **5** (0.20 g, 0.43 mmol) was cooled to -78°C in a dry ice/acetone bath. To this a 10 mL toluene solution of PCl₃ (34 μL, 0.43 mmol) was added via syringe pump at a rate of 1 mL/h. The reaction mixture was then warmed to rt. and stirred for 24 h. Upon completion the reaction was concentrated under reduced pressure and then taken up in 10 mL of Et₂O. The Et₂O solution was then centrifuged to remove the ammonium salt and was then concentrated yielding the desired product.

Yield: 90 % (0.22 g, 0.38 mmol);

m.p.: 98 -100 °C;

¹H NMR (CDCl₃ δ (ppm)): 7.33 (s, 2H, thienyl), 7.11(m, 6H, aryl), 4.04 (d, 4H, ³J_{H-P}=7.37 Hz, alkyl), 3.26 (sept. 4H, ³J_{HH} = 6.8 Hz), 1.14 (d, 24 H, ³J_{HH} = 6.8 Hz);

¹³C{¹H} NMR (CDCl₃ δ (ppm)): 147.4, 134.9 134.2, 131.4, 126.7, 125.4, 58.8, 28.7, 25.1, 24.2;

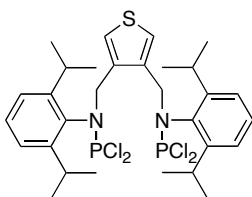
³¹P{¹H} NMR (CDCl₃ δ (ppm)): 152.2;

FT-IR (ranked intensity (cm⁻¹)): 526(5), 573(8), 731(10), 802(2), 932(13), 1055(4), 1113(14), 1194(7), 1258(6), 1302(15), 1382(11), 1459(3), 1587(9), 2961(1), 3090(12);

FT-Raman (ranked intensity (cm⁻¹)): 149(4), 169(9), 274(15), 676(8), 857(10), 889(5), 1042(7), 1110(11), 1247(6), 1446(2), 1589(3), 2862(13), 2906(14), 2961(1), 3089(12);

λ_{max}: 240 nm (1.8 x 10⁴ M⁻¹cm⁻¹), 280 (sh) nm (2.1 x 10³ M⁻¹cm⁻¹).

Compound 2.8



A 10 mL Et₂O solution of **4** (0.20 g, 0.43 mmol) was cooled to -78 °C. To this a 10 mL Et₂O solution of PCl₃ was added dropwise *via* cannula. A white precipitate formed immediately and the reaction mixture stirred -78 °C for 2 h. The reaction was then warmed to rt. and left to stir for an additional 24 h. Upon completion the solvent was removed in *vacuo* leaving an orange residue, which was

then taken up in CH₃CN. The orange solution was then concentrated again under reduced pressure yielding a yellow solid. The yellow solid was washed with 3 x 5 mL of CH₃CN yielding the product as a white solid.

Yield: 42 % (0.12 g, 0.18 mmol);

m.p.: 157 - 159 °C,

¹H NMR (CDCl₃ δ (ppm)): 7.21 (m, 2H, aryl), 7.03 (d, 4H, ³J_{HH} = 7.6 Hz, aryl), 6.30 (s, 2H, thienyl), 4.61 (d, 4H, ³J_{HP} = 2.4 Hz, alkyl), 2.79 (sept. 4H, ³J_{HH} = 6.8 Hz), 1.02 (d, 12H, ³J_{HH} = 6.8 Hz), 0.90 (d, 12H, ³J_{HH} = 6.8 Hz);

¹³C{¹H} NMR (CDCl₃ δ (ppm)): 149.9, 135.4, 134.1, 129.4, 126.7, 124.3, 46.3 (²J_{C-P} = 28.4 Hz), 28.8, 26.7, 22.6;

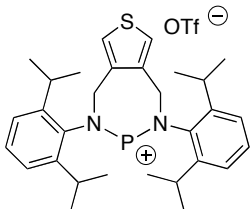
³¹P{¹H} NMR (CDCl₃ δ (ppm)): 154.8;

FT-IR (ranked intensity (cm⁻¹)): 454(10), 515(7), 637(2), 692(15), 751(14), 810(5), 857(9), 895(13), 1028(3), 1113(11), 1169(8), 1256(1), 1467(6), 1587(12), 2970(4);

λ_{max} = 226 nm (1.9 x 10⁴ M⁻¹cm⁻¹), 270 (sh) nm (7.9 x 10² M⁻¹cm⁻¹);

HRMS: (C₃₀H₄₀SN₂Cl₄P₂) Calcd (found) : 662.1142 (662.1135).

Compound 2.9



To a 5 mL CH₂Cl₂ of **5** (0.200 g, 0.38 mmol) neat (CH₃)₃SiOTf (0.20 mL, 0.114 mmol) was added. The reaction mixture stirred at rt. for 2 h until all of the chlorophosphine was converted to the phosphonium cation. Upon completion the reaction mixture was concentrated under reduced pressure yielding a white solid. The

product was then washed with 3 x 5 ml of Et₂O and dried under vacuum.

Yield: 51 % (0.08 g, 0.12 mmol);

m.p.: 260 - 263 °C;

¹H NMR (CDCl₃ δ (ppm)): 7.36 (t, 2H, ³J_{HH} = 8 Hz, aryl), 7.27 (s, 2H, thienyl), 7.19 (d, 4H, ³J_{HH} = 8 Hz, aryl), 5.48 (br. s, 4H, alkyl), 3.18 (br. sept., 4H), 1.28 (d, 12H, ³J_{HH} = 6.8 Hz), 1.07 (d, 12H, ³J_{HH} = 6.8 Hz);

¹³C{¹H} (CDCl₃ δ (ppm)): 147.4, 134.9, 134.2, 131.4, 126.7, 125.4, 58.8, 28.7, 25.1, 24.2;

³¹P{¹H} (CDCl₃ δ (ppm)): 257.1;

FT-IR (ranked intensity (cm⁻¹)): 454(10), 515(7), 637(2), 692(15), 751(14), 810(5), 857(9), 895(13), 1028(3), 1113(11), 1169(8), 1256(1), 1467(6), 1587(12), 2970(4);

FT-Raman (ranked intensity (cm⁻¹)): 201(10), 308(8), 693(1), 720(11), 882(7), 1027(3), 1043(6), 1116(2), 1239(5), 1586(4), 2870(9), 2980(12);

λ_{max}: 224 nm (7.1 x 10³ M⁻¹cm⁻¹), 241 nm (4.1 x 10³ M⁻¹cm⁻¹)

Elemental Analysis (%) calc for C₃₁H₄₀F₃O₃N₂S₂P₁: C 57.88, H 6.51, N 4.38, S 10.07 found C 58.11, H 6.29, N 4.37, S 10.01.

2.4 References

- (1) Crudden, C. M.; Allen, D. P. *Coord. Chem. Rev.* **2004**, *248*, 2247-2273.
- (2) Hahn, F. E.; Jahnke, M. C. *Angew. Chem., Int. Ed.* **2008**, *47*, 3122-3172.
- (3) Mercs, L.; Albrecht, M. *Chem. Soc. Rev.* **2010**, *39*, 1903-1912.
- (4) Peris, E.; Crabtree, R. H. *Coord. Chem. Rev.* **2004**, *248*, 2239-2246.
- (5) Trnka, T. M.; Grubbs, R. H. *Acc. Chem. Res.* **2001**, *34*, 18-29.
- (6) Arduengo, A. J., III; Harlow, R. L.; Kline, M. *J. Am. Chem. Soc.* **1991**, *113*, 361-363.
- (7) Gudat, D.; Haghverdi, A.; Hupfer, H.; Nieger, M. *Chem. Eur. J.* **2000**, *6*, 3414-3425.
- (8) Cowley, A. H.; Kemp, R. A. *Chem. Rev.* **1985**, *85*, 367-382.
- (9) Tuononen, H. M.; Roesler, R.; Dutton, J. L.; Ragogna, P. J. *Inorg. Chem.* **2007**, *46*, 10693-10706.
- (10) Caputo, C. A.; Jennings, M. C.; Tuononen, H. M.; Jones, N. D. *Organometallics* **2009**, *28*, 990-1000.
- (11) Romero-Nieto, C.; Durben, S.; Kormos, I. M.; Baumgartner, T. *Adv. Funct. Mater.* **2009**, *19*, 3625-3631.
- (12) Scheer, M.; Balazs, G.; Seitz, A. *Chem. Rev.* **2010**, *110*, 4236-4256.
- (13) Stephan, D. W. *Dalton Trans.* **2009**, *17*, 3129-3136.
- (14) Holthausen, M. H.; Weigand, J. J. *J. Am. Chem. Soc.* **2009**, *131*, 14210-14211.
- (15) Chen, C.; Roland, F.; Kehr, G.; Erker, G. *Chem. Commun.* **2010**, *46*, 3580-3582.

- (16) Perepichka, I. R.; Perepichka, D. F.; Meng, H.; Wudl, F. *Adv. Mater.* **2005**, *17*, 2281-2305.
- (17) Wolf, M. *Adv. Mater.* **2001**, *13*, 545-553.
- (18) Price, J. T.; Jones, N. D.; Ragogna, P. J. *Inorg. Chem.* **2012**, *51*, 6776 - 6783.
- (19) Price, J. T.; Lui, M.; Jones, N. D.; Ragogna, P. J. *Inorg. Chem.* **2011**, *50*, 12810-12817.
- (20) Powell, A. B.; Brown, J. R.; Vsudevan, K. V.; Cowley, A. H. *Dalton Trans.* **2009**, 2521-2527.
- (21) Powell, A. B.; Bielawski, C. W.; Cowley, A. H. *J. Am. Chem. Soc.* **2009**, *131*, 18232-18233.
- (22) Powell, A. B.; Bielawski, C. W.; Cowley, A. H. *J. Am. Chem. Soc.* **2010**, *132*, 10184-10194.
- (23) Caputo, C. A.; Price, J. T.; Jennings, M. C.; McDonald, R.; Jones, N. D. *Dalton Trans.* **2008**, 3461-3469.
- (24) Niecke, E.; Kröher, R. *Angew. Chem. Int. Ed.* **1976**, *15*, 692-693.
- (25) Brazeau, A. L.; Hänninen, M. M.; Tuononen, H. M.; Jones, N. D.; Ragogna, P. J. *J. Am. Chem. Soc.* **2012**, *134*, 5398-5414.
- (26) Powell, A. B.; Brown, J. R.; Vasudevan, K. V.; Cowley, A. H. *Dalton Trans.* **2009**, 2521-2527.

Chapter 3

3 Group 15 cations supported by a benzo[1,2-b:5,6-b']dithiophene core^Ω

3.1 Introduction

The current renaissance in p-block chemistry has borne witness to some remarkable developments for the main group elements, with many of the breakthroughs centering on new structure, bonding and reactivity.¹⁻⁷ An emerging tenet in this area of research is to use these novel molecules and their unique reactivity to bridge the gap into functional or applied chemical processes. Excellent examples have surfaced in the last few years including efforts in OLEDs, catalysis and small molecule activation.⁵⁻¹⁰ One of the limitations to further expanding p-block chemistry into the realm of the applied, has been the challenge of developing novel ligand frameworks with which to support low coordinate and low oxidation state main group element centres. New directions could be realized by installing various functionalities onto these supporting ligands and by taking advantage of the inherent electronic influence as well as the chemical versatility of the p-block elements. Combined, these can have a significant impact on the resulting materials that are not always possible in exclusively organic functionalized systems.^{7,11}

It has been well established that thiophene based materials lend themselves to the design of tunable, light emitting polymers and materials.¹² Related efforts in this area by other research groups have realized the synthesis of both a poly(thiophene) with orthogonal carbenes and a redox active thiophene substituted diazabutadiene ligand for the construction of phosphenium cations.¹³⁻¹⁵ Although each development is novel, a key drawback to the utility of these systems has been the lack of conjugation between the thiophene rings and the rest of the molecule. In this context, we have undertaken an effort to model a wholly new ligand system where two contiguous thiophene rings occupy the supporting backbone (Figure 3.1). The corresponding diaminochloropnictine and pnictenium cations (Pn = P, As, Sb) were readily

^Ω A version of this chapter has been published in Price, J. T., Lui, M., Jones, N. D. and Ragona, P. J., *Inorg. Chem.*, **2011**, *50*, 12810 and has been reproduced with permission.

synthesized using established dehydrohalogen coupling protocols between diamine ligands and p-block halides in high yields, and a platinum complex of both the phosphonium and arsenium cation were prepared. These achievements represent a unique opportunity to bring together the known and emerging chemistry of low coordinate p-block cations, with the alluring photophysical properties of thiophene based materials.

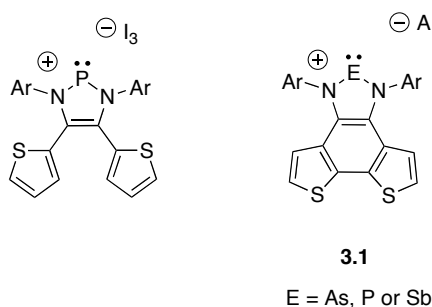
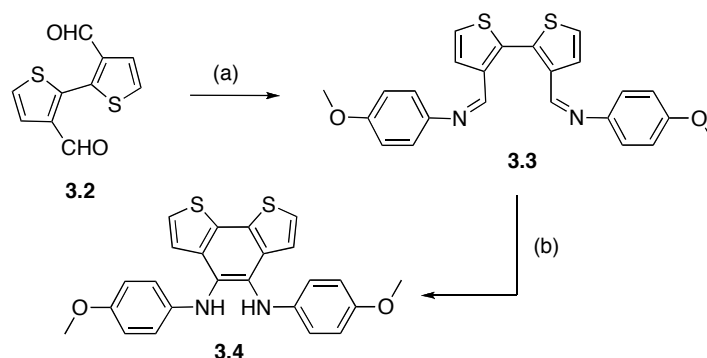


Figure 3.1: Previously reported phosphonium cation with the triiodide counter ion and the reported new pnictenium cations (**3.1**).

3.2 Results and Discussion

3.2.1 Synthesis

Our entry into the new thiophene-based systems (Scheme 3.1) rested on the known 2,2'-dithiophene-3,3'-biscarboxaldehyde (**3.2**).¹⁶



Scheme 3.1: Synthesis of **3.4**. (a) *p*-OMe-C₆H₄NH₂, EtOH, reflux 4 h, 82%; (b) NaCN, DMF, rt. 48 h, 80 %.

Compound **3.3** was prepared by a condensation reaction between a yellow ethanolic suspension of **3.2** with 2.1 stoichiometric equivalents of *p*-anisidine. Upon addition of the amine, the solution turned from yellow to black and during the 4 h reflux a

yellow solid precipitated. The slurry was then cooled to rt. and the yellow solid was isolated by filtration. The ^1H NMR spectrum of the redissolved yellow powder revealed the disappearance of the aldehyde proton ($\delta_{\text{H}} = 9.85$) and the appearance of a singlet ($\delta_{\text{H}} = 8.38$) consistent with an imine, along with the protons corresponding to the *p*-MeOPh group. A benzoin condensation of the diimine to form the corresponding diamine target (**3.4**) was carried out by the addition of DMF to solid NaCN and **3.3**. The mixture immediately became dark green, and was stirred at rt. for 2 days. The reaction mixture was diluted with CH_2Cl_2 and washed with water. Removal of the volatiles and the subsequent addition of MeOH caused precipitation of a bright orange solid. A sample of the bulk material was redissolved for ^1H NMR spectroscopy, which revealed the disappearance of the imine proton and no significant change in the aryl groups, indicating that the condensation was likely successful. Single crystals suitable for X-ray diffraction studies (Figure 3.5) were grown from a solution of MeOH at rt. confirming the successful synthesis of **3.4**, isolated in 86 % yield.

A 3:1:1 stoichiometric reaction between N-methylmorpholine (NMM), PCl_3 and **3.4** in THF resulted in an immediate colour change from brown/orange to a bright orange. The reaction was monitored by $^{31}\text{P}\{^1\text{H}\}$ NMR spectroscopy, which showed the reaction was complete after 4 days by the disappearance of PCl_3 ($\delta_{\text{p}} = 220$) and the appearance of a new peak ($\delta_{\text{p}} = 136$) which was tentatively assigned to the chlorophosphine **3.5**. X-ray quality, orange crystals were grown by $\text{CH}_2\text{Cl}_2/n$ -pentane vapour diffusion at rt. and subsequent X-ray diffraction analysis confirmed the production of the cyclic diaminochlorophosphine (**3.5**), isolated in 83 % yield (Figure 3.3). The corresponding diaminochloroarsine, **3.6** was synthesized using a similar procedure of a 3:1:1 stoichiometric reaction between NMM, AsCl_3 and **3.4** in THF, and resulted in a slight colour change of the solution from orange to red. The reaction was complete after 4 days, denoted by the proton shifts in the ^1H NMR spectrum (Scheme 3.2, B). The protons from the thiophene ring shifted significantly upfield **3.6** ($\delta_{\text{H}} = 7.04$ and 6.20), compared to the proligand **3.4** ($\delta_{\text{H}} = 7.18$ and 7.04), whereas the resonances in the phenyl rings were further split in compound **3.6** ($\delta_{\text{H}} = 7.48$ and 6.98 ; $\Delta\delta = 0.50$) compared to the free ligand, **3.4** ($\delta_{\text{H}} = 6.69$ and 6.59 ppm; $\Delta\delta = 0.10$). Another indication that the desired chloroarsine was synthesized was the disappearance of the NH peak in the ^1H NMR spectrum ($\delta_{\text{H}} = 5.63$) shown in Figure

3.2, C. X-ray quality, orange crystals were grown by CH₂Cl₂/pentane liquid diffusion at rt. and subsequent X-ray analysis confirmed the production of **3.6** isolated in 54% yield (Figure 3.5). The 3:1:1 stoichiometric reaction between NMM, SbCl₃ and **3.4** resulted in no reaction so the reaction mixture was heated to 50 °C for 48 h and 3 stoichiometric equivalents Et₃N were added. Upon completion of the reaction as detected by proton NMR spectroscopy (Figure 3.2, D), X-ray quality, red crystals were grown from CH₂Cl₂/Et₂O liquid diffusion at rt. confirming the synthesis of the diaminochlorostibine (Figure 3.5).

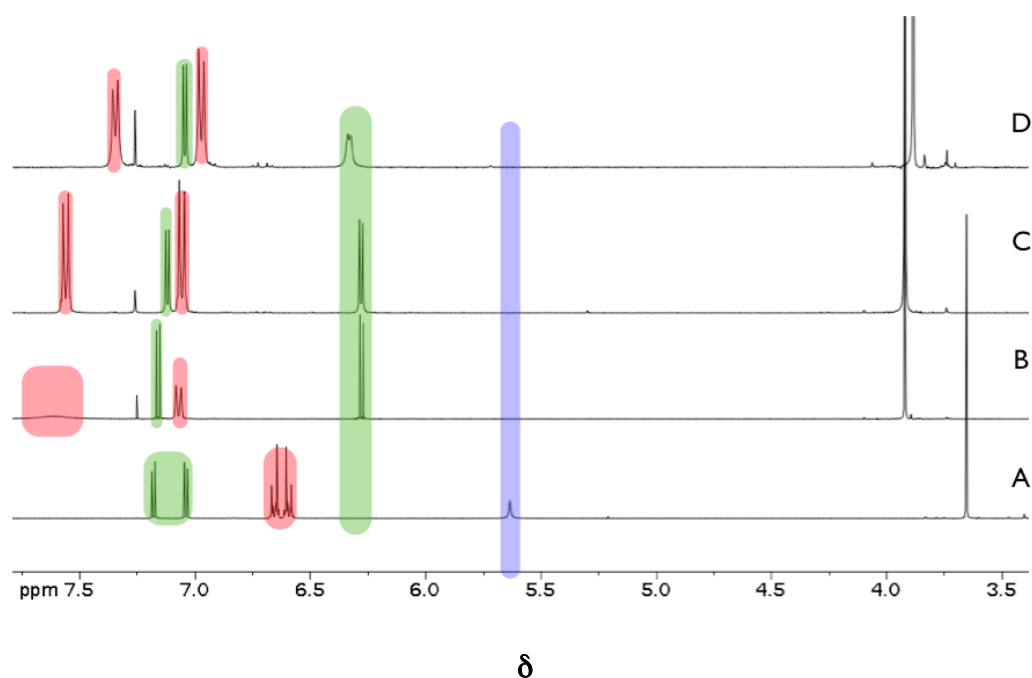
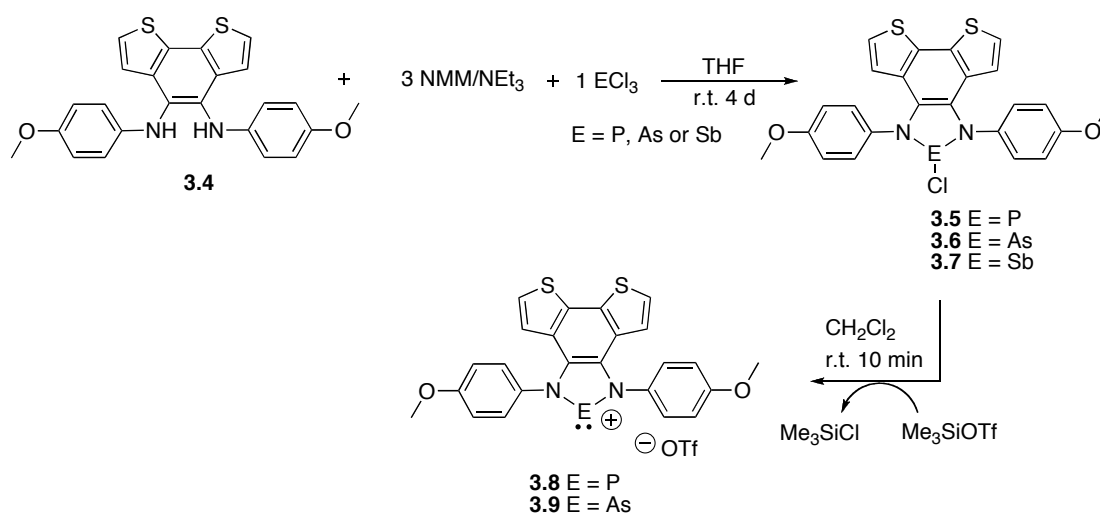


Figure 3.2: Stacked plot of the ¹H NMR spectra of A) the proligand, compound **3.4**; B) Compound **3.5**, Pn = P; C) Compound **3.6**, Pn = As; and D) Compound **3.7**, Pn = Sb.

Compound **3.5** was transformed to the corresponding phosphonium cation, (**3.8**) using two stoichiometric equivalents of trimethylsilyltrifluoromethanesulfonate (Me₃SiOTf) in CH₂Cl₂. The solution immediately turned from orange to red and after a few minutes a yellow solid precipitated from the reaction mixture. The red liquid was decanted and the remaining yellow powder dried *in vacuo*. A phosphorus-31 NMR spectrum of the redissolved yellow solid revealed a singlet ($\delta_P = 191$) and ionic triflate was detected in ¹⁹F {¹H} NMR spectrum ($\delta_F = -78.5$ cf. [Bu₄N]OTf $\delta_F = -78.7$),¹⁷ thus the solid was assigned as the triflate salt of the phosphonium cation (**3.8**). Crystals

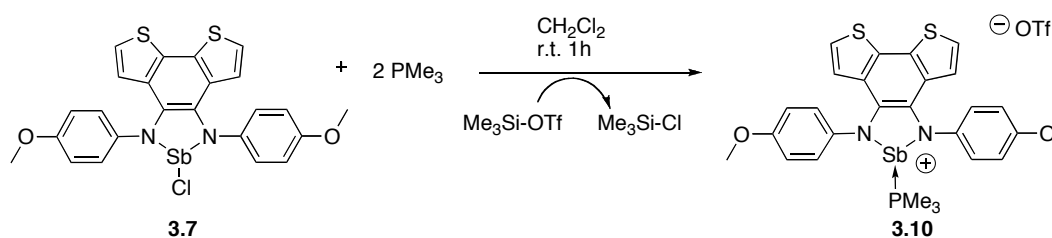
suitable for X-ray diffraction studies were obtained by vapour diffusion of *n*-pentane into a CH₂Cl₂ solution of **3.8**, confirming the production of the title compound, which was isolated in 90 % yield (Figure 3.5). The corresponding arsenium cation, **3.9** was synthesized from compound **3.6** by the addition of one stoichiometric equivalent of Me₃SiOTf in CH₂Cl₂ (Scheme 3.2). The solution remained red in colour, however after 15 min of stirring an orange solid began to precipitate from the reaction mixture. To this mixture 5 mL of Et₂O was added and the supernatant was decanted off leaving an orange solid, which was dried *in vacuo*. The fluorine-19 NMR spectrum revealed an ionic triflate, and in the ¹H NMR spectrum, both resonances attributed to the protons on thiophene and phenyl rings were shifted downfield by 0.1 ppm. Crystals suitable for X-ray diffraction studies were obtained by vapour diffusion of Et₂O into a CH₂Cl₂ solution of **3.9**, confirming the synthesis of the desired product in 93% yield (Figure 3.3).



Scheme 3.2: Synthesis of **3.5**, **3.6** and **3.7** then subsequent halide abstraction yielding compounds **3.8** and **3.9**.

The corresponding stibonium cation could not be isolated and only decomposition products were observed by ¹H NMR spectroscopy when halide-abstracting agents Me₃SiOTf or GaCl₃ were added to a CH₂Cl₂ solution of the diaminochlorostibine, **3.7**, however, the stibonium cation could be trapped using a Lewis base. To a CH₂Cl₂ solution of chlorostibine (**3.7**), two stoichiometric equivalents of PMe₃ and one stoichiometric equivalent of Me₃SiOTf were added (Scheme 3.3). A yellow solid precipitated from the orange solution after 15 min. of stirring and the orange solution

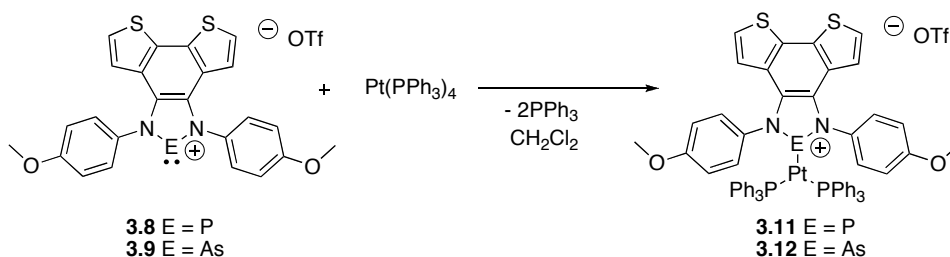
was decanted. The yellow solid was isolated in 37% yield. Upon redissolving the yellow solid in CDCl_3 and examination by ^{31}P NMR spectroscopy a peak at $\delta_{\text{P}} = -1.2$ was observed along with ionic triflate ($\delta_{\text{F}} = -78.7$) indicating the target product was likely synthesized. A doublet in the ^1H NMR spectrum at 1.55 ppm corresponding to the methyl groups on the PMe_3 was also observed providing further evidence that the desired product was isolated. Single crystals were grown by vapour diffusion of Et_2O into a CH_2Cl_2 solution of the product and single X-ray quality crystals were obtained confirming the target compound (**3.10**, Scheme 3.3, Figure 3.5).



Scheme 3.3: Synthesis of **3.10**.

The ability to readily modify the pnictenium framework is important for the successful manipulation of the photophysical and electronic properties of the thiophene system; metallation strategies are often useful in this regard.¹⁸ This was probed by the addition of $\text{Pt}(\text{PPh}_3)_4$ to a CH_2Cl_2 solution of **3.8**, causing an immediate colour change from yellow to deep red (Scheme 3.4). The reaction mixture was concentrated *in vacuo* to a red oil. Diethyl ether was added to precipitate a bright orange powder. A $^{31}\text{P}\{^1\text{H}\}$ NMR spectrum of the redissolved solid revealed an upfield doublet and a downfield triplet, each with corresponding ^{195}Pt satellites, in an approximate 2:1 integration ratio that were assigned to two PPh_3 and one phosphonium ligand, respectively ($\delta_{\text{P}} = 47$, $^1J_{\text{Pt-P}} = 2358$ Hz, $^2J_{\text{P-P}} = 490$ Hz; $\delta_{\text{P}} = 249$, $^1J_{\text{Pt-P}} = 2326$ Hz, $^2J_{\text{PP}} = 490$ Hz). Single crystals were grown by vapour diffusion of *n*-pentane into a CH_2Cl_2 solution of the product and subsequent X-ray diffraction studies revealed the coordinatively unsaturated $\text{Pt}(0)$ phosphonium complex (**3.11**) isolated in 77 % yield (Figure 3.5). The reactivity of **3.9** was also explored by the addition of one equivalent of $\text{Pt}(\text{PPh}_3)_4$ in CH_2Cl_2 causing an immediate colour change from red to dark purple (Scheme 3.4). The reaction mixture was concentrated *in vacuo* to give a purple oil, to which 3 mL of Et_2O was added precipitating a purple solid. A $^{31}\text{P}\{^1\text{H}\}$ NMR spectrum of the purple powder displayed a single peak ($\delta_{\text{P}} =$

41) with ^{195}Pt satellites ($^1J_{\text{Pt-P}} = 3579.6$ Hz) and the disappearance of the Pt precursor ($\delta_{\text{p}} = 23$). Upon examination of the ^1H NMR spectrum, again the protons on the thiophene backbone were diagnostic and shifted upfield from $\delta_{\text{H}} = 6.34$ in **3.6**, to $\delta_{\text{H}} = 5.97$ in the metal complex **3.12**. Single crystals were grown by vapour diffusion of Et_2O into a CH_2Cl_2 solution of the product and X-ray diffraction studies revealed the Pt(0) arsenium complex, **3.12** (Figure 3.5).



Scheme 3.4: Synthesis of pnictenium metal complexes.

3.2.2 Photophysical properties

The UV-visible absorption spectra of compounds **3.3** - **3.12** are shown in Figure 3.3 along with the fluorescence spectra of compounds **3.4**, **3.5**, **3.7**, **3.8** and **3.10** in Figure 3.4. The λ_{max} and the extinction coefficients are listed in Table 3.1. In comparison to the ligand **3.4** ($\lambda_{\text{abs}} = 279$ nm), upon the addition of the pnictogen center, phosphorus (**3.5**, $\lambda_{\text{abs}} = 266, 373$ nm), arsenic (**3.6**, $\lambda_{\text{abs}} = 271, 373$ nm) and antimony (**3.7**, $\lambda_{\text{abs}} = 252, 276, 372, 465$ nm), the absorption was blue-shifted to shorter wavelengths with antimony having an absorption maxima with the highest energy. Absorption maxima for the pnictenium cations were shifted to a higher energy as the charge is increased on the five membered ring for phosphorus (**3.8**, $\lambda_{\text{abs}} = 258, 377$ nm) and arsenic (**3.9**, $\lambda_{\text{abs}} = 256, 282$ nm), however in the base stabilized stibenium cation, the λ_{abs} was shifted to a lower energy (**3.10**, $\lambda_{\text{abs}} = 279, 386$ nm). As one goes down group 15, both the maximum absorption and emission wavelengths of these compounds were similar in CH_2Cl_2 solutions and suggests that the substitution did not cause significant changes in the conjugation of the molecular structure and the photophysical properties are dominated by the benzo[1,2-b:5,6-b']dithiophene backbone. The solvatochromic effects of the pnictenium compounds were investigated and upon changing the solvent composition from CH_3CN to Et_2O in 10 vol % increments, there was no dramatic shift in the UV-vis absorption, however the absorption coefficient decreased as the vol %

of Et₂O increased. The quantum yields were calculated against diphenylanthracene, which were low, ranging from 1.0% to 2.3%.¹⁹

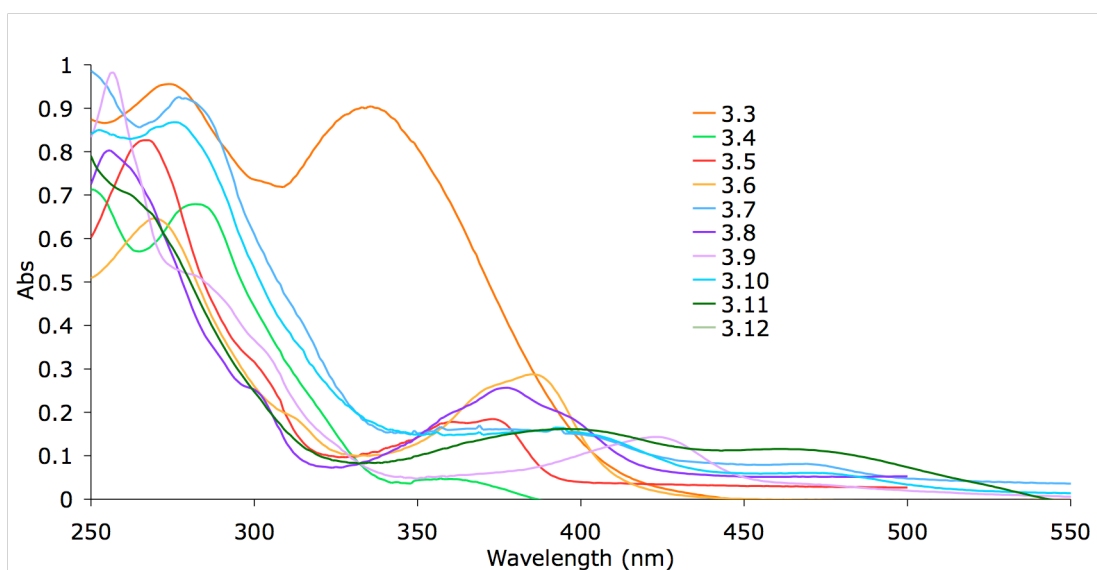


Figure 3.3: UV-absorption spectra of compounds 3.4 - 3.12 in CH₂Cl₂.

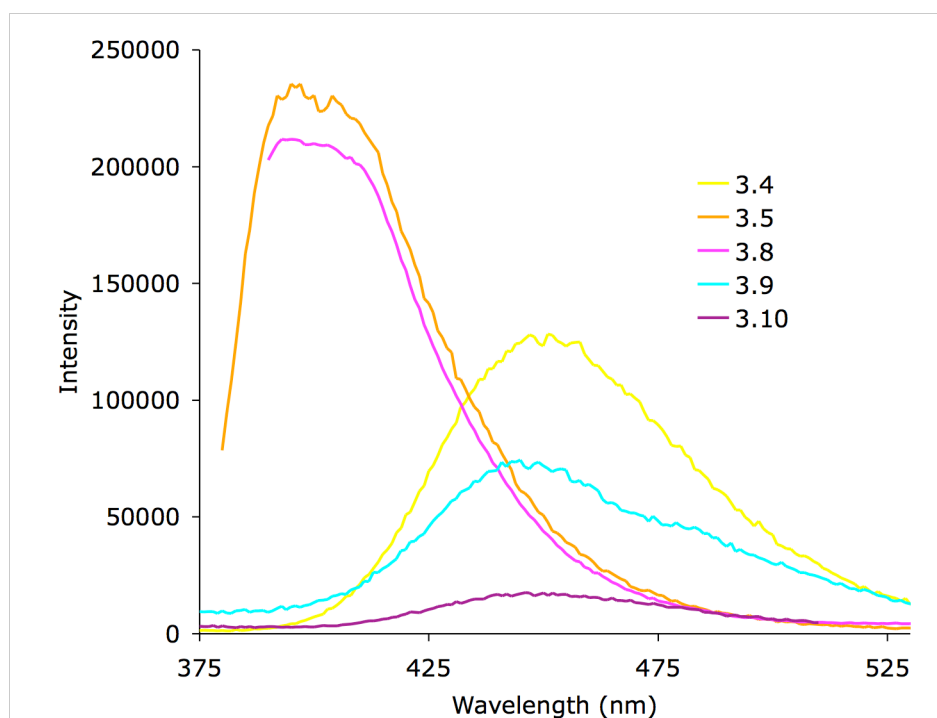


Figure 3.4: Fluorescence spectra of compounds 3.4, 3.5, 3.8, 3.9 and 3.10 in CH₂Cl₂.

Table 3.1. Optical properties of compounds **3.3 - 3.12**.

Compound	λ_{abs} nm (ϵ_{max} L mol ⁻¹ cm ⁻¹)	λ_{em} (nm)	ϕ_{FL}^*
3.3	273 (3.5×10^4)	-	-
	333 (3.3×10^4)		
3.4	279 (2.7×10^4)	450	0.011
3.5	266 (3.1×10^4)	400	0.023
	373 (7.1×10^3)		
3.6	271 (3.1×10^4)	-	
	383 (1.3×10^3)		
3.7	252 (4.8×10^5)	450	0.011
	276 (4.6×10^5)		
	372 (8.0×10^4)		
	465 (4.0×10^4)		
3.8	258 (2.5×10^4)	400	0.019
	377 (8.2×10^3)		
3.9	256 (5.6×10^4)		
	282 (2.9×10^4)		
	423 (3.9×10^3)		
3.10	279 (6.6×10^4)	450	0.010
	386 (1.2×10^4)		
3.11	259 (5.9×10^4)	-	
	394 (1.3×10^4)		
	466 (9.5×10^3)		
3.12	276 (3.2×10^4)	-	
	576 (2.7×10^4)		

*Fluorescence quantum yields measured in CH₂Cl₂ solution using 9,10 diphenylanthracene ($\phi_{\text{FL}} = 0.90$ in CH₂Cl₂) as a standard, excited at 260 nm.¹⁹

3.2.3 X-ray crystallography

Compounds **3.4** - **3.12** have been characterized by single X-ray diffraction studies. Views of the solid state structures are shown in Figure 3.3 and refinement details can be found in Table 3.2 and 3.3. Key bond lengths and angles are summarized in Table 3.4.

An examination of the solid-state structures of compounds **3.4** – **3.12** revealed that the metrical parameters for the C₂N₂ ring were all consistent with two C – N single bonds (1.388 - 1.415 Å *cf.* 1.420 Å (avg.) in the free ligand) and a C – C double bond (1.386 – 1.399 Å *cf.* 1.382 Å (avg.) in **3.4**). The C – N bonds are slightly shortened upon coordination to pnictogen and the C – C double bond in the backbone remained the same as in the free ligand (**3.4**).

Compounds **3.5**, **3.6** and **3.7** are all isostructural and feature long E(1) – Cl(1) bonds and are all pyramidal at the pnictogen center. Upon examination of the pnictogen halogen linkage the bond length increases down the group from 2.2123(9) Å for compound **3.5**, 2.3296(5) Å for **3.6** and 2.5129(6) Å for **3.7**, corresponding to the increase in size of the central element. The pnictogen atom is pyramidal which is expected from a three coordinate pnictogen center with a lone pair, however the Cl(1) - Pn(1) - N(1) angle decrease as one goes down the group from **3.5** ($\Sigma_{\text{ang}} = 102.81(7)^\circ$), **3.6** ($\Sigma_{\text{ang}} = 100.85(5)$) to **3.7** ($\Sigma_{\text{ang}} = 92.70(6)$) due to the decrease in hybridization at the pnictogen.

Upon examination compound **3.8** (**3.9** is isostructural) the thiophene – P(1) portion deviates from planarity only by 0.0348 Å. The *p*-MeOPh rings are twisted out of the plane by 96.0(7)° and are almost perpendicular to the plane of the benzo[1,2-*b*:5,6-*b'*]dithiophene backbone. In general, the metrical parameters of the phosphonium cation (**3.8**) are comparable to those reported for other NHP systems. Upon formation of the arsenium cation there is a contraction in the C - N bond from 1.405(2) Å for compound **3.6** to C(11) - N(2) 1.369(6) Å and C(12) - N(1) 1.372(6) Å. This contraction was also observed in the P - N bond, P(1) - N(1) 1.683(2) Å; P(1) - N(2) 1.6942(19) Å for compound **3.5** and P(1) - N(1) 1.649(5) Å, P(1) - N(2) 1.655(5) Å for **3.8**. The structural changes that were observed with the formation of the trimethylphosphine stabilized stibonium cation **3.10** from **3.7** are summarized in Table

3.3. There is a slight increase in the Sb - N bond lengths (Sb-N(1) = 2.057(2) Å, Sb-N(2) = 2.053 Å) and is slightly longer than previously reported examples of N-Heterocyclic stibonium cations.^{20,21} The Sb - P bond is elongated at 2.6171(11) Å and is outside the sum of the covalent radii (*cf.* 2.50 Å)²² and is in line with other values reported for P→Sb bonding modes.^{23,24} Figure 3.3 shows the crystal structure and packing motifs of compound **3.9** forming an extended network of zigzag chains. When viewed down the *c*-axis the molecules are π -stacked in a head to tail conformation orientated in a perpendicular fashion with the pnictogen center directed toward the centroid of the benzo[1,2-b:5,6-b']dithiophene unit on an adjacent molecule. They are packed in four non-equivalent stacks that are nearly vertical to each other (*ca.* 75.49°) due to the occurrence of As $\cdots\pi$ inter molecular contacts with an interplanar distance of 6.18 Å. This packing motif is most likely attributed to the existence of C-H $\cdots\pi$ and As $\cdots\pi$ interactions and is not observed in any of the other pnictogen complexes. These interactions are similar to those reported between three coordinate As(III) centers and arenes²⁵⁻²⁷ and other arsenium cations.²⁸

Table 3.2. Crystal data for compounds **3.4** to **3.8**.

	3.4	3.5	3.6	3.7	3.8
Empirical formula	C ₂₄ H ₂₀ N ₂ O ₂ S ₂	C ₂₄ H ₁₈ N ₂ O ₂ S ₂ PCl	C ₂₄ H ₁₈ N ₂ O ₂ S ₂ AsCl	C ₂₄ H ₁₈ N ₂ O ₂ S ₂ SbCl	C ₂₅ H ₁₈ F ₃ N ₂ O ₅ PS ₃
FW (g/mol)	432.54	496.94	540.89	587.72	610.56
Crystal system	Orthorhombic	Triclinic	Monoclinic	Triclinic	Monoclinic
Space group	P2 ₁ 2 ₁ 2 ₁	P $\bar{1}$	P2 ₁	P $\bar{1}$	P2 ₁
a (Å)	5.6639(4)	8.8245(18)	8.7034(4)	9.8620(4)	10.270(2)
b (Å)	18.2454(12)	10.045(2)	13.3155(6)	14.3596(6)	11.016(2)
c (Å)	19.7061(13)	13.898(3)	19.5851(9)	17.3069(7)	12.460(3)
α (deg)	90.00	80.52(3)	90.00	66.669(2)	90.00
β (deg)	90.00	74.17(3)	101.340(2)	89.298(2)	112.43(3)
γ (deg)	90.00	67.92(3)	90.00	86.426(2)	90.00
V (Å ³)	2036.4(2)	1095.7(4)	2225.41(18)	2245.92(16)	1303.0(5)
Z	4	2	4	4	2
D _c (mg m ⁻³)	1.411	1.506	1.861	1.559	1.556
R _{int}	0.0351	0.0411	0.0224	0.0222	0.0632
R1[I > 2 σ I] ^a	0.0451	0.0599	0.0266	0.0281	0.1452
wR2(F ²) ^a	0.0860	0.1177	0.0603	0.0576	0.1439
GOF(S)	0.992	1.112	1.033	1.119	0.977

^aR1($F[I > 2(I)]$) = $\sum ||F_o| - |F_c| || / \sum |F_o|$; wR2(F^2 [all data]) = $[w(F_o^2 - F_c^2)^2]^{1/2}$; S(all data) = $[w(F_o^2 - F_c^2)^2 / (n - p)]^{1/2}$ (n = no. of data; p = no. of parameters varied; $w = 1/[\sigma^2 (F_o^2) + (aP)^2 + bP]$ where $P = (F_o^2 + 2F_c^2)/3$ and a and b are constants suggested by the refinement program.

Table 3.3: Crystal data for compounds **3.9** - **3.12**.

	3.9	3.10	3.11	3.12
Empirical formula	C ₂₅ H ₁₈ F ₃ N ₂ O ₅ AsS ₃	C ₂₈ H ₂₇ F ₃ N ₂ O ₅ PS ₃ Sb	C ₆₂ H ₄₉ Cl ₃ F ₃ N ₂ O ₅ P ₃ PtS ₃	C ₆₂ H ₄₉ Cl ₃ F ₃ N ₂ O ₅ P ₂ AsPtS ₃
FW (g/mol)	654.51	862.34	1449.56	1374.14
Crystal system	Monoclinic	Triclinic	Monoclinic	Triclinic
Space group	P2 ₁	P $\bar{1}$	P2 ₁ /c	P $\bar{1}$
a (Å)	10.342(2)	9.1339(5)	19.897(4)	11.5899(8)
b (Å)	10.994(2)	11.8823(7)	11.949(2)	13.2732(10)
c (Å)	12.477(3)	16.8352(10)	25.874(5)	17.7278(13)
α (deg)	90.00	81.367(2)	90.00	85.961(2)
β (deg)	111.88(3)	79.485(2)	98.91(3)	83.564(2)
γ (deg)	90.00	71.365(2)	90.00	84.914(2)
V (Å ³)	1316.4(5)	1694.01(17)	6078(2)	2694.3(3)
Z	2	2	4	2
D _c (mg m ⁻³)	1.651	1.691	1.584	1.694
R _{int}	0.0501	0.0311	0.0388	0.0498
R1[I>2 σ I] ^a	0.0729	0.0501	0.0646	0.1091
wR2(F ²) ^a	0.1234	0.0673	0.1009	0.0669
GOF(S)	1.062	1.052	1.063	0.972

^aR1(F[I > 2(I)]) = $\sum ||F_o| - |F_c| | / \sum |F_o|$; wR2(F² [all data]) = $[w(F_o^2 - F_c^2)^2]^{1/2}$; S(all data) = $[w(F_o^2 - F_c^2)^2 / (n - p)]^{1/2}$ (n = no. of data; p = no. of parameters varied; $w = 1 / [\sigma^2 (F_o^2) + (aP)^2 + bP]$ where $P = (F_o^2 + 2F_c^2) / 3$ and a and b are constants suggested by the refinement program.

Table 3.4 Selected bond lengths [\AA] and angles [$^\circ$] for compounds **3.4** - **3.12**.

Compound Bond	3.4	3.5	3.6	3.7	3.8	3.9	3.10	3.11	3.12
N(1) - C(12)	1.404(4)	1.413(3)	1.405(2)	1.406(3)	1.396(8)	1.372(6)	1.417(4)	1.401(6)	1.394
N(2) - C(11)	1.434(4)	1.415(3)	1.406(2)	1.396(3)	1.388(8)	1.369(6)	1.423(4)	1.395(5)	1.388(7)
C(11) - C(12)	1.379(4)	1.399(3)	1.395(2)	1.412(3)	1.396(7)	1.408(6)	1.391(4)	1.386(6)	1.408(7)
Pn(1) - X(1)	N/A	2.2123(9)	2.3296(5)	2.5129(6)	N/A	N/A	2.6171(11)	N/A	N/A
N(1) - Pn(1)	N/A	1.683(2)	1.8224(13)	2.0203(19)	1.649(5)	1.790(4)	2.057(2)	1.660(4)	1.835(4)
N(2) - Pn(1)	N/A	1.6942(19)	1.8255(13)	2.0091(18)	1.655(5)	1.798(4)	2.053(3)	1.666(4)	1.825(5)
Pn(1) - Pt(1)	N/A	N/A	N/A	N/A	N/A	N/A	N/A	2.1157(12)	2.4462(7)
N(1) - Pn(1) - N(2)	N/A	89.79(10)	85.72(6)	79.67(7)	91.3(3)	85.89(17)	81.52(10)	90.90(18)	84.5(2)
N(1) - Pn(1) - X(1)	N/A	102.81(7)	100.85(5)	92.70(6)	N/A	N/A	89.17(8)	N/A	N/A
N(2) - Pn(1) - X(1)	N/A	100.40(7)	101.12(5)	95.81(6)	N/A	N/A	89.69(8)	N/A	N/A
N(1) - Pn(1) - Pt(1)	N/A	N/A	N/A	N/A	N/A	N/A	N/A	134.49(14)	107.78(14)
N(2) - Pn(1) - Pt(1)	N/A	N/A	N/A	N/A	N/A	N/A	N/A	131.48(14)	114.98(15)

The Pt complex **3.11** is trigonal planar at the metal ($\Sigma_{\text{ang}} = 360.00^\circ$) and at the phosphonium P-atom ($\Sigma_{\text{ang}} = 356.87^\circ$). The N(1) - P(1) - N(2) plane of the phosphonium makes a torsion angle of $78.9(2)^\circ$ with the coordination plane of the metal, likely due to the bulky nature of the triphenylphosphine ligands. The Pt - NHP bond P(1) - Pt(1) (2.1157(12) Å) is shorter than the Pt(1) - P(2) (2.3315(13) Å) and Pt(1) - P(3) bonds (2.2935(12) Å) suggesting strong backbonding from the Pt to the phosphonium similar to that observed in related phosphonium→Pt complexes (*cf.* 2.116(3) Å; 2.107(3) Å).^{29,30} Upon examination of the solid-state structure of **3.11**, it consists of a central Pt center with two triphenylphosphine ligands. In contrast to **3.11**, compound **3.12** is pyramidal at the pnictenium center and has a coordination geometry ($\Sigma_{\text{ang}} = 307.24$) consistent with a non-bonding lone pair still present on the arsenium and can be described as primarily M → L bonding.³¹ Progressing down group 15 from phosphorus to arsenic, the bonding changes from the filled sp^2 hybrid orbital on phosphorus interacting with the filled d-orbitals on Pt^0 , and metal backbonding to the empty p orbital on phosphorus yielding a coplanar arrangement, to arsenic, where only the metal is donating into the empty p orbital on arsenic leading to a pyramidal geometry. This bonding is similar to the heavy N-heterocyclic plumblylenes observed by Hahn. The metal (Pt^0 or Pd^0) acts as a d-electron donor to the empty p orbital on Pb^{II} and the lone pair of electrons on Pb, located in the sp^2 hybrid orbital, do not participate in bonding to the metal center. By going down group 14 in synthesizing the heavier group 14 NHC metal complexes the geometry at the coordinating atom changes from coplanar to tetrahedral.³¹

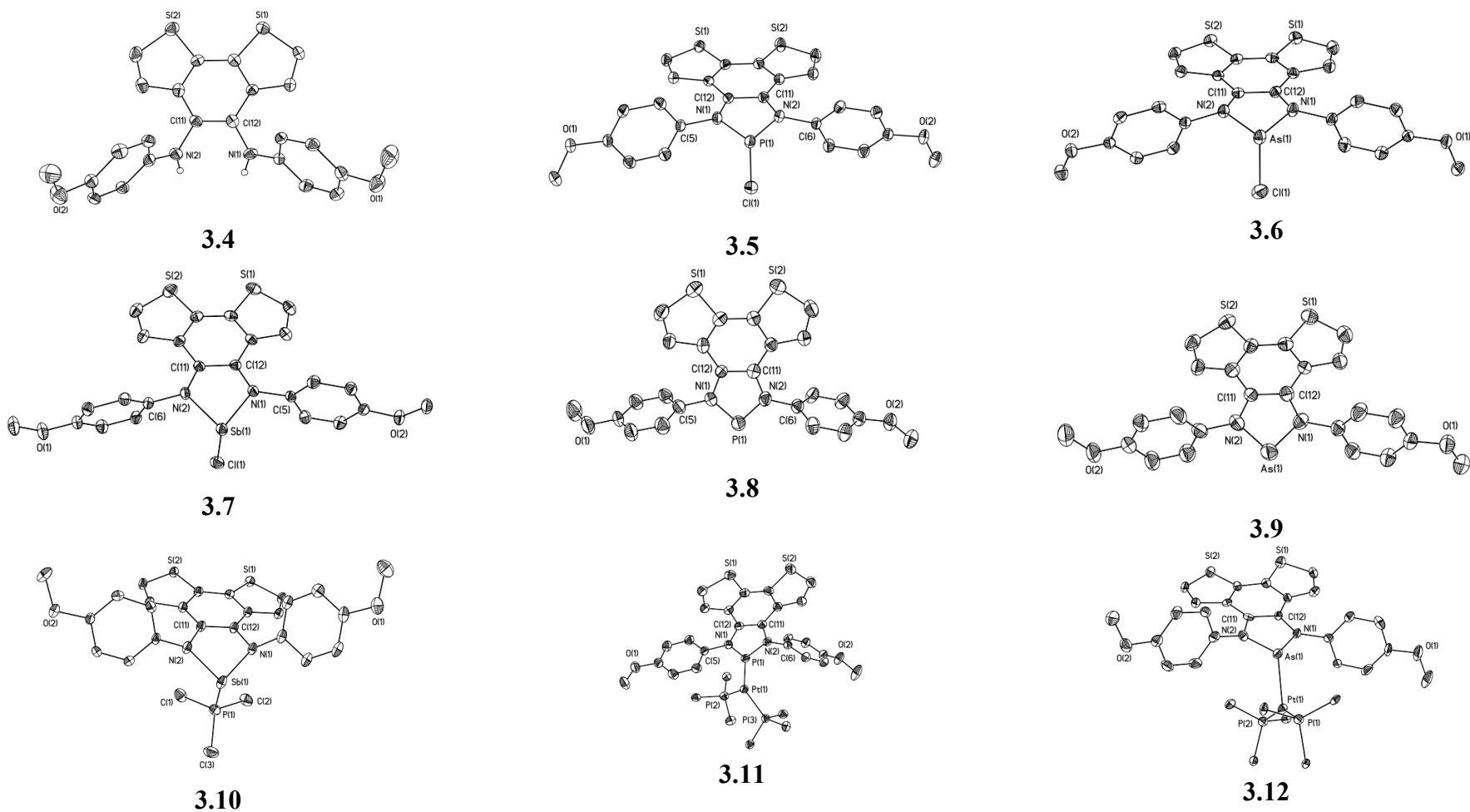


Figure 3.5: Solid-state structures of **3.4** to **3.12**. Ellipsoids are drawn to 50% probability. The triflate anions for compounds **3.8** - **3.12** and hydrogen atoms are removed except on the nitrogen atoms for compound **3.4** and the phenyl rings on compounds **3.11** and **3.12** for clarity.

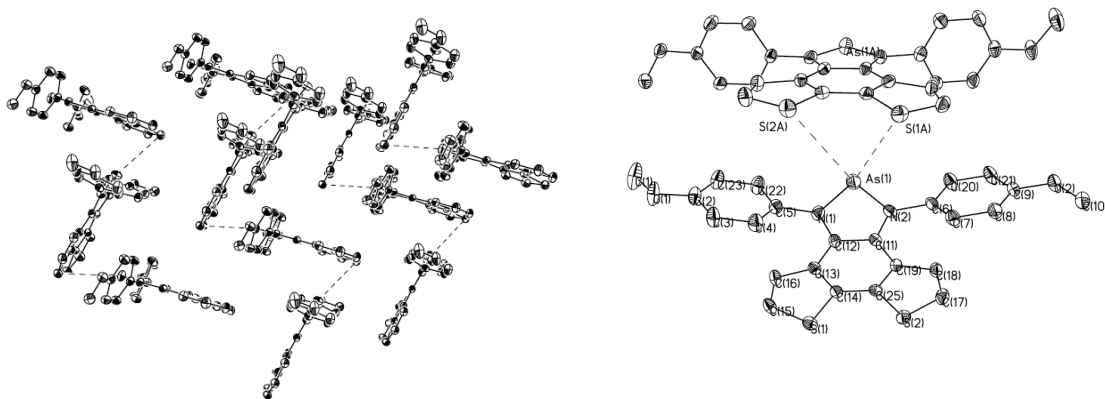


Figure 3.6: Crystal packing of **3.9**.

3.2.4 Conclusion

The successful synthesis of a new diamine ligand with a benzo[1,2-b:5,6-b']dithiophene backbone was achieved and was subsequently converted to the diaminochloropnictine and pnictenium cations. These complexes are the first examples of pnictogens containing a benzo[1,2-b:5,6-b']dithiophene backbone and the first example of a pnictogen containing a thiophene heterocycle complexed to a transition metal. These new complexes did not display any solvatochromic properties and their UV-vis absorption was dominated by benzo[1,2-b:5,6-b']dithiophene backbone with little influence from the pnictogen atom. Compounds **3.4**, **3.5**, **3.7**, **3.8** and **3.10** did display fluorescence, however, the efficiencies were low. This new ligand system opens the door to the preparation of other p-block derivatives, which could have new electronic or photophysical properties dependent on the Lewis acid or metal complex used.

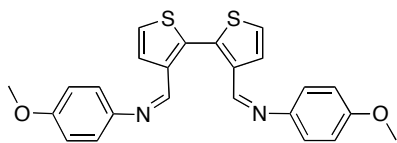
3.3 Experimental

3.3.1 General experimental

General synthetic and crystallography experimental details can be found in Appendix 1.

3.3.2 Synthetic procedures

Compound 3.3.



A solution of 2,2'-bithiophene-3,3'-biscarboxaldehyde (1.50 g, 6.70 mmol) in EtOH (40 mL) was cooled to 0 °C and a solution of *p*-anisidine (1.74 g, 14.10 mmol) in EtOH (10 mL) was added dropwise. The reaction

mixture was warmed to rt. and then heated to reflux for 4 h. The solvent was concentrated and the resulting yellow powder was collected by filtration and washed with cold EtOH (3 x 5 mL);

Yield: 86% (2.50 g, 5.78 mmol);

m.p.: 148 – 149°C;

¹H NMR (CDCl₃, δ (ppm)): 8.38 (s, 2H, CH), 7.81 (d, 2H, thienyl, ³J_{HH} = 5.2), 7.45 (d, 2H, thienyl, ³J_{HH} = 5.2), 7.08 (d, 4H, aryl, ³J_{HH} = 8.8), 6.83 (d, 4H, aryl, ³J_{HH} = 9.2), 3.78 (s, 6H, CH₃);

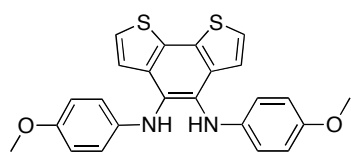
¹³C{¹H} NMR (CDCl₃, δ (ppm)): 158.4, 151.7, 144.6, 139.1, 136.2, 127.3, 127.0, 122.1, 114.3, 55.4;

FT-IR (ranked intensities (cm⁻¹)): 533(14), 630(9), 715(11), 728(13), 781(7), 826(4), 1034(2), 1105(12), 1207(6), 1251(1), 1293(10), 1458(8), 1500(3), 1611(5);

FT-Raman (ranked intensities (cm⁻¹)): 160(3), 679(12), 788(15), 968(13), 1166(7), 1209(4), 1247(14), 1295(11), 1355(8), 1392(9), 1462(5), 1501(6), 1592(1), 1624(2), 3101(15);

HRMS: C₂₄H₂₀N₂O₂S₂ Calcd (found) 432.0966 (432.0955).

Compound 3.4.



A DMF (5 mL) solution of **3.3** (2.50 g, 5.78 mmol) and sodium cyanide (0.28g, 5.78 mmol) stirred at rt. for 48 h. To the reaction mixture 10 mL of CH₂Cl₂ was added and washed with water (3 x 50 mL). The CH₂Cl₂ layer was then dried with MgSO₄ and concentrated. The product was then precipitated with MeOH and isolated by filtration. The resulting orange powder was washed with MeOH (3 x 5 mL).

Yield: 80% (2.05 g, 4.62 mmol);

m.p.: 173 - 175 °C;

¹H NMR (CDCl₃, δ (ppm)): 7.18 (d, 2H, thienyl, ³J_{HH} = 5.6), 7.04 (d, 2H, thienyl, ³J_{HH} = 5.6), 6.65 (m, 4H, aryl), 6.59 (m, 4H, aryl), 5.63 (s, 2H, NH), 3.65 (s, 6H, CH₃);

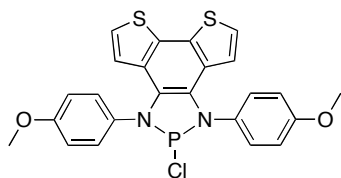
¹³C{¹H} (CDCl₃, δ (ppm)): 153.7, 139.8, 134.5, 130.5, 128.8, 123.9, 123.5, 117.5, 114.6, 55.6;

FT-IR (ranked intensities (cm⁻¹)): 653(9), 732(4), 806(6), 901(10), 1033(3), 1107(15), 1167(11), 1179(12), 1245(2), 1297(13), 1356(14), 1397(8), 1449(5), 1507(1), 3336(7);

FT-Raman (ranked intensities (cm⁻¹)): 1314(4), 1462(2), 1499(1), 1587(3), 2061(15), 2076(13), 2146(14), 2157(7), 2171(12), 2205(11), 2220(10), 2243(9), 2265(8), 2732(5), 3059(6);

HRMS: (C₂₄H₂₂N₂O₂S₂) Calcd (found) 432.0966 (432.0955).

Compound 3.5.



A THF (5 mL) solution of **3.4** (0.30g, 0.69 mmol) and n-methylmorpholine (0.29 mL, 2.08 mmol) stirred for 10 min. at rt. PCl₃ (0.06 mL, 0.69 mmol) was added to the solution. The reaction then stirred for 4 days at rt. The white precipitate was removed by centrifuge and the resulting orange solution was concentrated *in vacuo* yielding an orange solid.

Yield: 83 % (0.28g, 0.57 mmol);

m.p.: 207 - 211 °C;

¹H NMR (CDCl₃, δ (ppm)): 7.62 (br. s, 4H, aryl), 7.16 (d, 2H, thienyl, ³J_{HH} = 6.0), 7.07 (d, 4H, aryl, ³J_{HH} = 7.6), 6.28 (d, 2H, thienyl, ³J_{HH} = 5.2), 3.92 (s, 6H, CH₃);

$^{13}\text{C}\{^1\text{H}\}$ NMR (CDCl_3 , δ (ppm)): 159.9, 130.0, 129.9, 129.4, 129.1, 125.2, 124.2, 120.9, 114.8, 55.5;

$^{31}\text{P}\{^1\text{H}\}$ NMR (CDCl_3 , δ (ppm)): 136.5;

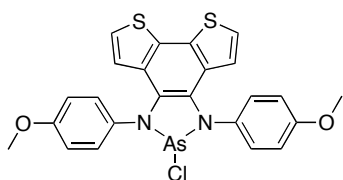
FT-IR (ranked intensities (cm^{-1})): 532(12), 724(2), 817(7), 918(10), 978(5), 1031(9), 1104(13), 1124(4), 1167(8), 1247(2), 1280(11), 1437(15), 1463(14), 1363(6), 1508(1);

FT-Raman (ranked intensities (cm^{-1})): 215(2), 384(3), 795(8), 1238(5), 1365(1), 1500(6), 2619(7), 3321(7);

HRMS: ($\text{C}_{22}\text{H}_{18}\text{N}_2\text{O}_2\text{PS}_2$)⁺ Calcd (found) 461.0547 (461.0547);

Elemental Analysis (%) calc for $\text{C}_{22}\text{H}_{18}\text{N}_2\text{O}_2\text{PS}_2\text{Cl}$: C 58.00, H 3.65, N 5.64; found C 57.86, H 3.70, N 5.44.

Compound 3.6.



A THF (40 mL) solution of **3.4** (1.00g, 23.00 mmol) and n-methylmorpholine (0.76 mL, 69.00 mmol) stirred for 10 min. at rt. AsCl_3 (0.20 mL, 23.00 mmol) was added to the solution.

The reaction then stirred for 4 days at rt. The white precipitate was removed by centrifuge and the resulting red solution was concentrated *in vacuo* yielding a red solid.

Yield: 54 % (0.67 g, 12.4 mmol);

m.p.: 208 - 213°C;

^1H NMR (CDCl_3 , δ (ppm)): 7.48(d, 4H, aryl, $^3J_{\text{HH}}=8.8$) 7.04 (d, 2H, thienyl, $^3J_{\text{HH}}=5.2$), 6.98 (d, 4H, aryl $^3J_{\text{HH}}=8.8$), 6.20 (d, 2H, thienyl, $^3J_{\text{HH}}=5.6$), 3.84 (s, 6H, CH_3);

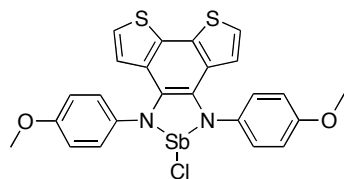
$^{13}\text{C}\{^1\text{H}\}$ NMR (CDCl_3 , δ (ppm)): 159.6, 142.2, 132.2, 129.8, 129.0, 126.0, 123.5, 121.5, 114.8, 55.5;

FT-IR (ranked intensities (cm^{-1})): 485(15), 521(6), 642(5), 728(3), 812(10), 912(8), 945(12), 1028(4), 1116(13), 1244(1), 1277(11), 1363(7), 1455(14), 1505(2), 1602(9);

HRMS: ($\text{C}_{22}\text{H}_{18}\text{N}_2\text{O}_2\text{As}$)⁺ Calcd (found) 505.0026 (505.0029);

Elemental Analysis (%) calc for $\text{C}_{22}\text{H}_{18}\text{N}_2\text{O}_2\text{AsS}_2\text{Cl}$: C 53.29, H 3.35, N 5.18; found C 53.29, H 3.33, N 5.15.

Compound 3.7.



In a pressure tube a THF (30 mL) solution of **3.4** (1.0g, 23.00 mmol) and NEt_3 (0.96 mL, 69.00 mmol) stirred for 10 min. at rt. A THF solution (5 mL) of SbCl_3 (0.52g, 23.00 mmol) was added to the solution. The reaction was then heated to 60° C for 48 hours. The precipitate was removed

by centrifuge and the resulting red solution was concentrated *in vacuo* yielding a red solid.

Yield: 95% (1.27 g, 21 mmol);

d.p.: 152 °C;

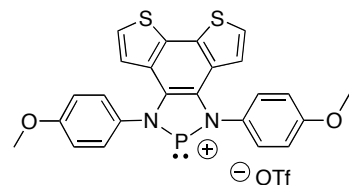
^1H NMR (CDCl_3 , δ (ppm)): 7.33 (d, 4H, aryl, $^3J_{\text{HH}}=8.4$), 7.03 (d, 2H, thienyl, $^3J_{\text{HH}}=5.6$), 6.96 (d, 4H, aryl, $^3J_{\text{HH}}=8$), 6.32 (d, 2H, thienyl, $^3J_{\text{HH}}=4.8$), 3.88 (s, 6H, CH_3);

$^{13}\text{C}\{^1\text{H}\}$ NMR (CDCl_3 , δ (ppm)): 158.2, 136.5, 134.6, 128.0, 122.5, 114.7, 110.7, 45.7

FT-IR (ranked intensities (cm^{-1})): 638(10), 704(8), 722(4), 814(11), 909(5), 942(14), 1030(6), 1102(12), 1178(8), 1241(2), 1274(7), 1349(3), 1450(9), 1503(1), 1601(15);

FT- Raman (ranked intensities (cm^{-1})): 96.7(5), 173(11), 195(13), 227(4), 245(1), 676(8), 784(10), 1098(12), 1224(3), 1270(6), 1307(9), 1348(2), 1388(14), 1449(15), 1496(7);

Compound 3.8.



To a solution of **3.4** (0.10 g, 0.20 mmol) in CH_2Cl_2 (4 mL) the halide-abstracting agent Me_3SiOTf (0.04 mL, 0.22 mmol) was added dropwise. The solution was stirred for 10 min. at rt. during which time a yellow solid precipitated from the solution. The red solution was decanted and the

remaining yellow solid was dried *in vacuo*. The product was washed with Et_2O (2 x 3 mL) and dried.

Yield: 90 % (0.11 g, 0.18 mmol);

m.p.: > 300 °C;

^1H NMR (CDCl_3 , δ (ppm)): 7.84 (d, 4H, aryl, $^3J_{\text{HH}} = 8.4$), 7.36 (d, 2H, thienyl, $^3J_{\text{HH}} = 5.2$), 7.20 (d, 4H, aryl, $^3J_{\text{HH}} = 8.8$), 6.41 (d, 2H, thienyl, $^3J_{\text{HH}} = 5.2$), 3.97 (s, 6H, CH_3);

$^{13}\text{C}\{^1\text{H}\}$ NMR (Pyridine- d_5 , δ (ppm)): 159.4, 129.7, 128.2, 127.8, 127.6, 125.2, 123.8, 119.5, 114.5, 54.3;

$^{31}\text{P}\{^1\text{H}\}$ NMR (CDCl_3 , δ (ppm)): 191.0;

$^{19}\text{F}\{^1\text{H}\}$ NMR (CDCl_3 , δ (ppm)): -78.5;

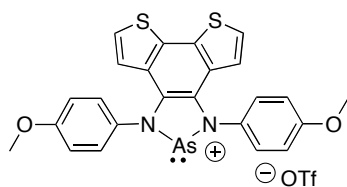
FT-IR (ranked intensities (cm^{-1})): 527(13), 635(5), 649(11), 724(12), 740(9), 824(8), 1030(2), 1159(3), 1174(6), 1221(7), 1257(1), 1307(10), 1325(15), 1509(3), 1608(14);

FT-Raman (ranked intensities (cm^{-1})): 633(9), 709(10), 736(12), 794(13), 1029(6), 1180(5), 1325(14), 1366(15), 1433(7), 1491(1), 1605(4), 1892(8), 2115(3), 2609(2), 3081(11);

HRMS: ($\text{C}_{24}\text{H}_{18}\text{N}_2\text{O}_2\text{PS}_2$) $^+$ Calcd (found) 461.0547 (461.0538);

Elemental Analysis (%) calc for $\text{C}_{25}\text{H}_{18}\text{F}_3\text{N}_2\text{O}_5\text{PS}_3 \cdot \text{C}_{0.25}\text{H}_{0.5}\text{Cl}_{0.5}$: C 48.00, H 2.95, N 4.43, S 15.23; found C 47.91, H 3.03, N 4.43, S 15.39.

Compound 3.9



To a solution of **3.6** (0.18 g, 0.33 mmol) in CH_2Cl_2 (4 mL) the halide-abstracting agent Me_3SiOTf (0.11 mL, 0.66 mmol) was added dropwise. The solution was stirred for 45 min. at rt. during which time the solution turned red and a dark

yellow solid precipitated from the solution. The red solution was decanted and the remaining yellow solid was dried *in vacuo*. The product was washed with Et_2O (2 x 3 mL) and dried.

Yield: 93 % (0.20 g, 0.31 mmol);

m.p.: >300 °C;

^1H NMR (CDCl_3 , δ (ppm)): 7.68 (d, 4H, aryl, $^3J_{\text{HH}}=8.0$), 7.27 (d, 2H, thienyl, $^3J_{\text{HH}}=8.0$)
 δ 7.15 (d, 4H, aryl, $^3J_{\text{HH}}=8.4$), 6.34 (d, thienyl, $^3J_{\text{HH}}=4.8$), 3.94 (s, 6H, CH_3);

$^{13}\text{C}\{^1\text{H}\}$ NMR (CDCl_3 , δ (ppm)): 161.4, 136.4, 135.1, 128.9, 125.7, 124.9, 122.2, 116.3, 115.3, 55.7;

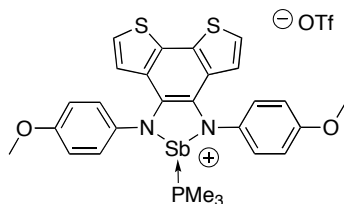
$^{19}\text{F}\{^1\text{H}\}$ NMR (CDCl_3 , δ (ppm)): -78.2;

FT-IR (ranked intensities (cm^{-1})): 521 (8), 635 (4) 715 (10), 738 (7), 819 (5), 1029 (3), 1157 (5), 1173 (14), 1221 (15), 1256 (10), 1458 (13), 1508 (2), 1540 (11), 1606 (9), 3084 (12);

HRMS: (C₂₄H₁₈N₂O₂AsS₂)⁺ Calcd (found) 505.0020 (505.0003);

Elemental Analysis (%) calc for C₂₅H₁₈AsClF₃N₂O₅S₃: C 45.88, H 2.77, N 4.28; found C 45.72, H 2.49, N 4.12.

Compound 3.10.



To an orange solution of **3.7** (0.10 g, 0.17 mmol) in CH₂Cl₂ (3 mL) was added PMe₃ (0.035 mL, 0.034 mmol) and Me₃SiOTf (0.031 mL, 0.17 mmol). The reaction mixture stirred at rt. for 1 h and was then concentrated. The CH₂Cl₂ was decanted leaving a yellow solid, which was washed (2 x

5 mL) with pentane.

Yield: 36% (0.13 g, 0.06 mmol);

d.p.: 223 - 225 °C;

¹H NMR (CDCl₃, δ (ppm)): 7.15 (m, 6H, aryl), 6.82 (d, 4H, aryl, ³J_{HH} = 8.4), 6.68 (d, 2H, thienyl, ³J_{HH} = 5.4), 3.78 (s, 6H, CH₃), 1.55 (d, 9H, CH₃, ²J_{PH} = 12.0);

¹³C{¹H} NMR (CD₃CN, δ (ppm)): 156.4, 141.5, 140.8, 137.8, 125.6, 124.4, 123.0, 114.2, 55.1, 9.5 (¹J_{PC} = 106.8);

¹⁹F {¹H} NMR (CD₃CN, δ (ppm)): -78.2;

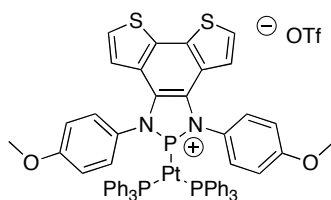
³¹P{¹H} NMR (CD₃CN, δ (ppm)): δ -1.2;

FT-IR (ranked intensities (cm⁻¹)): 510(6), 633(4), 704(14), 732(6), 810(13), 901(9), 956(8), 1024(3), 1109(12), 1161(7), 1237(1), 1291(5), 1386(10), 1453(15);

FT-Raman (ranked intensities (cm⁻¹)): 87(3), 194(10), 244(2), 674(12), 780(6), 1025(11), 1221(8), 1262(15), 1312(7), 1361(5), 1387(9), 1452(13), 1497(1), 1606(4), 2914(14);

Elemental Analysis: (%) calc for C₂₈H₂₇F₃N₂O₅PS₃Sb · C_{0.5}H₁Cl₁: C 41.75, H 3.44, N 3.42, S 11.73; found C41.48, H 3.61, N 3.47, S 11.71.

Compound 3.11.



To a solution of **3.8** (0.015 g, 0.032 mmol) in CH₂Cl₂ (2 mL) was added to a CH₂Cl₂ (2 mL) solution of Pt(PPh₃)₄ (0.04 g, 0.032 mmol). The solution turned from yellow to red and was stirred for 10 min at rt. The CH₂Cl₂ was removed *in vacuo*, yielding a red oil. After triturating the red oil with

Et₂O (3 mL) for 10 min. an orange solid precipitated from solution. The Et₂O was decanted off and dried under reduced pressure.

Yield: 77% (0.028 g, 0.024 mmol);

m.p.: 146 - 148 °C .

¹H NMR (CDCl₃, δ (ppm)): 7.29 (t, 6H, aryl, ³J_{HH} = 7.6), 7.21(d, 2H, thienyl, ³J_{HH} = 5.6), 7.10 (m, aryl, 12H), 6.91 (m, 15H, aryl), 6.82 (d, 2H, aryl, ³J_{HH} = 5.5), 3.85 (s, 6H, CH₃);

¹³C{¹H} NMR (CDCl₃, δ (ppm)): 160.9, 133.4, 131.6, 130.9, 129.3, 128.8, 128.7, 127.6, 127.5, 125.9, 123.6, 120.6, 115.4, 55.8;

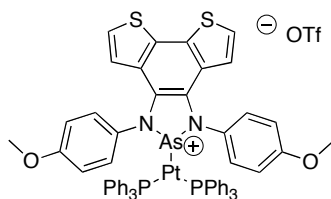
³¹P{¹H} NMR (CDCl₃, δ (ppm)): 47.4 (d, ²J_{P-P} = 490.8, ¹J_{P-Pt} = 2358), 249.5 (t, ²J_{P-P} = 490.8, ¹J_{P-Pt} = 2326);

¹⁹F {¹H} NMR (CDCl₃, δ (ppm)): -78.4;

FT-IR (ranked intensities (cm⁻¹)): 514(5), 528(2), 636(3), 693(3), 743(9), 922(11), 998(14), 1030(4), 1094(10), 1130(8), 1248(1), 1435(7), 1478(15), 1507(2), 1605(12);

FT- Raman (ranked intensities (cm⁻¹)): 174(6), 363(7), 999(3), 1027(12), 1096(14), 1131(2), 1236(3), 1375(1), 1494(11), 1321(15), 1585(5), 1887(8), 2112(13), 2560(10), 3057(9).

Compound 3.12.



To a solution of **3.9** (0.015 g, 0.032 mmol) in CH₂Cl₂ (2 mL) was added to a CH₂Cl₂ (2 mL) solution of Pt(PPh₃)₄ (0.04g, 0.032 mmol). The solution turned from orange to purple and was stirred for 10 min at rt. The CH₂Cl₂ was removed *in vacuo*, yielding a purple oil. After triturating the purple oil

with Et₂O (3 mL) for 10 min a purple solid precipitated from solution. The Et₂O was decanted off and dried under reduced pressure.

Yield: 92% (0.035 g, 0.029 mmol);

d.p.: 225 °C;

¹H NMR (CDCl₃, δ (ppm)): 7.28 (m, 6H, aryl), 7.20 (m, 15H, aryl), 7.07 (m, 15H, aryl), 6.81 (d, 4H, aryl, ³J_{HH} = 8.8), 5.97 (d, 2H, aryl, ³J_{HH} = 5.6), 3.87 (s, 6H, CH₃);

¹³C{¹H} NMR (CDCl₃, δ (ppm)): 156.6, 134.6, 131.3, 129.1, 128.5, 124.5, 123.9, 122.9, 114.5, 55.8;

³¹P{¹H} NMR (CDCl₃, δ (ppm)): 41.9 (s, ¹J_{Pt} = 5347.6);

¹⁹F {¹H} NMR (CDCl₃, δ (ppm)): - 78.3;

FT-IR (ranked intensities (cm⁻¹)): 515(2), 538(10), 636(6), 695(4), 744(7), 1025(5), 1097(11), 1157(8), 1222(12), 1263(1), 1303(13), 1386(14), 1435(9), 1478(15), 1506(3).

3.4 References

- (1) Chivers, T.; Konu, J. *Comments on Inorganic Chemistry* **2009**, *30*, 131-176.
- (2) Prabusankar, G.; Gemel, C.; Parameswaran, P.; Flener, C.; Frenking, G.; Fisher, R. A. *Angew. Chem. Int. Ed.* **2009**, *48*, 5526 - 5529.
- (3) Power, P. P. *Chem. Rev.* **1999**, *99*, 3463-3503.
- (4) Fisher, R. C.; Power, P. P. *Chem. Rev.* **2010**, *110*, 3877-3923.
- (5) Holthausen, M. H.; Weigand, J. J. *J. Am. Chem. Soc.* **2009**, *131*, 14210-14211.
- (6) Scheer, M.; Balazs, G.; Seitz, A. *Chem. Rev.* **2010**, *110*, 4236-4256.
- (7) Romero-Nieto, C.; Durben, S.; Kormos, I. M.; Baumgartner, T. *Adv. Funct. Mater.* **2009**, *19*, 3625-3631.
- (8) Chen, C.; Roland, F.; Kehr, G.; Erker, G. *Chem. Commun.* **2010**, *46*, 3580-3582.
- (9) Stephen, D. W. *Dalton Trans.* **2009**, *17*, 3129-3136.
- (10) Stephan, D. W.; Erker, G. *Angew. Chem. Int. Ed.* **2010**, *49*, 46-76.

- (11) Hill, N. J.; Vargus-Baca, I.; Cowley, A. H. *Dalton Trans.* **2009**, 240-253.
- (12) Perepichka, I., R.; Perepichka, D. F.; Meng, H.; Wudl, F. *Adv. Mater.* **2005**, *17*, 2281-2305.
- (13) Powell, A. B.; Brown, J. R.; Vasudevan, K. V.; Cowley, A. H. *Dalton Trans.* **2009**, 2521-2527.
- (14) Powell, A. B.; Bielawski, C. W.; Cowley, A. H. *J. Am. Chem. Soc.* **2010**.
- (15) Powell, A. B.; Brown, J. R.; Vasudevan, K. V.; Cowley, A. H. *Dalton Trans.* **2009**, 2521-2527.
- (16) Mitsumori, T.; Inoue, K.; Koga, I.; Iwamura, H. *J. Am. Chem. Soc.* **1995**, *117*, 2467-2478.
- (17) Boersma, A. D.; Goff, H. M. *Inorg. Chem.* **1982**, *21*, 581-586.
- (18) Wolf, M. *Adv. Mater.* **2001**, *13*, 545-553.
- (19) Zhang, X.; Chi, Z.; Yang, Z.; Chen, M.; Xu, B.; Zhou, L.; Wang, C.; Zhang, Y.; Liu, S.; Xu, J. *Optical Materials* **2009**, *32*, 94 - 98.
- (20) Spinney, H. A.; Korobkov, I.; DiLabio, G. A.; Yap, G. P. A.; Richeson, D. S. *Organometallics* **2007**, *26*, 4972-4982.
- (21) Spinney, H. A.; Korobkov, I.; Richeson, D. S. *Chem. Commun.* **2007**, 1647-1649.
- (22) Blom, R.; Haaland, A. *J. Mol. Struct.* **1985**, *128*, 21-27.
- (23) Kilah, N. L.; Petrie, S.; Stranger, R.; Wielandt, J. W.; Willis, A. C.; Wild, S. B. *Organometallics* **2007**, *26*, 6106-6113.
- (24) Wielandt, J. W.; Kilah, N. L.; Willis, A. C.; Wild, S. B. *Chem. Commun.* **2006**, 3679-3680.
- (25) Schmidbaur, H.; Bublak, W.; Huber, B.; Muller, G. *Angew. Chem. Int. Ed.* **1987**, *26*, 234-237.
- (26) Probst, T.; Steigelmann, O.; Riede, H.; Schmidbaur, H. *Chem. Ber.* **1991**, *124*, 1089-1093.
- (27) Schmidbaur, H.; Nowak, R.; Steigelmann, O.; Muller, G. *Chem. Ber.* **1990**, *123*, 1221-1226.
- (28) Spinney, H. A.; Korobkov, I.; DiLabio, G. A.; Yap, G. P. A.; Richeson, D. S. *Organometallics* **2007**, *26*, 4972-4982.

- (29) Caputo, C. A.; Jennings, M. C.; Tuononen, H. M.; Jones, N. D. *Organometallics* **2009**, *28*, 990-100.
- (30) Hardman, N. J.; Abrams, M. B.; Pribisko, M. A.; Gilbert, T. M.; Martin, R. L.; Kubas, G. J.; Baker, R. T. *Angew. Chem. Int. Ed.* **2004**, *43*, 1955-1958.
- (31) Burck, S.; Daniels, J.; Gans-Elchler, T.; Gudat, D.; Nattinen, K.; Nieger, M. *ZAAC* **2005**, *631*, 1403-1412.

Chapter 4

4 An N-Heterocyclic carbene containing a benzo[1,2-b:5,6-b']dithiophene backbone: Synthesis and coordination chemistry^Ω

4.1 Introduction

The discovery of conjugated polymers in the 1970's have since drawn significant interest in the field of materials science.¹ Their ability to combine both the electronic and photophysical properties of inorganic semi-conductors along with the flexibility and processability of organic plastics have resulted in their wide use in many applications.¹⁻³ Conjugated organic polymer-based materials have found broad applicability in light emitting diodes (LED) or light emitting electrochemical cells (LEC), plastics, lasers, solar cells, field effect transistors and sensors.^{4,5} More specifically, thiophene based polymers are one of the most studied classes of organic conjugated polymers because of their synthetic versatility and their ability to be polymerized both chemically and electrochemically.⁵⁻⁷ It has been demonstrated that the incorporation of transition metals or main group elements into these thiophene-based systems can significantly heighten their conductivity and optical properties, thus providing a potential handle by which one can tune the polymers for specific applications.⁸ Despite functional modifications of thiophene being well established in the literature, the synthetic challenges of designing a thiophene containing scaffold to support either metals or main group elements has proven to be challenging because of their rigid coordination sites, difficult carbon-carbon coupling chemistry and lengthy work-up procedures.^{9,10}

Inspiration for this work has come from the widely used bis(arylimino)acenaphthene (**i**) which has been shown to readily coordinate s-, p-, and d-block elements.¹¹ We sought to synthesize a similar type of framework containing two fused thiophene rings in the

^Ω A version of this chapter has been previously published in Price, J. T., Jones, N. D. and Ragogna, P. J., *Inorg. Chem.* **2012**, *51*, 6776, and has been reproduced with permission.

backbone, supporting two flanking α -diamines (**3.4**). This system would allow for chemical versatility at the donor nitrogen sites while maintaining conjugation between the thiophene fragments in the backbone, which have the potential to undergo polymerization in a subsequent step.

N-Heterocyclic carbenes (NHC) have been extensively studied over the last two decades because of their ability to act as a strong two-electron donor for transition metals as well as stabilizing highly reactive main group species.¹²⁻²⁰ The use of an NHC would be an ideal fragment within a poly(thiophene) system because of its ability to act as a strong Lewis base.²¹ This would enable the facile incorporation of both Lewis acidic transition metals and main group elements into a polymeric system and enhance or modify the electronic and photophysical properties of the end compound.^{22,23} Incorporating a NHC into a conjugated polymer would allow for chemical versatility that is desirable but often difficult to achieve. While there are many examples of polymeric NHCs,^{16,24-29} there is only one recent example combining an NHC within a polythiophene framework, in which the NHC is orthogonal to the polymer backbone (**ii**, Figure 4.1). Further functionalization of the system can be achieved *via* coordination of the NHC to a metal center.^{30,31} This is a substantial development in metal functionalized NHC polymers, however one downfall is that the thiophene rings are not conjugated. Conjugated thiophene polymers are desirable because they possess a characteristic reduced band gap and one of the most successful methods of achieving this has been the application of a fused thiophene ring system, giving a quinoidal structure (**iii**), resulting in significant reduction in the band gap.¹

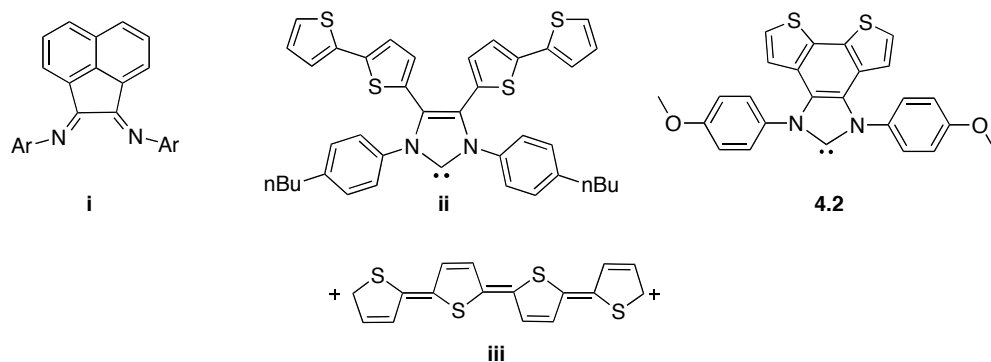


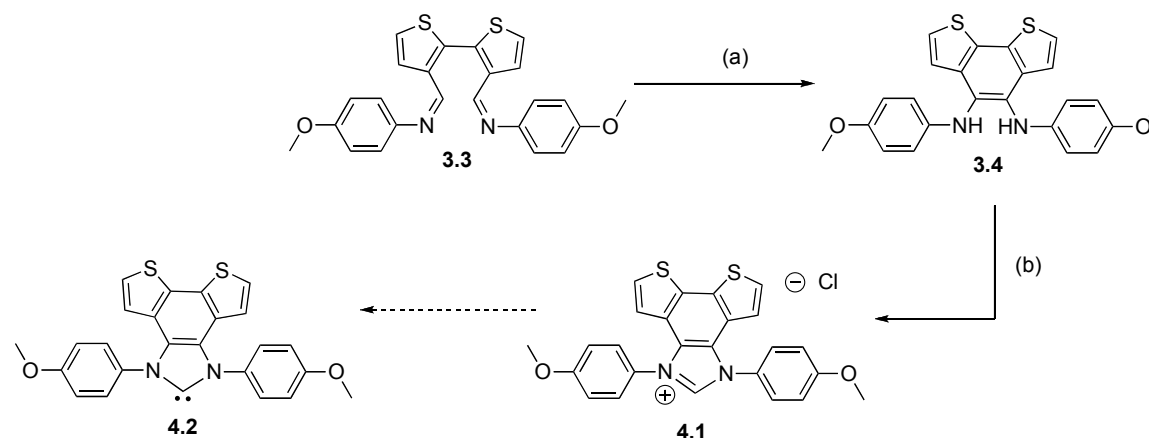
Figure 4.1: (i) bis(imino)acenaphthene, (ii) NHC orthogonal to the thiophene rings, quinoidal structure of tert-thiophene(iii) and our NHC (4.2).

In this context, we report the synthesis of the first bithiophene-annulated backbone substituted imidazole-2-ylidene, **4.1**. The N-Heterocyclic carbene (**4.2**) can act as a Lewis base and form adducts with the Lewis acidic BPh_3 and metal complexes with both silver and rhodium. The donor ability of **4.2** was also determined by measuring IR stretching frequencies of the carbonyl ligands in $(\text{NHC})\text{Rh}(\text{CO})_2\text{Cl}$ (**4.8**). The photophysical properties of all compounds have been investigated, where the absorbance and emission is dominated by the benzo[1,2-b:5,6-b']dithiophene backbone and not by substitution at the carbenic carbon.

4.2 Results and Discussion

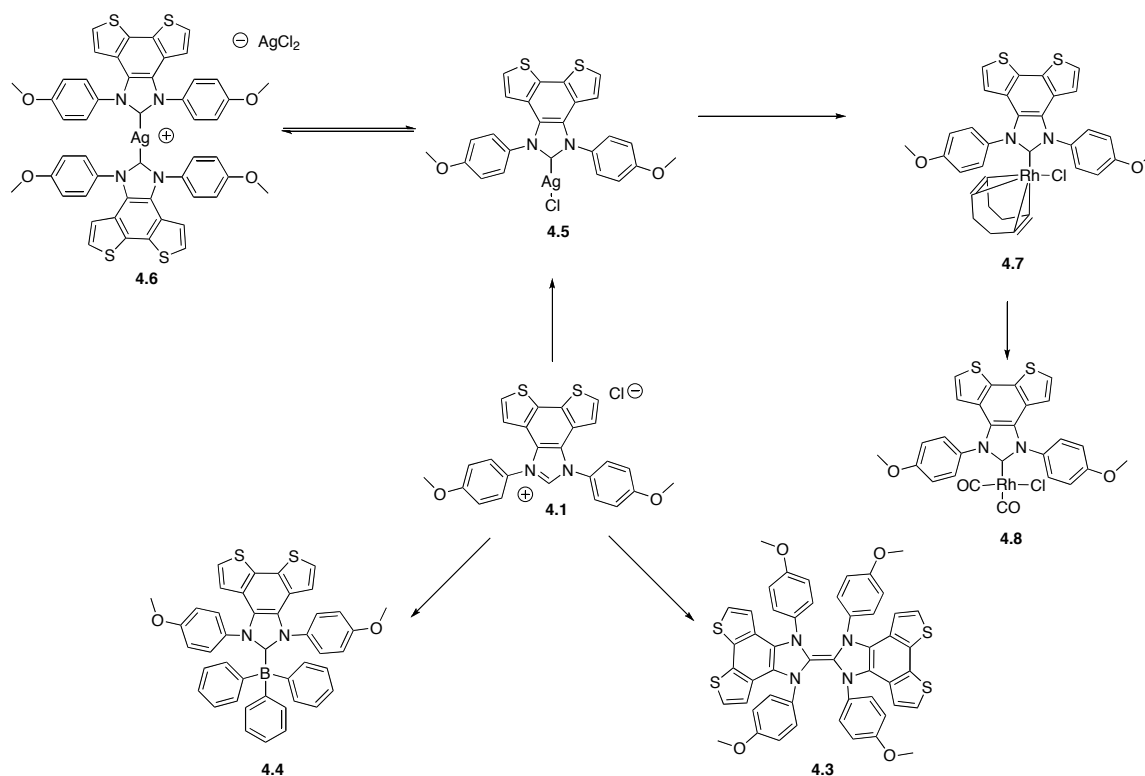
4.2.1 Synthesis

The precursor (**3.4**) to the imidazolium salt (**4.1**) was synthesized *via* a benzoin condensation of the diimine (**3.3**) using NaCN in dimethylformamide (DMF) yielding the diamine as described in Chapter 3. Compound **3.4** was placed in a pressure tube, with 2 stoichiometric equivalents of 4M HCl in dioxane and triethylorthoformate at 145 °C for 2 min. (Scheme 4.1). The yellow precipitate was isolated by filtration and washed with Et_2O . Upon examination of the redissolved powder by ^1H NMR spectroscopy, the imidazolium proton was observed downfield ($\delta_{\text{H}} = 10.44$) as well as the disappearance of the NH proton ($\delta_{\text{H}} = 5.63$). Single crystals suitable for X-ray diffraction studies were grown from vapor diffusion of Et_2O into a concentrated CH_2Cl_2 solution of the bulk powder at rt. confirming the synthesis of **4.1** (Figure 4.2).



Scheme 4.1: Synthesis of the imidazolium salt **4.1**; a) DMF, NaCN, rt., 48 h; b) 4M HCl, HC(OEt)₃, 145°C, 2 min.

Compound **4.3** was synthesized from a 1:1 stoichiometric reaction between LiHMDS (lithium bis(trimethylsilyl)amide) and **4.1** in toluene. This resulted in a color change from an orange to yellow solution with the formation of a white precipitate. The white precipitate was removed by centrifugation, the yellow solution was decanted and upon concentration of the supernatant, a yellow solid formed. Examination of the redissolved solid by ¹H NMR spectroscopy revealed the imidazolium proton ($\delta_{\text{H}} = 10.44$) had disappeared and the aryl peaks shifted significantly upfield ($\Delta\delta_{\text{H}} = 0.6$). The successful deprotonation of the imidazolium salt was sensitive to the base employed; when either the sodium or potassium salts of HMDS were used, multiple products were observed by ¹H NMR spectroscopy. In solution, an equilibrium between the free carbene and the dimer was observed. This was confirmed through ¹³C {¹H} NMR spectroscopy and the addition of a Lewis acid. Heating the dimer to 80 °C in a solution of C₆D₆ the carbenic carbene was observed ($\delta_{\text{C}} = 214.6$). X-ray quality single crystals of compound **4.3** were grown from vapor diffusion of a pentane/benzene solution confirming the connectivity (Scheme 4.2, Figure 4.3).



Scheme 4.2: Synthetic scheme of the bithiophene substituted NHCs.

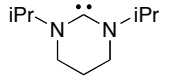
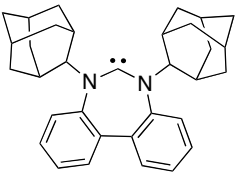
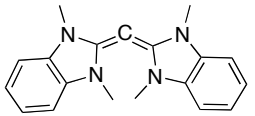
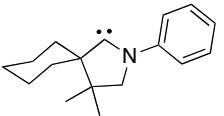
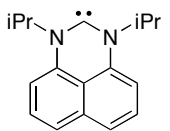
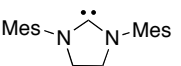
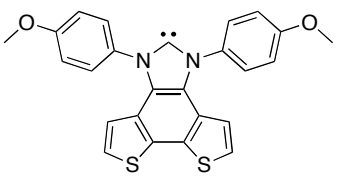
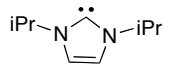
Given the observed dimerization of the NHC, we sought to trap the free carbene by the addition of a Lewis acid (BPh_3). A THF solution of a 1:1:1 mixture of the imidazolium salt, LiHMDS and triphenylborane was stirred at room temperature for 45 min., where the solution turned from orange to yellow along with the formation of a white precipitate. The precipitate was separated by centrifuge and the volatiles were removed under reduced pressure yielding a yellow powder. Examination of the redissolved yellow solid by ^1H NMR spectroscopy revealed that the imidazolium proton ($\delta_{\text{H}} = 10.44$) was again absent. Signals belonging to the thiophene ring were shifted upfield ($\delta_{\text{H}} = 7.48$ and $\delta_{\text{H}} = 6.79$ to $\delta_{\text{H}} = 7.19$ and $\delta_{\text{H}} = 5.88$). The $^{11}\text{B}\{^1\text{H}\}$ NMR spectrum showed a peak with an upfield shift from $\delta_{\text{B}} = 86.0$ for free BPh_3 to $\delta_{\text{B}} = -8.2$ and is similar to other NHCs coordinated to triphenylborane.³² Single crystals were grown from vapor diffusion of *n*-pentane/ CH_2Cl_2 and X-ray diffraction studies confirmed the synthesis of the carbene \rightarrow borane adduct (**4.4**, Scheme 4.2, Figure 4.3).

Access to the silver NHC complex (**4.5**) was obtained by metallation of the imidazolium chloride using Ag₂O. Upon collection of the ¹H NMR spectrum, the imidazolium proton ($\delta_{\text{H}} = 10.44$) was not observed and the aromatic signals shifted significantly upfield, reminiscent of the carbene triphenylborane adduct. The signal for the carbenic carbon was lacking in the ¹³C{¹H} NMR spectrum at room temperature, suggesting a fast exchange in solution between **4.5** and **4.6** due to the silver carbon bond lability.³³ This has previously been observed in other reported silver NHC species.^{31,33} Cooling the solution to -50 °C and recollecting the ¹³C{¹H} NMR spectrum, two sets of doublets were observed as a result of carbon silver coupling ($\delta_{\text{C}} = 183.9$, $^1J_{^{13}\text{C} - ^{107}\text{Ag}} = 226.3$ Hz and $^1J_{^{13}\text{C} - ^{109}\text{Ag}} = 296.1$ Hz). The NHC bis-carbene complex, (**4.6**) was also detected by ESI mass spectrometry providing further evidence that in solution the bis-carbenic species **4.6** exists. Single crystals of the silver complex containing one NHC ligand were grown in the dark from the vapor diffusion of Et₂O into CH₂Cl₂ (Scheme 4.2, Figure 4.3).

Synthesizing the NHC rhodium complex (**4.8**) provided the opportunity to evaluate the donor properties of my NHC ligand relative to others. The (NHC)Rh(COD)Cl precursor (**4.7**) was made by the transmetalation of **4.5** with [Rh(COD)Cl]₂ (COD = 1,5 cyclooctadiene) in refluxing toluene for 12 h.³⁴ In comparison to the starting material, the aryl protons shifted downfield in the ¹H NMR spectrum ($\delta_{\text{H}} = 8.04$ to 8.51) and the vinyl protons belonging to the COD ligand were now distinct as separate multiplets ($\delta_{\text{H}} = 3.04$ (*cis*); $\delta_{\text{H}} = 4.00$ (*trans*)). Upon examination of the ¹³C{¹H} NMR spectrum, the COD C_{CH} for the rhodium complex **4.7**, two doublets ($\delta_{\text{C}} = 67.9$, $^1J_{^{13}\text{C}-^{103}\text{Rh}} = 14.9$ Hz, *trans* to the carbene) and ($\delta_{\text{C}} 98.1$, $^1J_{^{13}\text{C}-^{103}\text{Rh}} = 6.2$ Hz, *cis* to the carbene) and the C_(carbene) could only be observed at -40 °C appearing as a doublet downfield ($\delta_{\text{C}} = 191.3$, $^1J_{^{13}\text{C} - ^{103}\text{Rh}} = 49.2$ Hz). Single crystals suitable for X-ray diffractions studies were grown from vapour diffusion of Et₂O into a concentrated CH₂Cl₂ solution of **4.7** could be obtained confirming the connectivity, however the quality of the full structure solution does not permit the discussion of the metrical parameters. The synthesis of **4.8**, was accomplished by bubbling CO gas into a CH₂Cl₂ solution of **4.7** over a period of 2 h. The yellow solution was concentrated under reduced pressure, yielding a yellow powder. The ¹H NMR spectrum of the redissolved yellow powder revealed that the COD peaks were no

longer present and the aryl peaks appeared as a broad singlet. Similar to the other metal-NHC complexes, the carbenic carbon, as well as the carbonyl carbons were not observed at room temperature. When the sample was cooled to -50 °C three sets of doublets appeared downfield, the C_{CO} ($\delta_C = 185.4$, $J_{^{13}C-^{103}Rh} = 55.3$ Hz and $\delta_C = 180.8$, $J_{^{13}C-^{103}Rh} = 42.9$ Hz) and the $C_{carbene}$ ($\delta_C = 182.4$, $J_{^{13}C-^{103}Rh} = 75.2$ Hz). The relative donor ability of the bithiophene NHC (**4.2**) was determined by the IR stretching frequencies of the carbonyl ligands and compared to other (NHC)Rh(CO)₂Cl complexes. The IR stretching frequencies of **4.8** (2074 cm⁻¹ and 1991 cm⁻¹, $\nu_{avg.} = 2033$ cm⁻¹) indicate that **4.8** is a stronger donor than the saturated and unsaturated 5-membered NHCs, however not quite as strong as the acyclic and 6-membered NHC derivatives (Table 4.1).

Table 4.1: Average CO stretching frequencies (ν_{avg}) of various (carbene)Rh(CO)₂Cl Complexes.

Entry	Carbene	$\nu_{\text{ave}}/\text{cm}^{-1}$	Ref.	Entry	Carbene	$\nu_{\text{ave}}/\text{cm}^{-1}$	Ref.
1		2012	35	5		2033	36
2		2014	37	6		2036	38
3		2020	39	7		2038	40
4		2033	This work	8		2041	40

4.2.2 Photophysical properties

The photophysical properties of the NHCs were examined and are summarized in Figure 4.2 and Table 4.2. All of the compounds were yellow in colour and absorbed UV-light in the 300 - 400 nm region. Examination of the UV-spectrum for compound **4.1**, two λ_{max} values at 310, 323 nm and a broad peak of lower intensity at 410 nm were observed. A hypsochromic shift upon the formation of the enetetramine, **4.3**, was observed with λ_{max} values of 282, 308, 327, 342 nm along with a shoulder at 416 nm respectively. These bands are attributed to both $\pi - \pi^*$ transitions from the phenyl and thiophene rings and $n - \pi^*$ transitions from thiophene. Upon coordination to a metal centre, a third absorption band appears at a lower energy for compound **4.4**, ($\lambda_{\text{max}} = 307, 320$ and 334 nm) and compound **4.7**, ($\lambda_{\text{max}} = 305, 318, 332$ nm). Compounds **4.7** and **4.8** also have 3 intense bands similar to those observed in compounds **4.4** and **4.5** in addition to a smaller band at a lower energy appearing at 400 nm for compound **4.4** and 367 nm for compound **4.5**. These peaks are also attributed to both the $\pi - \pi^*$ and $n - \pi^*$ transitions from the phenyl and thiophene rings. Compounds **4.1**, **4.3**, **4.4** and **4.5** fluoresce when irradiated with light at 300 nm. Compound **4.1** fluoresces at the longest wavelength (460 nm) whereas compounds **4.3** - **4.5** had two fluorescent bands in the blue region, between 330 and 360 nm.

Table 4.2: Photophysical properties of compounds **4.1**, **4.3** - **4.8**.

Compound	λ_{abs} nm	ϵ_{max} L mol ⁻¹ cm ⁻¹	λ_{em} (nm)
4.1	310	1.5×10^4	460
	323	1.6×10^4	
	427	4.4×10^3	
4.3	282	3.3×10^4	348
	308	2.5×10^4	362
	327	1.8×10^4	
	342	1.7×10^4	
4.4	307	1.7×10^4	336
	320	1.8×10^4	350
	334	1.8×10^4	364(sh)
4.5	305	1.6×10^4	333
	318	1.7×10^4	347
	332	1.6×10^4	364(sh)
4.7	293	1.5×10^4	-
	308	1.3×10^4	
	344	1.2×10^4	
	397	2.6×10^3	
4.8	307	1.8×10^4	-
	320	1.7×10^4	
	332	1.8×10^4	
	370	1.5×10^3	

All UV-visible spectra were collected in a 5×10^{-5} M concentration in CH₂Cl₂ with the exception of compound **4.3**, which was done in a 3.75×10^{-5} M solution of toluene.

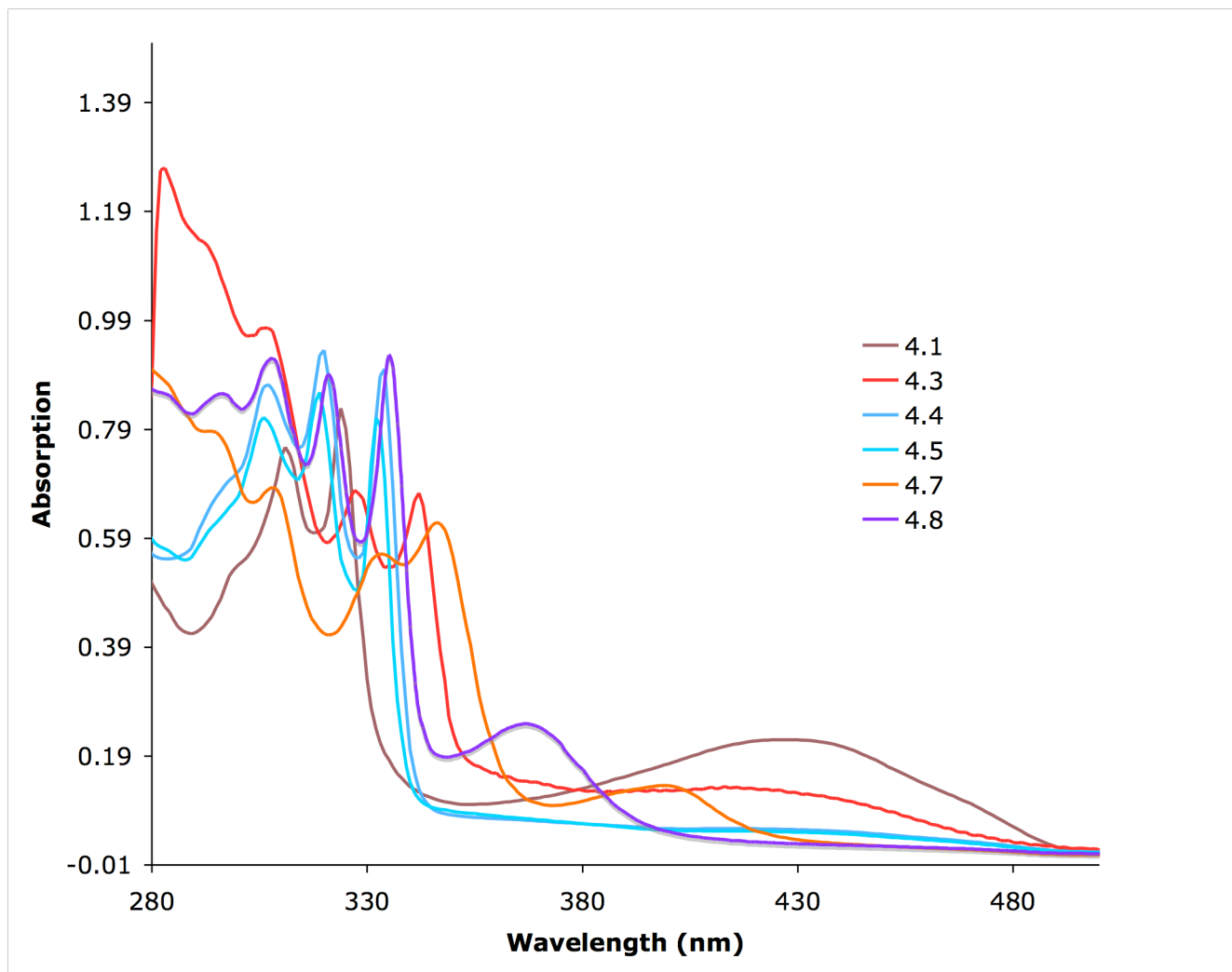


Figure 4.2: UV-visible spectra of compounds **4.1**, **4.4**, **4.5**, **4.7** and **4.8** in CH_2Cl_2 and compound **4.3** in toluene.

4.2.3 X-ray crystallography

Single crystals of compounds **4.1**, **4.3**, **4.4** and **4.5** were grown by vapor diffusion using various solvent combinations and their solid-state structures were determined by X-ray diffraction studies. The relevant crystallographic data, and connectivity for compounds **4.1**, **4.3**, **4.4** and **4.5** are detailed in Table 4.3 and Figure 4.3, respectively. Examination of the solid-state structures of compounds **4.1**, **4.3**, **4.4** and **4.5** revealed that the metrical parameters of the C₂N₂ ring are consistent with two C - N single bonds (1.386 - 1.405 Å *cf.* 1.420 Å (avg.) and a C - C double bond (1.368 - 1.389 Å *cf.* 1.382 Å (avg.) in the free ligand (**3.4**)). Upon coordination of the NHC to a metal center and in the NHC dimer, the metrical parameters of the C₂N₂ ring remain unchanged.

The NHC dimer, **4.3** contains a shortened C - C double bond of 1.354(11) Å between the carbenic carbons C(7) - C(6). There is a slight contraction in the bond angle between N(3) - C(7) - N(2) and N(4) - C(6) - N(1) (107.9(6)° and 108.2(6)°) in comparison to that found in the imidazolium salt 109.9(2)°. The sum of the bond angles around N(1) and N(4) ($\sum_{\text{ang}} = 339.2$ and 339.6) are congruous with a pyramidal geometry whereas the geometry around N(2) and N(3) ($\sum_{\text{ang}} = 352.1$ and 349.2) is more consistent with a trigonal planar arrangement.

Compound **4.4** crystallizes with two independent molecules in the asymmetric unit and consists of a four coordinate boron(III) center with a C₃ propeller like geometry about the boron atom ($\sum_{\text{ang}} = 332.8^\circ$). The C(6) - B(1) bond length is 1.658(4) Å and a slight elongation in the C - N bonds (1.393(3)Å *cf.* 1.378 Å (avg.)) in the imidazole-2-ylidene from **4.1** is observed, along with a contraction of the N - C - N bond angle (104.3(2)° *cf.* 109.9(2)°).

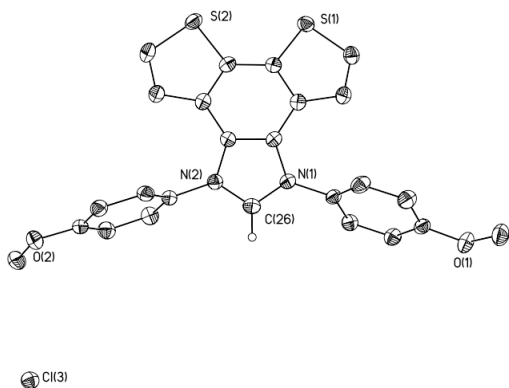
Examination of the (NHC)AgCl complex, **4.5**, consists of a two coordinate silver (I) ion in a linear environment with a C - Ag - Cl bond angle of 179.42(4)°. The C - Ag bond length is 2.082(1) Å, which is in accordance with other silver mono or bis-carbene complexes. The Ag - Cl bond length is 2.335(4) Å, and is within the range of other silver(I) chloride complexes reported. In the solid-state, the silver complex is monomeric

with no evidence of argentophilic (Ag(I)...Ag(I)) interactions. All distances between Ag(I) centers are greater than 3.44 Å, the sum of twice the van der Waals radius of Ag(I).^{34,41}

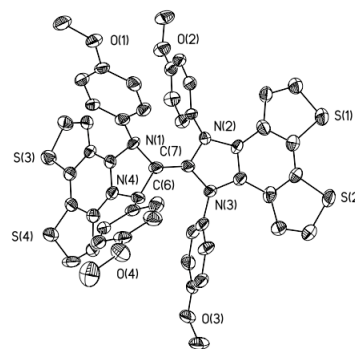
Table 4.3: Crystal data for compounds **4.1**, **4.3**, **4.4** and **4.5**.

Compound	4.1	4.3	4.4	4.5
Empirical formula	C ₂₇ H ₂₃ N ₂ Cl ₅ O ₂ S ₂	C ₅₀ H ₄₀ N ₄ O ₄ S ₄	C ₄₃ H ₃₄ N ₂ O ₂ S ₂ B ₁	C ₂₆ H ₂₀ N ₂ Ag ₁ Cl ₁ O ₂ S ₂
FW (g/mol)	648.84	947.55	684.64	670.78
Crystal system	Triclinic	Triclinic	Monoclinic	Monoclinic
Space group	P $\bar{1}$	P $\bar{1}$	P2 ₁ /c	P2 ₁ /c
a (Å)	9.2020(4)	10.3630(7)	20.285(4)	10.3668(4)
b (Å)	9.2504(4)	14.7130(11)	12.280(3)	17.3763(6)
c (Å)	17.1345(7)	16.9285(12)	28.040(6)	15.0656(5)
α (deg)	95.675(2)	93.514(2)	90	90
β (deg)	91.790(2)	96.846(2)	105.45(3)	103.229(2)
γ (deg)	92.530(2)	99.525(2)	90	90
V (Å ³)	1449.03(11)	2518.7(3)	6832(2)	2639.30(16)
Z	2	2	8	4
D _c (mg m ⁻³)	1.487	1.249	1.351	1.688
R _{int}	0.0421	0.0690	0.0522	0.0261
R1[I > 2σI] ^a	0.0528	0.1077	0.1126	0.0379
wR2(F ²) ^a	0.1059	0.2094	0.1080	0.0607
GOF(S) ^a	1.030	1.078	1.004	1.021

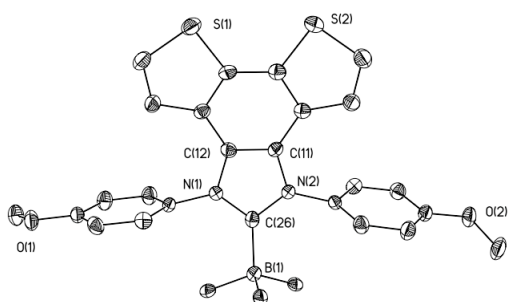
^aR1(F[I > 2(I)]) = $\sum ||F_o| - |F_c| || / \sum |F_o|$; wR2(F² [all data]) = $[w(F_o^2 - F_c^2)^2]^{1/2}$; S(all data) = $[w(F_o^2 - F_c^2)^2 / (n - p)]^{1/2}$ (n = no. of data; p = no. of parameters varied; w = 1/[σ²(F_o²) + (aP)² + bP] where P = (F_o² + 2F_c²)/3 and a and b are constants suggested by the refinement.



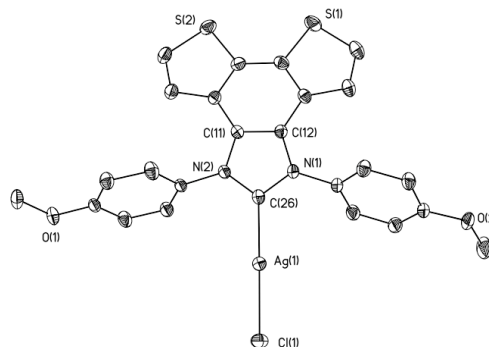
4.1



4.3



4.4



4.5

Figure 4.3: Solid state structures of compounds **4.1**, **4.3**, **4.4** and **4.5**. Ellipsoids are drawn to 50% probability and hydrogen atoms have been removed for clarity.

4.2.4 Conclusions

The successful synthesis of a novel imidazolium salt with a benzo[1,2-b:5,6-b']dithiophene backbone was synthesized. The imidazolium salt was generated from a diamine precursor using a sealed pressure tube and was complete in less than 5 minutes. The NHC could be used as a ligand for both BPPH_3 and Ag(I) salts in which rapid exchange was observed in solution between $(\text{NHC})\text{AgCl}$ and $(\text{NHC})_2\text{Ag}$ due to the labile C - Ag bond. The Ag(I) salt was also used as a transfer reagent to synthesize the $(\text{NHC})\text{Rh}(\text{COD})\text{Cl}$ complex, which was utilized in the synthesis of the $(\text{NHC})\text{Rh}(\text{CO})_2\text{Cl}$. A comparison of the donor abilities of our NHC compared to a selection of those reported, demonstrated that **4.2** is a stronger Lewis base than a 5-

membered NHC, but weaker than the acyclic and 6-membered NHCs. Upon examination of the photophysical properties all of the compounds absorbed in the UV-visible region between 300 and 360 nm whereas only compounds **4.1** and **4.3** - **4.5** fluoresced when excited at 300 nm light. Future work will encompass the extension of the thiophene backbone and further exploring its potential in fluorescent and polymeric materials.

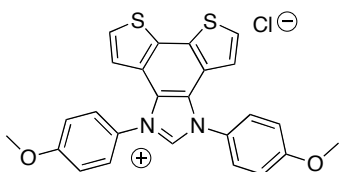
4.3 Experimental

4.3.1 General experimental

General synthetic and crystallography experimental details can be found in Appendix 1.

4.3.2 Synthetic procedures

Compound 4.1



In a 10 mL pressure tube, triethylorthoformate (6.00 mL), **3.4** (2.00 g, 4.60 mmol) and 4M HCl in dioxane (2.30 mL, 9.20 mmol) stirred at room temperature for 5 min. The reaction mixture was then heated to 145°C for 2 min. The resulting orange powder was isolated by filtration and washed with

Et₂O (3 x 5 mL).

Yield: 72 % (1.60 g, 3.38 mmol);

d.p.: 156 - 158 °C;

¹H NMR (CDCl₃ δ (ppm)): 10.44 (s, 1H, CH), 8.04 (d, 4H, aryl, ³J_{HH} = 8.0 Hz), 7.48 (d, 2H, thienyl, ³J_{HH} = 5.2 Hz), 7.16 (d, 4H, aryl, ³J_{HH} = 8.4 Hz), 6.79 (d, 2H, thienyl, ³J_{HH} = 5.6 Hz), 3.92 (s, 6H, CH₃);

¹³C{¹H} NMR (CDCl₃ δ (ppm)): 161.6, 140.0, 134.6, 128.7, 127.2, 126.0, 125.4, 122.7, 120.2, 115.3, 55.7;

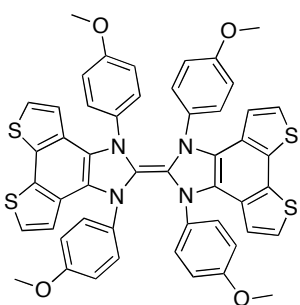
FT-IR (ranked intensity (cm⁻¹)): 656(10), 700(14), 752(8), 838(3), 879(6), 1027(7), 1169(2), 1257(7), 1305(11), 1366(15), 1442(13), 1507(1), 1556(4), 1609(9), 3019(12);

FT-Raman (ranked intensity (cm⁻¹)): 659(12), 796(5), 1123(13), 1238(10), 1339(8), 1363(2), 1405(3), 1433(9), 1462(6), 1491(1), 1586(4), 1608(7), 3099(11);

HRMS: (C₂₅H₁₉N₂O₂S₂)⁺ Calcd (found) 443.5600 (443.8661);

Elemental Analysis (%) calc for C₂₅H₁₉N₂O₂S₂Cl·0.5CH₂Cl₂: C 58.73, H 3.87, N 5.37, S 12.61; found C 58.74, H 4.45, N 5.50, S 12.80.

Compound 4.3



A 2 mL THF solution of LiHMDS (0.70 g, 0.42 mmol) was added to a 5 mL toluene solution of **4.1** (0.20 g, 0.42 mmol) at rt. The reaction mixture stirred at room temperature for 2 h. Upon completion a white precipitate was removed by centrifugation and the resulting yellow solution was concentrated yielding a yellow solid.

Yield: 48 % (0.09 g, 0.20 mmol);

m.p.: 147 - 150 °C;

¹H NMR (C₆D₆ δ (ppm)): 7.25 (d, 4H, aryl, ³J_{HH} = 8.9), 6.87 (d, 2H, thienyl, ³J_{HH} = 5.5), 6.71 (d, 2H, thienyl, ³J_{HH} = 5.5), 6.53 (d, 4H, aryl, ³J_{HH} = 8.9), 3.22 (s, 6H, CH₃);

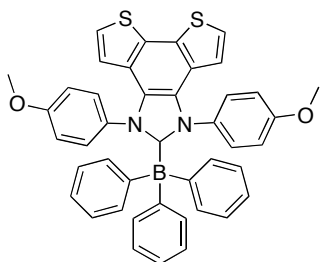
¹³C{¹H} NMR (C₆D₆ δ (ppm)): 156.9, 138.7, 132.6, 129.1, 128.9, 128.1, 126.6, 124.9, 124.0, 121.8, 113.6, 54.5;

FT-IR (ranked intensity (cm⁻¹)): 551(7), 599(13), 634(15), 730(6), 820(4), 856(12), 1034(3), 1104(14), 1176(5), 1246(2), 1298(8), 1366(9), 1463(10), 1505(1), 1583(11);

HRMS: (C₅₀H₃₇N₄O₄S₄)⁺ Calcd (found) 885.1700 (885.1698);

Elemental Analysis (%) calc for C₅₀H₃₆N₄O₄S₄: C 67.85, H 4.10, N 6.33, S 14.40; found C 67.10, H 4.26, N 5.98, S 14.17.

Compound 4.4



A 2 mL THF solution of LiHMDS (0.14 g, 0.63 mmol) was added dropwise to a 5 mL THF slurry of **4.1** (0.30 g, 0.63 mmol). The reaction mixture stirred for 10 min after which a 3 mL THF solution of B(C₆H₅)₃ (0.15 g, 0.63 mmol) was added. The reaction stirred at rt. for 1 h. The white precipitate was removed by centrifugation and the resulting yellow

solution was concentrated yielding a yellow powder.

Yield: 70 % (0.30 g, 0.43 mmol);

m.p.: 136 - 138 °C;

¹H NMR (CDCl₃ δ (ppm)): 7.19 (d, 2H, thienyl, ³J_{HH} = 5.2 Hz), 7.07 (d, 6H, aryl, ³J_{HH} = 6 Hz), 6.88 (m, 12H, aryl), 6.50 (d, 4H, aryl, ³J_{HH} = 8.8 Hz), 5.88 (d, 2H, thienyl, ³J_{HH} = 5.2 Hz), 3.77 (s, 6H, CH₃);

$^{13}\text{C}\{^1\text{H}\}$ NMR (CDCl_3 δ (ppm)): 159.5, 135.8, 132.5, 129.6, 127.6, 127.5, 126.1, 125.6, 123.3, 123.1, 120.7, 113.9, 55.4;

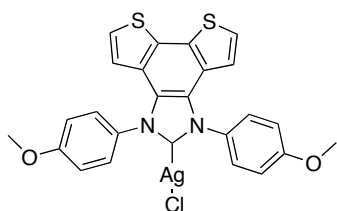
$^{11}\text{B}\{^1\text{H}\}$ NMR (CDCl_3 δ (ppm)): -8.2 (br. s);

FT-IR (ranked intensity (cm^{-1})) ν = 644(11), 706(10), 732(2), 821(5), 897(6), 1027(4), 1107(15), 1167(8), 1251(3), 1300(7), 1361(12), 1440(14), 1510(1), 3031(13) cm^{-1} ;

HRMS: ($\text{C}_{43}\text{H}_{34}\text{N}_2\text{O}_2\text{S}_2\text{BNa}$)⁺ Calcd (found) 707.1974 (707.2006);

Elemental Analysis (%) calc for $\text{C}_{43}\text{H}_{34}\text{N}_2\text{O}_2\text{S}_2\text{B}$: C 74.07, H 5.13, N 4.32, S 9.89; found C 74.53, H 4.86, N 4.05, 9.24.

Compound 4.5



A 5 mL CH_2Cl_2 solution of **4.1** (1.00 g, 2.10 mmol) was added dropwise to a 5 mL CH_2Cl_2 slurry of Ag_2O (0.24 g, 1.05 mmol). The reaction stirred at rt. over 4 Å molecular sieves in the dark for 48 h. The yellow powder was isolated

by filtration and washed with Et_2O (3 x 5 mL).

Yield: 82 % (1.22 g, 2.08 mmol);

d.p.: 195 - 197 °C;

^1H NMR (CDCl_3 δ (ppm)): 7.52 (d, 4H, aryl, $^3J_{\text{HH}} = 8.8$ Hz), 7.38 (d, 2H, thienyl, $^3J_{\text{HH}} = 5.6$ Hz), 7.14 (d, 4H, aryl, $^3J_{\text{HH}} = 8.8$ Hz), 6.67 (d, 2H, thienyl, $^3J_{\text{HH}} = 5.6$ Hz), 3.95 (s, 6H, CH_3);

$^{13}\text{C}\{^1\text{H}\}$ NMR (CDCl_3 δ (ppm)): 160.9, 132.3, 131.3, 128.8, 127.8, 126.0, 123.6, 115.3, 55.8;

$^{13}\text{C}\{^1\text{H}\}$ NMR (- 50°C, CDCl_3 δ (ppm)): 183.9 ($^1J_{^{13}\text{C} - ^{107}\text{Ag}} = 226.3$ Hz and $^1J_{^{13}\text{C} - ^{109}\text{Ag}} = 296.1$ Hz).

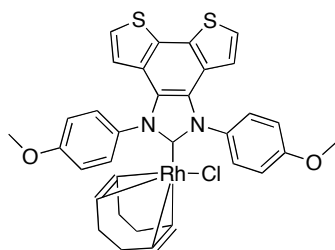
FT-IR (ranked intensity (cm^{-1})): 640 (12), 737(4), 802(9), 835(3), 887(6), 1027(5), 1104(11), 1164(8), 1251(2), 1301(2), 1333(15), 1441(15), 1513(1), 1607(10), 3060(12);

FT-Raman (ranked intensity (cm^{-1})): 640(12), 737(4), 802(9), 835(3), 887(6), 1027(5), 1104(11), 1164(8), 1251(2), 1301(7), 1333(15), 1441(14), 1513(1), 1607(10), 3060(12);

HRMS: ($\text{C}_{50}\text{H}_{36}\text{N}_4\text{O}_4\text{S}_4\text{Ag}$)⁺ Calcd (found) 991.0654 (991.0697);

Elemental Analysis (%) calc for $\text{C}_{50}\text{H}_{38}\text{N}_4\text{O}_4\text{S}_4\text{Ag}$: C 51.16, H 3.26, N 4.77, S 10.93; found C 51.45, H 2.77, N 4.70, S 10.74.

Compound 4.7^Ω



A 10 mL toluene solution of compound **4.5** (0.12 g, 0.20 mmol) and [Rh(cod)Cl]₂ (0.10 g, 0.20 mmol) was heated to 120 °C in a pressure tube in the dark for 12 h. Upon completion the yellow reaction mixture was filtered to remove the salt and concentrated yielding a yellow powder.

Yield: 87 % (0.12 g, 0.17 mmol);

d.p.: 164 °C;

¹H NMR (CDCl₃ (δ (ppm)): 8.51 (dd, 2H, aryl, ³J_{HH} = 8.7, ⁴J_{HH} = 2.6), 7.44 (dd, 2H, aryl, ³J_{HH} = 8.5, ⁴J_{HH} = 2.6), 7.31 (d, 2H, thienyl, ³J_{HH} = 5.5), 7.27 (dd, 2H, aryl, ³J_{HH} = 8.7, ⁴J_{HH} = 2.9), 7.12 (dd, 2H, aryl, ³J_{HH} = 8.5, ⁴J_{HH} = 2.9), 6.72 (d, 2H, thienyl, ³J_{HH} = 5.5), 4.80 (t, 2H, COD, ³J_{HH} = 2.96), 4.00 (s, 6H, CH₃), 3.04 (t, 2H, COD, ³J_{HH} = 2.40), 1.87 (m, 2H, COD), 1.62 (m, 6H, COD);

¹³C{¹H} NMR (CDCl₃ (δ (ppm)): 159.9, 132.2, 131.6, 130.5, 128.5, 128.2, 125.3, 122.6, 120.8, 114.0, 98.1 (¹J_{C-Rh} = 6.2), 68.0 (¹J_{C-Rh} = 14.5), 55.7;

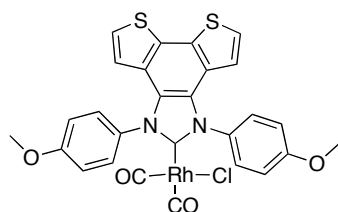
¹³C {¹H} NMR (CDCl₃ δ (ppm)) at -50 °C: 191.3 (¹J_{Carbene-Rh} = 50.1);

FT-IR (ranked intensity (cm⁻¹)): 557(9), 640(13), 702(3), 736(4), 802(5), 835(10), 887(12), 1033(7), 11170(8), 1250(2), 1302(3), 1332(6), 1440(14), 1458(15), 1513(1) cm⁻¹;

FT-Raman (ranked intensity (cm⁻¹)): 440(3), 557(13), 797(6), 1119(15), 1233(14), 1284(9), 1303(12), 1361(7), 1400(4), 1464(5), 1495(2), 1587(11), 1609(8), 3103(10);

Elemental Analysis (%) calc for C₃₃H₂₇N₂O₂S₂ClRh: C 57.77, H 3.97, N 4.08, S 9.35; found C 56.65, H 4.25, N 3.78, S 9.55.^Ω

Compound 4.8



A 25 ml flask was charged with a 10 mL CH₂Cl₂ solution of **4.7** (0.80 g, 0.12 mmol) and CO_(g) was bubbled through for 2 h at rt. Upon completion the reaction mixture was concentrated yielding a yellow oil. The yellow oil was triturated with hexanes

^Ω Several attempts were made to collect the elemental analysis but carbon was consistently low. ¹H NMR verifying its synthesis can be found in Appendix 3.

precipitating a yellow solid. The hexanes were decanted off and the yellow solid dried in *vacuo*.

Yield: 58 % (0.045 g, 0.07 mmol);

d.p.: 158 °C;

¹H NMR (CDCl₃ δ (ppm)): 7.67 (br. s, 4H, aryl), 7.36 (d, 2H, thienyl, ³J_{HH} = 5.5), 7.18 (d, 4H, aryl, ³J_{HH} = 9.0), 6.60 (d, 2H, thienyl, ³J_{HH} = 5.5), 3.99 (s, 6H, CH₃).

¹³C{¹H} NMR (CDCl₃ δ (ppm)): 160.6, 131.7, 130.7, 128.6, 125.8, 122.9, 120.5, 114.7, 55.6;

¹³C{¹H} NMR (- 50°C, CDCl₃ δ (ppm)): 185.4 (¹J_{CO-Rh} = 55.0), 182.5 (¹J_{C-Rh} = 75.4), 180.8 (¹J_{CO-Rh} = 42.9);

FT-IR (ranked intensity (cm⁻¹)): 588(14), 640(13), 701(8), 731(5), 805(4), 835(3), 889(9), 1030(6), 1106(15), 1167(12), 1251(2), 1301(11), 1512(1), 1995.0(10), 2074(7);

FT-Raman (ranked intensity (cm⁻¹)): 667(9), 797(6), 992(11), 1122(10), 1238(5), 1286(13), 1348(3), 1367(14), 1404(1), 1466(15), 1494(2), 1610(8), 1991(7), 2076(4);

Elemental Analysis (%) calc for C₂₇H₂₁N₂O₂S₂RhCl: C 49.97, H 2.90, N 4.48, S 10.26; found C 50.43, H 2.81, N 4.19, S 10.00.

4.4 References

- (1) Rasmussen, S. C.; Schwiderski, R. L.; Mulholland, M. E. *Chem. Commun.* **2011**, *47*, 11394 - 11410.
- (2) Skotheim, T. A.; Reynolds, J. R. *Handbook of Conducting Polymers*; 3rd ed.; CRC Press: Boca Raton, FL, 2007.
- (3) Perepichka, I. F.; Perepichka, D. F. *Handbook of Thiophene-based Materials*; Hoboken, NJ, 2009.
- (4) Marshall, N.; Sontag, S. K.; Locklin, J. *Chem. Commun.* **2011**, *47*, 5681 - 5689.
- (5) Roncali, J. *Mater. Chem.* **1999**, *9*, 1875-1893.
- (6) McCullough, R. D. *Adv. Mater.* **1998**, *10*, 93-116.
- (7) Perepichka, I. F.; Perepichka, D. F. *Adv. Mater.* **2005**, *17*, 2281 - 2305.
- (8) Wolf, M. O. *Adv. Mater.* **2001**, *13*, 545 - 553.
- (9) Sauvage, J. P.; Kern, J. M.; Bidan, G.; Divisia-Blohorn, B.; Vidal, P. L. *New. J. Chem.* **2002**, *26*, 1287 - 1290.

- (10) Joussetme, B.; Blanchard, P.; Ocafrain, M.; Allain, M.; Levillain, E.; Roncali, J. *J. Mater. Chem.* **2004**, *14*, 421 - 427.
- (11) Hill, N. J.; Vargas-Baca, I.; Cowley, A. H. *Dalton Trans.* **2009**, 240-253.
- (12) Diez-Gonzalez, S.; Marion, N.; Nolan, S. P. *Chem. Rev.* **2009**, *109*, 3612-3676.
- (13) Herrmann, W. A. *Angew. Chem., Int. Ed.* **2002**, *41*, 1290-1309.
- (14) Jahnke, M. C.; Hahn, F. E. *Top. Organomet. Chem.* **2010**, *30*, 95-129.
- (15) Marion, N.; Nolan, S. P. *Acc. Chem. Res.* **2008**, *41*, 1440-1449.
- (16) Mercs, L.; Albrecht, M. *Chem. Soc. Rev.* **2010**, *39*, 1903-1912.
- (17) Pugh, D.; Danopoulos, A. A. *Coord. Chem. Rev.* **2007**, *251*, 610-641.
- (18) Wang, Y.; Robinson, G. H. *Dalton Trans.* **2012**, *41*, 337-345.
- (19) Wang, Y.; Robinson, G. H. *Inorg. Chem.* **2011**, *50*, 12326-12337.
- (20) Dutton, J. L.; Tuononen, H. M.; Ragoona, P. J. *Angew. Chem., Int. Ed.* **2009**, *48*, 4409-4413.
- (21) Cowley, A. H. *J. Organomet. Chem.* **2001**, *617-618*, 105-109.
- (22) Murata, M.; Watanabe, T.; Nishihara, H. *J. Am. Chem. Soc.* **2003**, *125*, 12420 - 12421.
- (23) Kingsborough, R. P.; Swagar, T. M. *J. Am. Chem. Soc.* **1999**, *121*, 8825 - 8834.
- (24) Boydston, A. J.; Williams, K. A.; Bielawski, C. W. *J. Am. Chem. Soc.* **2005**, *127*, 12496-12497.
- (25) Coady, D. J.; Khramov, D. M.; Norris, B. C.; Tennyson, A. G.; Bielawski, C. W. *Angew. Chem., Int. Ed.* **2009**, *48*, 1587-1590.
- (26) Khramov, D. M.; Coady, D. J.; Bielawski, C. W. *Polym. Prepr.* **2008**, *49*, 139-140.
- (27) Norris, B. C.; Bielawski, C. W. *Macromolecules* **2010**, *43*, 3591-3593.
- (28) Mercs, L.; Neels, A.; Stoeckli-Evans, H.; Albrecht, M. *Dalton Trans.* **2009**, 7168-7178.
- (29) Zhou, H.; Zhang, W.-Z.; Wang, Y.-M.; Qu, J.-P.; Lu, X.-B. *Macromolecules* **2009**, *42*, 5419-5421.
- (30) Powell, A. B.; Bielawski, C. W.; Cowley, A. H. *J. Am. Chem. Soc.* **2009**, *131*, 18232-18233.

- (31) Powell, A. B.; Bielawski, C. W.; Cowley, A. H. *J. Am. Chem. Soc.* **2010**, *132*, 10184-10194.
- (32) Monot, J.; Brahmi, M. M.; Ueng, S.-H.; Robert, C.; Desage-El, M. M.; Curran, D. P.; Malacria, M.; Fensterbank, L.; Lacote, E. *Org. Lett.* **2009**, *11*, 4914-4917.
- (33) Newman, C. P.; Clarkson, G. J.; Rourke, J. P. *Organomet. Chem.* **2007**, *692*, 4962 - 4968.
- (34) Wang, H. M. J.; Lin, I. J. B. *Organometallics* **1998**, *17*, 972 - 975.
- (35) Mayr, M.; Wurst, K.; Ongania, K.-H.; Buchmeiser, M. R. *Chem. Eur. J.* **2004**, *10*, 1256-1266.
- (36) Scarborough, C. C.; Guzei, I. A.; Stahl, S. S. *Dalton Trans.* **2009**, 2284-2286.
- (37) Dyker, C. A.; Lavallo, V.; Donnadiou, B.; Bertrand, G. *Angew. Chem. Int., Ed.* **2008**, *47*, 3206-3209.
- (38) Lavallo, V.; Canac, Y.; DeHope, A.; Donnadiou, B.; Bertrand, G. *Angew. Chem., Int. Ed.* **2005**, *44*, 7236-7239.
- (39) Bazinet, P.; Yap, G. P. A.; Richeson, D. S. *J. Am. Chem. Soc.* **2003**, *125*, 13314-13315.
- (40) Türkment, H.; Çetinkaya, B. *J. Organomet. Chem* **2006**, *691*, 3749 - 3759.
- (41) de Frémont, P.; Scott, N. M.; Stevens, E. D.; Ramnial, T.; Lightbody, O. C.; Macdonald, C. L. B.; Clyburne, J. A. C.; Abernethy, C. D.; Nolan, S. P. *Organometallics* **2005**, *24*, 6301-6309.

Chapter 5

5 A versatile dithienylethene functionalized Ph-DAB ligand: From photoswitchable main group molecules to photochromic polymers^Ω

5.1 Introduction

Within the past decade photochromic materials have received considerable attention because of their ability to function as a potential workhorse within photoswitchable molecular devices and optical memory storage systems.¹ Among these materials, dithienylethenes (DTE) have proven to have the greatest promise in this field because of their excellent fatigue resistance and thermal irreversibility.^{1,2} Under irradiation of UV-light the ring-open DTE chromophore, that exists in both the anti-parallel and parallel states, can undergo a conrotatory cyclization from the anti-parallel conformation generating the ring-closed isomer (Figure 5.1). Extensive studies have focused on reversible DTE systems contained within organic frameworks, however recent explorations where the DTE fragment incorporates transition metal complexes have begun to emerge. Such modifications have shown distinct enhancements in the stability of the photochromic system and in modulating their photochromic reactivity.³

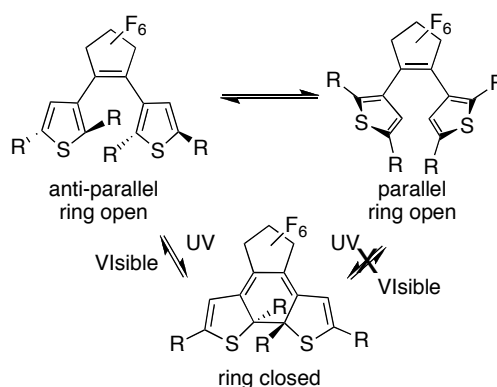


Figure 5.1: The anti-parallel and parallel ring open isomers and the photo-switching to the ring closed-isomer.

^Ω A version of this chapter has been previously published Price, J. T. and Ragogna, P. J., *Chem. Eur. J.*, **2013**, DOI: 10.1002/chem.201301086 and has been reproduced with permission.

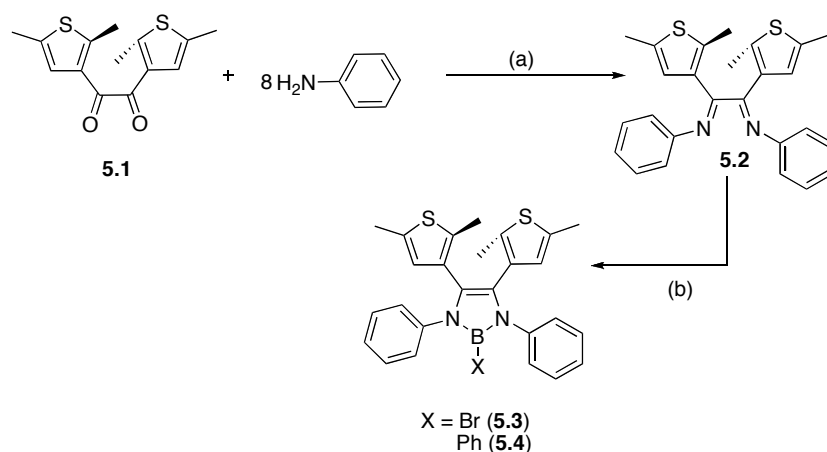
While diazabutadiene (DAB) ligands are well known for their ability to be redox active, bind to transition metals and support low valent, low oxidation-state main group elements,⁴⁻⁶ there has been no report on the modification of this ligand class with a diarylethene. We envision that the incorporation of a DTE functionality into the diazabutadiene framework would open up new pathways and opportunities for the development of photochromic materials, as this ligand set would have the potential to bind to a wide variety of elements spanning the periodic table. Ultimately this could reveal new discoveries for photochromic reactivity. The incorporation of p-block elements into DTE systems are particularly well suited for optoelectronic materials and sensing,⁷⁻¹² however such derivatives are limited. Yam and coworkers have tethered a diketonate onto a thiophene substituted DTE, which was used to incorporate B(III)⁷ and ultimately generated a gated "lock-unlock" system with triphenylborane.⁸ Another key development in main group DTE chemistry was reported by Bielawski *et al.*, where they were able to attenuate the activity of their DTE functionalized NHC catalyst using UV-light to promote *trans*-esterification and amidation reactions. The catalytic activity of the corresponding organocatalyst could be remotely tuned by exposure to visible and UV light.^{13,14} These results have been critical in the expansion of DTE chemistry, however the synthesis of these compounds, (especially those containing the hexafluorocyclopentene ring; e.g. Fig. 5.1) require costly starting materials, difficult metal catalyzed C-C coupling chemistry and lengthy purification steps, which can obviate their applicability in larger scale and broader applications. In this context, we have developed a new diazabutadiene framework decorated with photochromic thiophene rings, which can be synthesized over a small number of simple, high yielding standard transformations. We have demonstrated the potential versatility of this new ligand system by synthesizing both boron and phosphorus heterocycles. A key feature in the development of our small molecules is that these units can be further functionalized with a polymerizable group without the need for any modification to the diarylethene framework and then subsequently converted to the corresponding polymer. This final polymeric material retains the "switching" features one expects from DTE systems and as an added bonus has excellent recyclability with no apparent degradation once polymerized. Substitution of our ligand system reveals varied photophysical properties, where one could envision a wide expansion by the incorporation of other p-, d- or f-block elements. These results represent a wholly new

and versatile DTE ligand system that has the potential for the incorporation of a wide variety of elements through simple donor-acceptor chemistry.

5.2 Results and Discussion

5.2.1 Synthesis

The diazabutadiene (**5.2**) was synthesized from a condensation reaction between 1,2-bis(2,5-dimethyl-3thienyl)ethanedione (**5.1**) with aniline and TiCl_4 in a 1:8:1 stoichiometric ratio yielding the target product as a yellow solid in 78 % yield (Scheme 5.1). Single crystals suitable for X-ray diffraction studies were grown from a concentrated solution of EtOH confirming the synthesis of **5.2** (Figure 5.6).

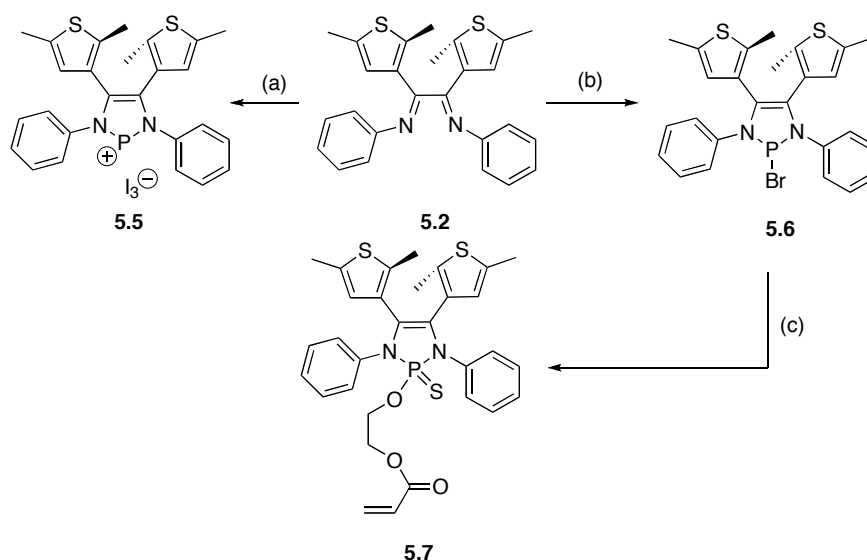


Scheme 5.1: Synthesis of B(III) substituted DTE; a) TiCl_4 , CH_2Cl_2 , 12 h, 76 %; b) $\text{Li}_{(s)}$, Et_2O , 2 d, rt.; $\text{NEt}_3\cdot\text{HCl}$, 2 h; b) CH_2Cl_2 , BBr_3 or BPhCl_2 , 12 h, rt.; c) $\text{Et}(\text{Pr})_2\text{N}$, 2 h, (X = Br, 32 %, X = Ph, 48 %).

Upon examination of the ^1H NMR spectrum of compound **5.2**, all thiophene signals were shifted noticeably upfield (methyl group: $\delta_{\text{H}} = 2.72$ and 2.35 to 2.59 and 1.90 ; 3-position: $\delta_{\text{H}} = 6.91$ to 6.79). Subsequent reaction of compound **5.2** with BBr_3 or BPhCl_2 afforded the air sensitive boron(III) compounds **5.3** and **5.4**, respectively as white solids in 32% to 48 % yields (Scheme 1). The synthesis of **5.3** and **5.4** were achieved by the reduction of **5.2** with 3 stoichiometric equivalents of $\text{Li}_{(s)}$, where the resulting reaction mixture was then quenched with $\text{NEt}_3\cdot\text{HCl}$. The product amine was redissolved in CH_2Cl_2 and subsequently BBr_3 or BPhCl_2 was added. Upon completion, the reaction mixture was quenched with $(\text{Pr})_2\text{NEt}$, filtered, concentrated and washed with CH_3CN resulting in a white solid.¹⁵ Subsequent ^{11}B NMR spectroscopy of the product revealed a single broad

resonance at $\delta_B = 21$ and 26 , respectively for compounds **5.3** and **5.4**. Crystals of compounds **5.3** and **5.4** suitable for X-ray diffraction studies were grown from a concentrated solution of benzene or in CH_2Cl_2 at -30°C respectively. X-ray diffraction experiments on these samples confirmed the expected connectivity (Figure 5.6).

Ligand versatility was an important feature in the design and synthesis of this particular dithienylethene and the facile installation of different elements into the ligand framework was a key goal. Thus from boron, our next target was the incorporation of phosphorus. This was accomplished through a two electron reduction of the ligand with PI_3 as developed by Cowley *et al.* to give the corresponding phosphonium cation (**5.5**) as an orange powder in 78 % yield shown in Scheme 5.2.¹⁶ The orange powder was dissolved in CDCl_3 and upon examination of the $^{31}\text{P}\{^1\text{H}\}$ NMR spectrum, two peaks were observed at $\delta_P = 191$ and 192 attributed to both the parallel and anti-parallel conformations present in solution.² X-ray quality single crystals were grown from a concentrated CH_2Cl_2 solution confirming the structure of **5.5** (Figure 5.6). Unfortunately upon exposure to UV light there was no observable change in the UV-vis spectrum and it was suspected that the presence of the I_3^- anion quenches the desired ring-closing reaction. Therefore an alternate route was chosen to avoid this counter ion and we utilized the now established procedure of reacting the α -diimine of choice (**5.2**) with PBr_3 and excess cyclohexene to give the cyclic diaminobromophosphine (**5.6**, Scheme 5.2).¹⁷ Upon the addition of PBr_3 the colourless solution turned orange and examination of the crude mixture by $^{31}\text{P}\{^1\text{H}\}$ NMR spectroscopy showed two new signals at $\delta_P = 163$ and 164 ppm, again attributed to an equilibrium of parallel and anti-parallel conformation present in solution, along with a disappearance of the PBr_3 resonance ($\delta_P = 220$). Upon no further change, the reaction mixture was concentrated and washed with pentane giving the desired product as a white solid, which was confirmed by X-ray diffraction studies, and was isolated in 92 % yield. The bromophosphine (**5.6**) was then dissolved in THF, and NEt_3 and hydroxyethylacrylate (HEA) were added. A crude $^{31}\text{P}\{^1\text{H}\}$ NMR spectrum of the reaction mixture revealed the disappearance of compound **5.6** ($\delta_P = 163$ and 164) and the appearance of a new single peak ($\delta_P = 100$). To this mixture, 1/8 stoichiometric equivalents of S_8 were added, and upon no further reaction as indicated by $^{31}\text{P}\{^1\text{H}\}$ NMR spectroscopy (12 hrs; $\delta_P = 68$), a white solid (**5.7**) was isolated in 65 % yield (Scheme 5.2). X-ray quality crystals were grown from a concentrated solution of hexanes and, where X-ray diffraction experiments confirmed the synthesis of **5.7** (Figure 5.6).



Scheme 5.2: Synthesis of compounds **5.5**, **5.6** and **5.7**; a) CH₂Cl₂, PI₃, 12 h, 95 %; b) CH₂Cl₂, PBr₃, 12 h, 92 %; c) THF, NEt₃, HEA, S₈, 65 %.

Variable temperature ¹H NMR spectroscopic studies were conducted on compounds **5.4**, **5.5**, **5.6** to determine their respective coalescence temperature (T_c) and the activation energy between the anti-parallel and parallel conformations as both conformations were observed in the ¹H NMR spectrum (Figures 5.2 - 5.4). The T_c for compounds **5.4**, **5.5** and **5.6** were determined to be 20, 40 and 30 °C, respectively. The activation energy was determined by plotting ln(k) vs T⁻¹ and using the Arrhenius equation, the activation energy was calculated as 64, 51 and 59 kJ mol⁻¹ for compounds **5.4**, **5.5** and **5.6**, respectively. Substitution did not have dramatic effect on the parallel/anti-parallel energy barrier, which is not unexpected as steric, not electronic effects usually direct such a phenomenon. This rationale explains why only one conformation was observed for compounds **5.7** and **5.8**.

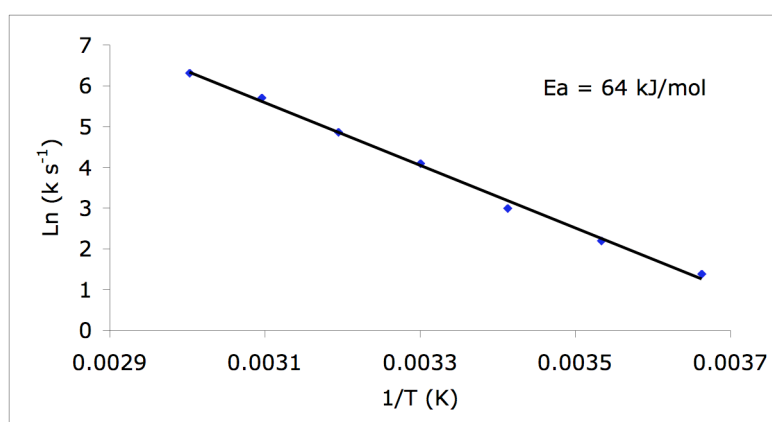
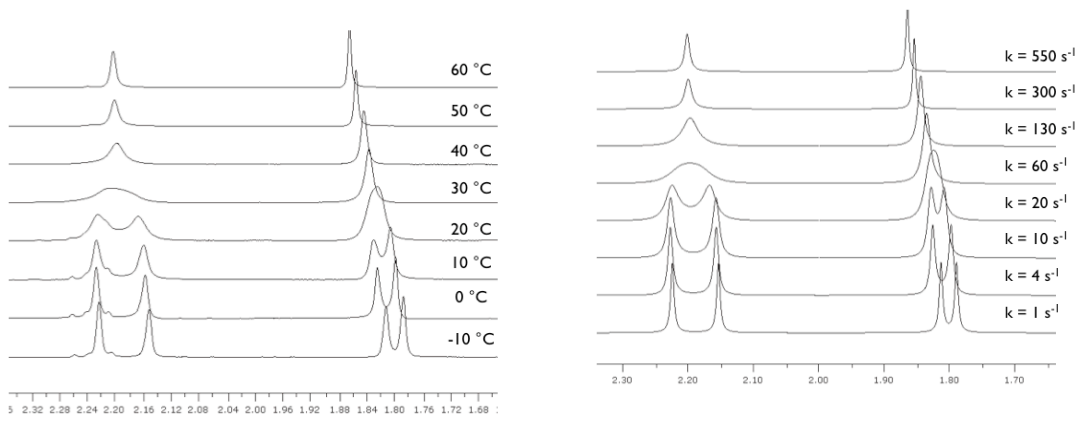


Figure 5.2: Variable temperature ^1H NMR of compound **5.4** (top left); Simulated variable temperature ^1H NMR of compound **5.4** (top right); Arrhenius plot of the rate of conversion between parallel and anti-parallel states vs. $1/T$ and the calculated activation energy required for the conversion between parallel and anti-parallel states for compound **5.4**.

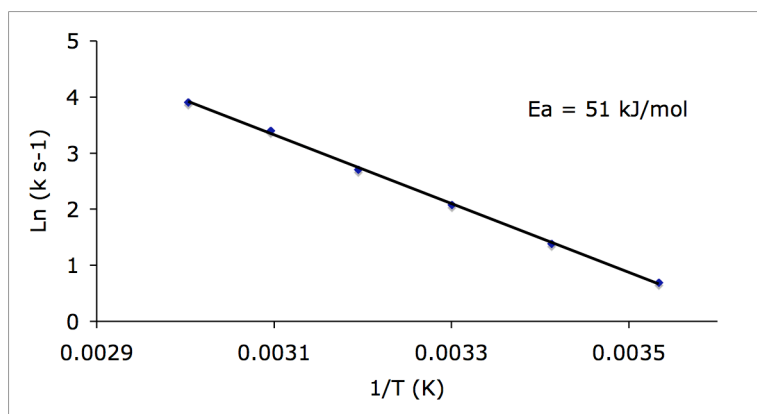
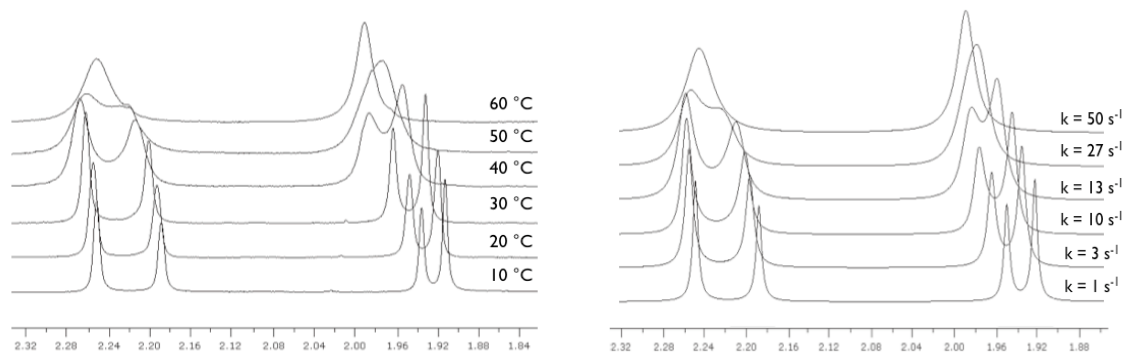


Figure 5.3: Variable temperature ^1H NMR of compound **5.5** (top left); Simulated variable temperature ^1H NMR of compound **5.5** (top right); Arrhenius plot of the rate of conversion between parallel and anti-parallel states vs. $1/T$ and the calculated activation energy required for the conversion between parallel and anti-parallel states for compound **5.5**.

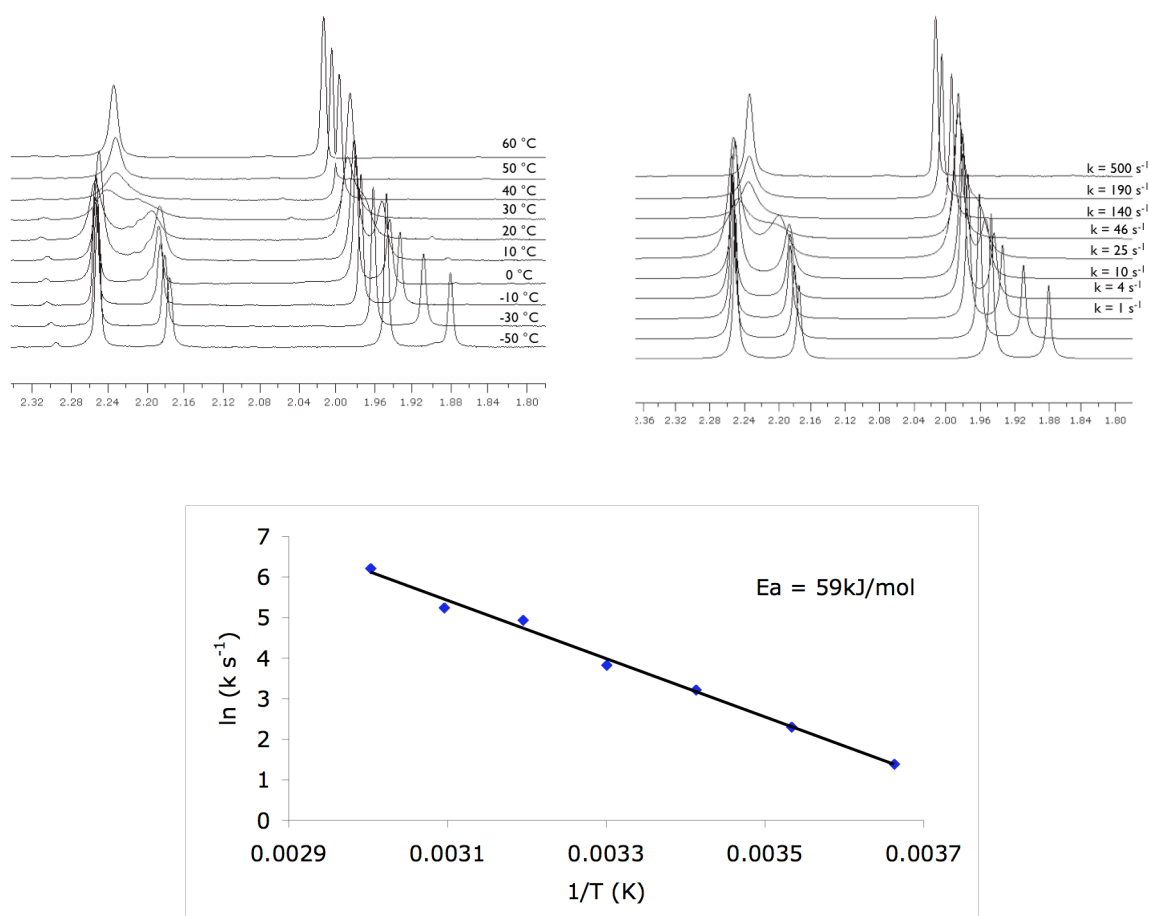


Figure 5.4: Variable temperature ¹H NMR of compound **5.6** (top left); Simulated variable temperature ¹H NMR of compound **5.6** (top right); Arrhenius plot of the rate of conversion between parallel and anti-parallel states vs. 1/T and the calculated activation energy required for the conversion between parallel and anti-parallel states for compound **5.6**.

To synthesize the polymer, **5.8**, reversible addition-fragmentation chain-transfer polymerization (RAFT) conditions were used to polymerize the acrylate functionalized monomer, (**5.7**). The side chain dithienylethene polymer was prepared using the side chain transfer reagent (**5.9**) in the presence of a radical initiator AIBN (azobisisobutyronitrile) in deoxygenated benzene at 80 °C (Figure 5.5). The reaction progress was monitored by ¹H NMR spectroscopy and the formation of the polymer increased linearly with time, which is characteristic of a controlled polymerization. Examination of the ¹H NMR spectrum of the polymer, **5.8**, (Figure 5.5) shows the disappearance of the vinylic (5.7 - 6.3 ppm) protons and a general broadening of the ¹H

NMR spectrum. Molecular weights and PDI's were determined by gel permeation chromatography (GPC), which indicate that **5.8** is a low molecular weight polymer ($M_n = 4200$ g/mol) with a narrow PDI (1.1). The thermogravimetric analysis (TGA) of the polymer revealed that it was stable up to 292°C and differential scanning calorimetry (DSC) experiments measured a glass transition (T_g) temperature of 79.7°C .^Ω

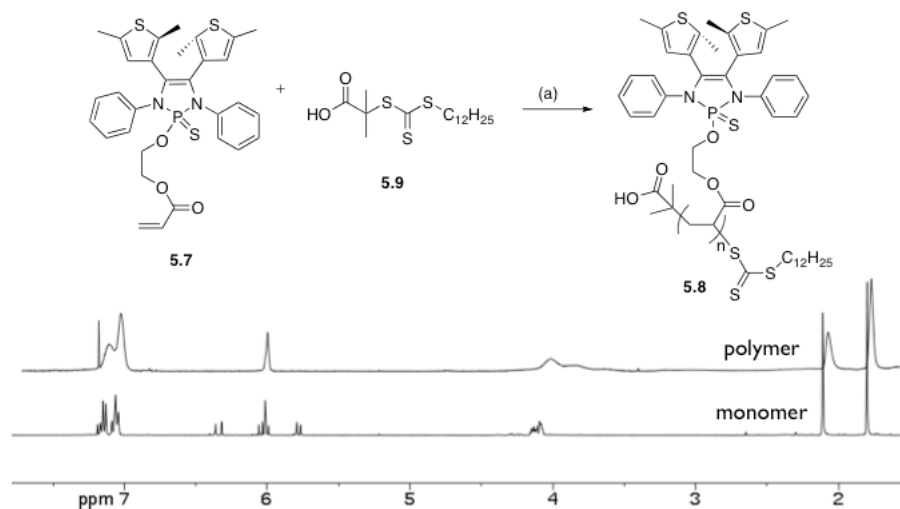


Figure 5.5: Polymerization of monomer **5.7**; a) AIBN; C_6H_6 ; 80°C ; 8 h; 42 %; Proton NMR spectra of monomer (bottom) and polymer (top) in CDCl_3 .

5.2.2 X-ray crystallography

Single crystals of compounds **5.2**, **5.3**, **5.4** and **5.7** were grown from various vapour diffusion combinations and were analyzed by single crystal X-ray diffraction (Figure 5.4, Table 5.1). Compound **5.2** contains shortened C - N linkages (1.269(3) and 1.273(3) Å) consistent with double bonds and a lengthened C - C connection (1.516(4) Å). The phenyl groups are arranged in a *cis* geometry, with the thiophene rings oriented parallel to each other (Figure 5.4). The $\text{C}_2\text{N}_2\text{B}$ five membered ring in compound **5.3** possesses two C - N single bonds (1.414(3) - 1.426(3) Å vs. 1.271 Å (avg) double bonds, **5.2**) and a C(5) - C(6) double bond (1.371(3) Å compared to 1.518(4) Å in **5.2**). The lengthening of the C - N and shortening of the C - C bonds is evidence of a two electron reduction of the diimine framework as expected from the reduction of **5.2** with lithium. The thiophene

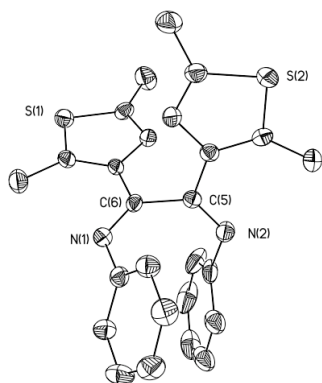
^Ω See Appendix 3 for the plot of polymer formation, the GPC, T_g and DSC trace.

rings have adopted an anti-parallel geometry and the planes of the thiophene rings are twisted with respect to the 5-membered borane ring with interplanar angles of 44.1 - 46.9 °. This is also observed within compound **5.4**, where a shortening of the C(5) - C(6) bond (1.355(5) Å compared to 1.518(4) Å in **5.2** and a lengthening of the C - N to two single bonds (1.419(4) - 1.415(4) Å vs. 1.271 Å (avg)) is observed. Also similar is the adoption of an anti-parallel geometry of the thiophene rings, which are twisted with respect to the C₂N₂B core with inter-planar angles of 55.33 and 56.75 ° (Figure 5.4). Compound **5.7** also exhibits the hallmarks of a 2 electron reduction of the ligand with a shortening of the C(5) - C(6) bond (1.341(4) Å) and lengthening of the C - N bond (1.43 avg.) compared to that of the free ligand and the thiophene rings having an interplanar angle of 57.12 and 51.25° with respect to the five membered C₂N₂P ring.

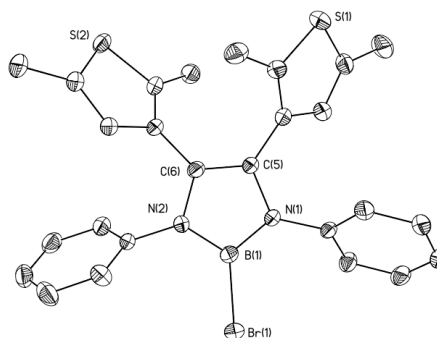
Compound	5.2	5.3	5.4	5.7
Empirical formula	C ₂₆ H ₂₄ N ₂ S ₂	C ₂₆ H ₂₄ B ₁ Br ₁ N ₂	C ₃₂ H ₂₉ B ₁ N ₂ S ₂ , C ₁ H ₂ Cl ₂	C ₃₁ H ₂₈ N ₂ O ₃ PS 3
FW (g/mol)	428.59	519.31	601.43	603.70
Crystal system	Orthorhombic	Triclinic	Monoclinic	Triclinic
Space group	Pbca	P $\bar{1}$	P2 ₁ /c	P $\bar{1}$
a (Å)	15.276(3)	11.1005(7)	16.703(2)	9.7809(7)
b (Å)	9.780(2)	11.3448(7)	9.3800(11)	11.3086(8)
c (Å)	30.178(6)	11.5243(7)	21.751(3)	15.0139(11)
α (deg)	90	91.024(4)	90	88.564(2)
β (deg)	90	113.928(4)	117.506(3)	74.331(2)
γ (deg)	90	112.193(4)	90	71.918(2)
V (Å ³)	4508.6(16)	1202.93(13)	3017.6(6)	1516.85(19)
Z	8	2	4	2
D _c (mg m ⁻³)	1.263	1.434	1.324	1.322
R _{int}	0.0478	0.0549	0.0638	0.0569
R1[I > 2 σ I] ^a	0.0955	0.1512	0.1141	0.1150
wR2(F ²) ^a	0.1333	0.1243	0.1462	0.1423
GOF(S) ^a	1.029	1.002	1.028	1.045

Table 5.1: X-ray details for compounds **5.2**, **5.3**, **5.4** and **5.7**.

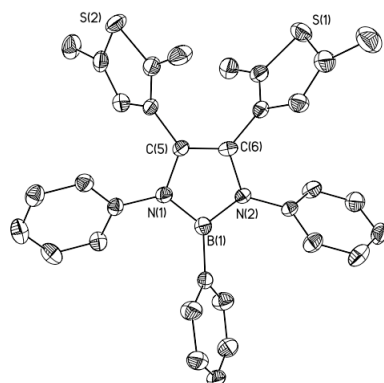
^aR1($F[I > 2(I)]$) = $\sum ||F_o| - |F_c| || / \sum |F_o|$; wR2(F^2 [all data]) = $[w(F_o^2 - F_c^2)^2]^{1/2}$; S(all data) = $[w(F_o^2 - F_c^2)^2 / (n - p)]^{1/2}$ (n = no. of data; p = no. of parameters varied; $w = 1/[\sigma^2(F_o^2) + (aP)^2 + bP]$ where $P = (F_o^2 + 2F_c^2)/3$ and a and b are constants suggested by the refinement.



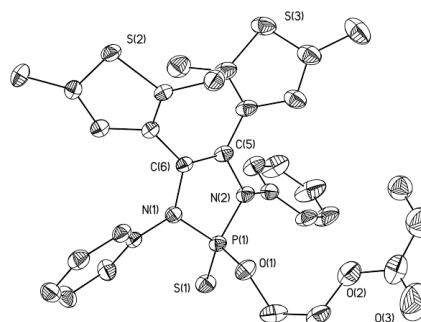
5.2



5.3



5.4



5.7

Figure 5.6: Solid state structures of compounds **5.2**, **5.3**, **5.4** and **5.7**. Thermal ellipsoids are drawn to 50 %. Hydrogen atoms and solvent were removed for clarity.

5.2.3 Photophysical properties

All complexes were found to be soluble in *n*-pentane with the exception of the polymer (**5.8**), which was soluble in toluene. The electronic spectra of compounds **5.2** - **5.8** show an intense absorption band at 270 - 300 nm attributed to both $\pi - \pi^*$ and $n - \pi^*$ transitions. Upon the photoexcitation of compounds **5.4**, **5.7** and **5.8**, each exhibited reversible photochromism, as revealed by changes in the UV-vis absorption spectra (Figures 5.7 and 5.9) with a well defined isosbestic point, whereas compounds **5.3**, **5.5** and **5.6** did not. Photoexcitation of compound **5.4** with 254 nm light brings about the appearance of a lower energy absorption at $\lambda_{\text{max}} = 498$ nm corresponding to the ring

closed isomer with an isosbestic point at 304 nm. Ring opening of compound **5.4** is achieved by irradiation with visible light and is marked by the disappearance of the lower energy absorption at $\lambda_{\text{max}} = 498$ nm. When excited with 300 nm light compound **5.4** fluoresces blue in the ring open state having a $\lambda_{\text{max}} = 378$ nm and orange in the ring closed state with a $\lambda_{\text{max}} = 558$ nm again with isosbestic points at 335 and 443 nm (Figure 5.7).

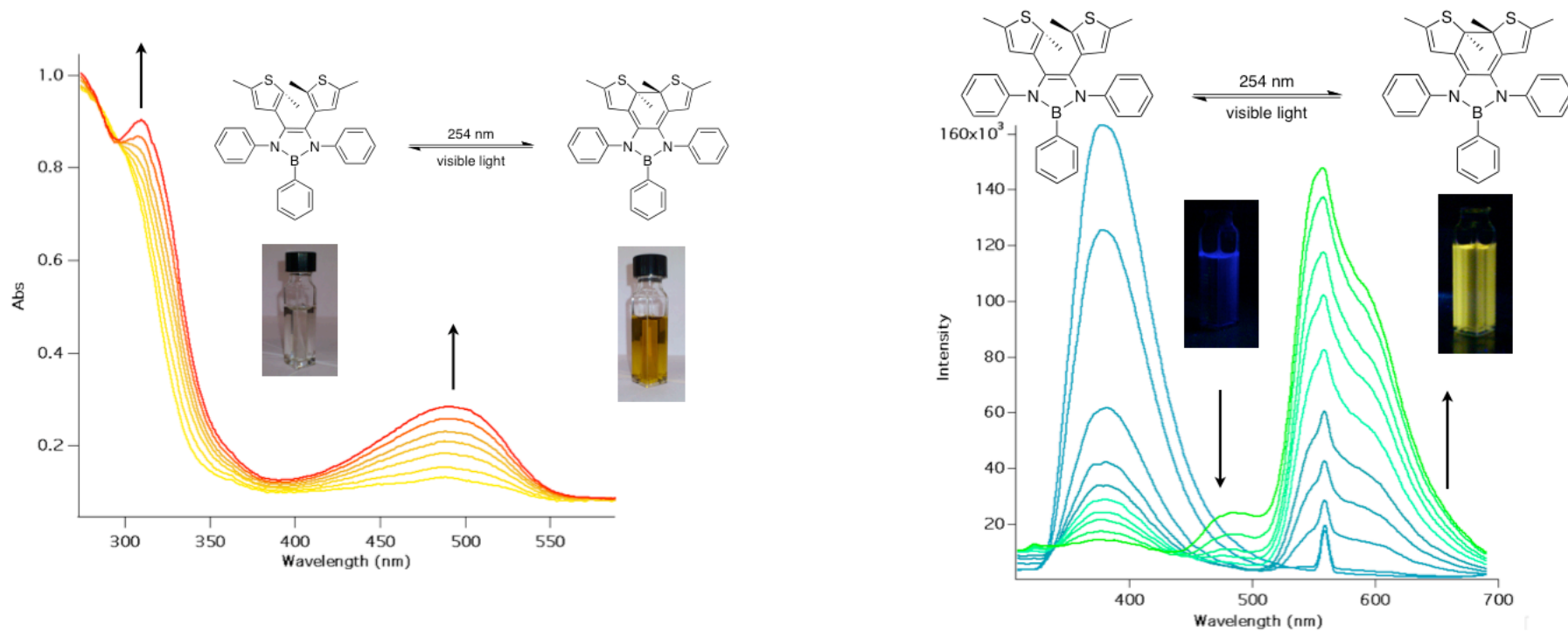


Figure 5.7: Left) Changes in the UV-vis absorption spectra (**5.4**) when a *n*-pentane solution (5×10^{-5} M) is irradiated with 254 nm light as a function of time; Right) Changes in the fluorescence spectra (**5.4**) when a *n*-pentane solution (5×10^{-5} M) is irradiated with 254 nm light as a function of time.

Examination of the ^1H NMR spectra of compound **5.4** irradiated in cyclohexane- d_{12} with 254 nm light, generated three new signals ($\delta_{\text{H}} = 4.49, 2.00$ and 1.65) from the reversible ring-closed isomer as well as signals ($\delta_{\text{H}} = 5.36, 2.43, 2.39$, and 1.52) attributed to possibly a six membered irreversible rearrangement product (IR, **5.9** in Figure 5.8). This was further confirmed after leaving the sample under ambient light, only those resonances consistent with the ring-closed isomer were no longer present, while those belonging to the irreversible rearrangement product remained. (Figure 5.8).^{18,19}

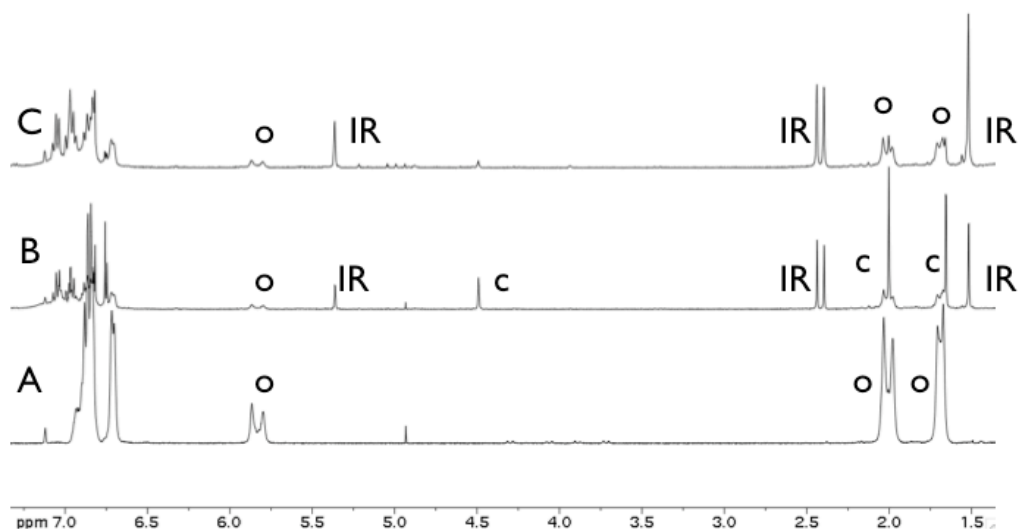
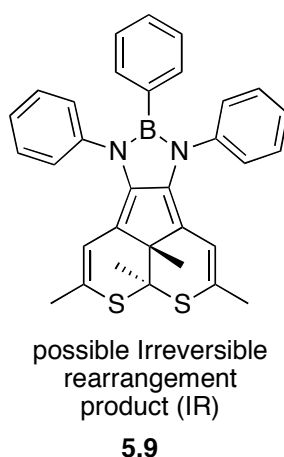


Figure 5.8: Stacked ^1H spectra of compound **5.4**, where o = open, c = closed and IR = irreversible rearrangement product. A) the ring open isomer before irradiation. B) after irradiation for 90 min with 254 nm light and C) after being left out in ambient light for 8 h.

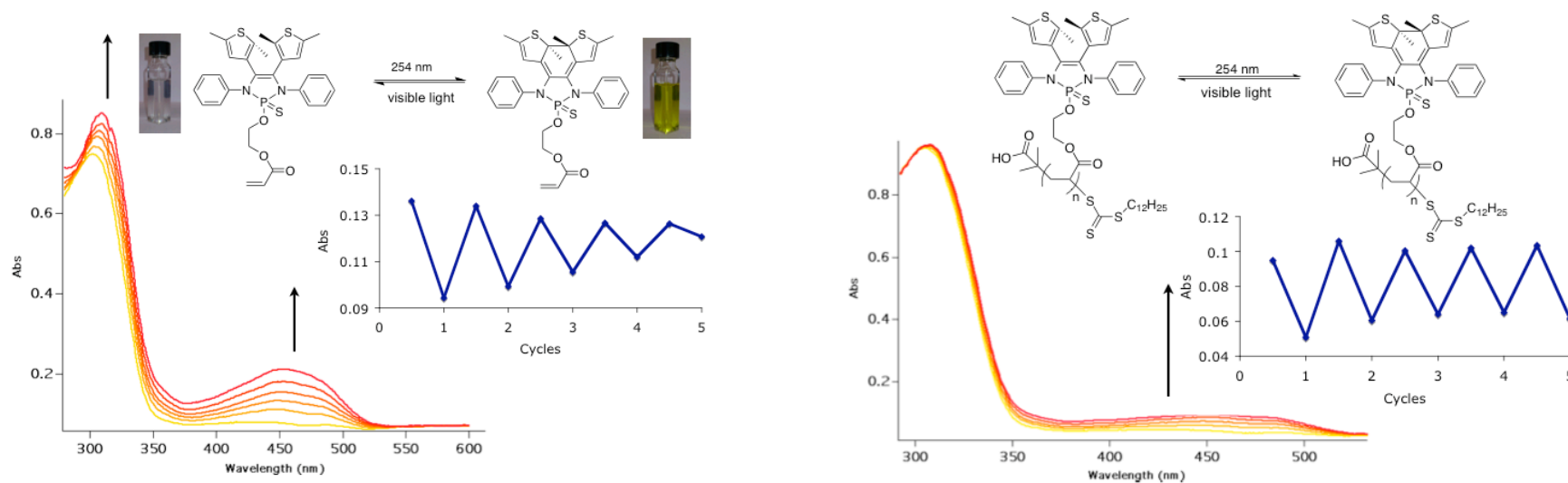


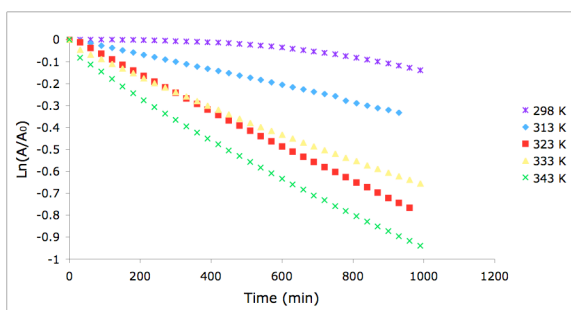
Figure 5.9: Left) Changes in the UV-vis absorption spectra of **5.7** when a pentane (1×10^{-5} M) solution is irradiated with 254 nm light and its decomposition after 5 cycles; Right) Changes in the UV-vis absorption spectra of **5.8** when a toluene (1×10^{-5} M) solution is irradiated with 254 nm light and its decomposition after 5 cycles.

Irradiation of the phosphorus(V) monomer (**5.6**), and polymer (**5.7**) a new band was observed with a λ_{\max} = at 448 nm, signifying the formation of the ring closed isomer, which is at a shorter wavelength than the boron derivative (**5.4**). This was also confirmed by the $^{31}\text{P}\{^1\text{H}\}$ NMR spectra of an irradiated sample of compound **5.6**, in which a new phosphorus peak was observed further downfield ($\delta_{\text{P}} = 69.0$ to 69.5) in cyclohexane- d_{12} . Again these compounds were reversible and when exposed to a longer wavelength visible light, the ring open isomer was observed, which can be monitored by the disappearance of the low energy band at 448 nm. The recyclability of these compounds were measured and it was found that the monomer (**5.6**) underwent a 65 % decomposition after 5 cycles however in the case of the polymer, very little decomposition is observed and after 5 cycles only 5 % decomposition was detected (Figure 5.9)

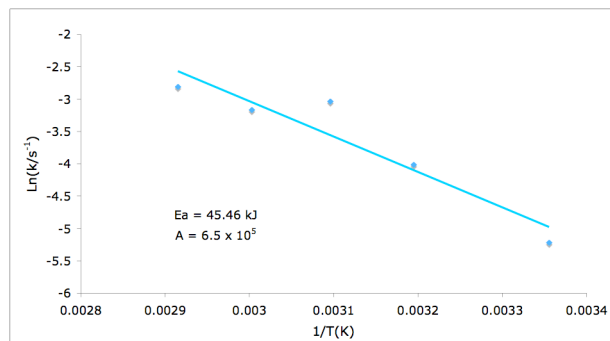
The quantum yields for both the photocyclization and photocycloreversion processes have been determined. The $\phi_{\text{O}\rightarrow\text{C}}$ values of the dithienylethenes containing either phosphorus or boron ranged from 0.12 - 0.17, where as the $\phi_{\text{C}\rightarrow\text{O}}$ values were determined to be 0.012 - 0.027. The DTE containing both boron (**5.4**), and phosphorus (**5.7**), had similar $\phi_{\text{O}\rightarrow\text{C}}$ values of 0.16 and 0.17 respectively, however once compound **5.7** was incorporated into a polymer the $\phi_{\text{O}\rightarrow\text{C}}$ decreased slightly to 0.12. This, however was not the case in the $\phi_{\text{C}\rightarrow\text{O}}$, as once compound **5.7** was incorporated into a polymer the $\phi_{\text{C}\rightarrow\text{O}}$ increased from 0.012 to 0.027 respectively.

An examination of the thermal stability of the closed form of compounds **5.4**, **5.7** and **5.8** were carried out and the plots of $\ln(A/A_0)$ vs. time for the absorbance decay at 498 for compound **5.4** and 448 for compounds **5.7** and **5.8** were measured at various temperature (Figure 5.10). The half life for the closed forms at 298 and 343 K for compounds **5.4**, **5.7** and **5.8** were found to be 4877, 49738, 25662 and 737, 2547, 10124 min respectively. The activation energy of the thermal cycloreversion of compounds **5.4**, **5.7** and **5.8** were determined by plotting $\ln(k)$ vs. T^{-1} using the Arrhenius equation were determined to be 43.5, 52.5 and 30.7 kJ mol^{-1} , suggesting the incorporation of the DTE functionality into a polymer increases the thermal stability of the closed form (Figure 5.10).

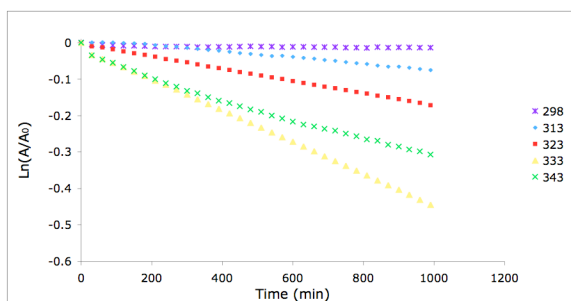
Compound 5.4



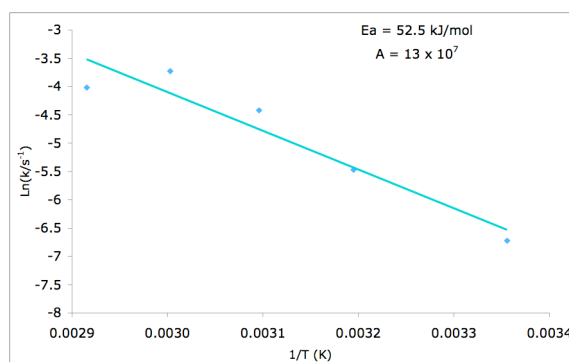
Compound 5.4



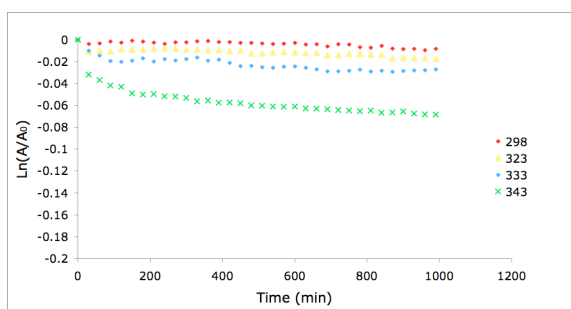
Compound 5.7



Compound 5.7



Compound 5.8



Compound 5.8

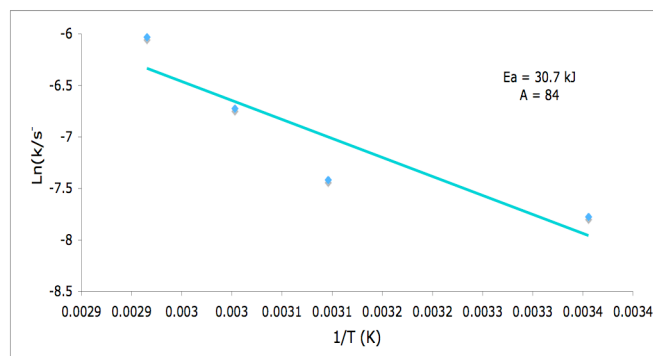


Figure 5.10: Left) Decay trace of the closed ring isomer by thermal cycloreversion at various temperatures in deoxygenated hexanes (5.4 and 5.7) and deoxygenated toluene (5.8) at 498 nm (5.4) and 448 nm (5.7 and 5.8); Right) Arrhenius plot of the thermal backward reaction of the closed ring isomer.

5.2.4 Conclusions

In summary, a new class of dithienylethenes (DTEs) that are contained within a diazabutadiene ligand framework were prepared in high yields without the use of column chromatography or any C - C coupling reactions that often require expensive metal catalysts. Being able to utilize the DTE as a ligand has enabled easy incorporation of different elements into the C₂N₂ framework without any modification to the parent ligand. The final compounds displayed vastly different photophysical properties depending on the nature of the incorporated main group element. When B(III) was incorporated the ring closed isomer a $\lambda_{\text{max}} = 498$ nm was observed, whereas the P(V) monomer and polymer both had $\lambda_{\text{max}} = 448$ nm, a hypsochromic shift of 50 nm. Also the B(III) DTE fluoresced blue in the open conformation while orange in the closed state. The facile functionalization of the DTE with an acrylate group also enabled the formation of a side chain functionalized polymer, which had a very high recyclability with almost no decomposition after 5 cycles. Although these compounds have low quantum efficiencies, they were thermally stable upon heating especially compound **5.7** upon polymerization. These compounds represent the first example in which DTE has been used as a ligand in which different elements can easily be incorporated into its framework. Future work will consist of incorporating both transition and lanthanide metals into this manifold.

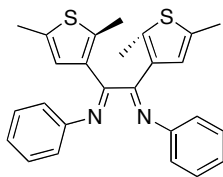
5.3 Experimental

5.3.1 General experimental

General synthetic and crystallography experimental details can be found in Appendix 1.

5.3.2 Synthetic procedures

Compound 5.2



A 10 mL CH_2Cl_2 solution of aniline (10.87 mL, 119.80 mmol) was cooled to 0 °C in an ice bath. To the reaction mixture TiCl_4 (1.61 mL, 14.80 mmol) was added *via* syringe and the reaction stirred for 20 min. at 0 °C. A 10 mL CH_2Cl_2 solution of 1,2-Bis(2,5-dimethyl-3-thienyl)ethandione (4.15 g, 14.80 mmol) was then added *via* cannula and the dark red solution stirred at rt. for 12 hours. Upon completion 5 mL of water was added to the reaction mixture and a white solid precipitated immediately, which was removed by filtration. The orange filtrate was then subsequently washed with water and dried with MgSO_4 and concentrated. The resulting residue was crystallized from EtOH.

Yield: 76 % (4.82 g, 11.20 mol);

m.p.: 140 - 142 °C;

^1H NMR (C_6D_6 , δ (ppm)): 6.99 (m, 4H, aryl), 6.85 (m, 6H, aryl), 6.79 (s, 2H, thienyl), 2.59 (s, 6H, CH_3), 1.90 (s, 6H, CH_3);

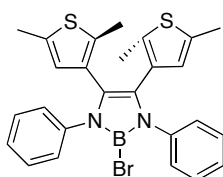
^{13}C NMR (CDCl_3 , δ (ppm)): 160.9, 149.3, 141.4, 135.2, 134.8, 128.2, 126.6, 124.2, 120.2, 15.6, 15.1;

FT-IR (ranked intensity (cm^{-1})): 488(14), 535(9), 664(11), 694(2), 752(3), 789(13), 833(5), 852(15), 1120(6), 1194(10), 1214(8), 1244(12), 1477(1), 1547(7);

FT-Raman (ranked intensity (cm^{-1})): 219(1), 500(9), 687(7), 1005(3), 1031(10), 1295(11), 1496(8), 1597(5), 1642(2), 2917(4), 3065(6);

HRMS: ($\text{C}_{26}\text{H}_{24}\text{N}_2\text{S}_2$) Calcd (found) 428.1381 (428.1387).

Compound 5.3.



Lithium metal (0.05 g, 6.99 mmol) was added to a 10 mL Et_2O solution of compound 5.2 (1.00 g, 2.33 mmol) and the reaction stirred at rt. for 2 days. Upon completion the reaction mixture was filtered and $\text{NEt}_3\cdot\text{HCl}$ (0.66 g, 4.80 mmol) was added and the reaction stirred for 1 h at rt., filtered through Elite and concentrated. The residue was then taken up in 20 mL of CH_2Cl_2 and cooled to 0 °C and a 1 M CH_2Cl_2 solution of BBr_3 (2.56 mL, 2.56 mmol) was added *via* syringe and stirred for 12 h at rt. The reaction was quenched using

$N(iPr)_2Et$ (0.41 mL, 2.33 mmol) and concentrated. The residue was taken up in 200 mL of hexanes, filtered through Celite and concentrated resulting in a red solid. The red solid was then washed with 3 x 5 mL of CH_3CN yielding the product, a white powder.

Yield: 33 % (0.48 g, 0.92 mmol);

m.p.: 179 - 180 °C;

1H NMR ($CDCl_3$, δ (ppm)): 7.09 (m, 10H, aryl), 5.93 (s, 2H, thienyl), 2.11 (s, 6H, CH_3), 1.73 (s, 6H, CH_3);

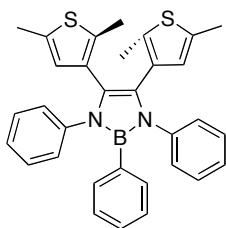
$^{13}C\{^1H\}$ NMR ($CDCl_3$, δ (ppm)): 140.1, 134.5, 127.1, 125.4, 123.9, 15.0, 13.7;

$^{11}B\{^1H\}$ NMR ($CDCl_3$, δ (ppm)): 21;

FT-IR (ranked intensity (cm^{-1})): 492(14), 560(10), 695(2), 759(5), 802(7), 1028(6), 1074(9), 1140(11), 1209(12), 1260(3), 1375(4), 1438(13), 1497(1), 1597(8), 2915(15);

FT-Raman (ranked intensity (cm^{-1})): 203(2), 233(6), 502(12), 691(4), 930(13), 1002(5), 1155(7), 1274(8), 1397(9), 1495(10), 1598(11), 1616(1), 2076(14), 2146(15).

Compound 5.4.



Lithium metal (0.05 g, 6.99 mmol) was added to a 10 mL Et_2O solution of compound **5.2** (1.00 g, 2.33 mmol) and the reaction stirred at rt. for 2 d. Upon completion the reaction mixture was filtered and $NEt_3 \cdot HCl$ (0.66 g, 4.80 mmol) was added the reaction stirred for 1 h at rt., filtered through Celite and concentrated. The residue was then taken up in 20 mL of CH_2Cl_2 and cooled to 0 °C and a 1 M CH_2Cl_2 solution of $BPhCl_2$ (0.33 ml, 2.53 mmol) was added via syringe and stirred for 12 h at rt. The reaction was quenched using $N(iPr)_2Et$ (0.95 mL, 5.63 mmol) and concentrated. The residue was then washed with 3 x 15 mL of CH_3CN yielding the product, a white powder.

Yield: 48 % (0.58 g, 1.4 mmol);

d.p.: 163 °C;

1H NMR (-20 °C) ($CDCl_3$, δ (ppm)): 7.10 (m, 8H, aryl), 6.94 (m, 2H, aryl), 6.88 (m 5H, aryl), 5.98 (s, 1H, thienyl), 5.89 (s, 1H, thienyl), 2.22 (s, 3H, CH_3), 2.15 (s, 3H, CH_3), 1.80 (s, 3H, CH_3), 1.78 (s, 3H, CH_3);

^{13}C NMR (-20 °C) (CDCl_3 , δ (ppm)): 141.2, 141.0, 134.9, 134.8, 134.7, 134.3, 134.2, 133.9, 128.7, 128.6, 128.1, 128.0, 127.4, 127.3, 127.1, 124.5, 123.3, 123.2, 15.4, 15.3, 14.1, 14.0;

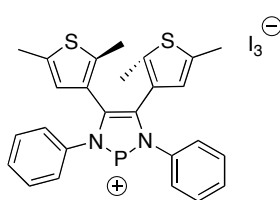
$^{11}\text{B}\{^1\text{H}\}$ NMR (CDCl_3 , δ (ppm)): 26;

FT-IR (ranked intensity (cm^{-1})): 489(11), 547(9), 604(6), 656(14), 737(4), 756(10), 791(15), 913(1), 1026(13), 1069(7), 1191(2), 1261(12), 1136(8), 2116(5), 3045(3);

FT-Raman (ranked intensity (cm^{-1})): 225(1), 701(9), 1000(4), 1376(5), 1497(6), 1597(3), 1629(2), 2911(7), 3057(8).

HRMS: ($\text{C}_{32}\text{H}_{29}\text{N}_2\text{S}_2\text{B}_1\text{Na}_1$) Calcd (found) 539.1768 (539.1777).

Compound 5.5.



To a 5 mL CH_2Cl_2 solution of compound **5.2** (0.20 g, 0.46 mmol) PI_3 (0.17 g, 0.46 mmol) was added and the reaction stirred for 12 h at rt. The reaction mixture was concentrated yielding the desired product as a red solid.

Yield: 95 % (0.23 g, 0.39 mmol);

m.p.: 78 - 81 °C;

^1H NMR (CDCl_3 , δ (ppm)): 7.51(m, 4H, aryl), 7.40(m, 6H, aryl), 6.32(s, 1H, thienyl), 6.22(s, 1H, thienyl), 2.25(s, 3H, CH_3), 2.19(s, 3H, CH_3), 1.96(s, 3H, CH_3), 1.92(s, 3H, CH_3);

^{13}C NMR (CDCl_3 , δ (ppm)): 139.9, 138.3, 137.3, 137.2, 134.9, 134.8, 134.7, 130.2, 130.0, 129.8, 126.7, 126.5, 126.1, 123.2, 122.9, 15.1, 15.0, 14.7, 14.7;

$^{31}\text{P}\{^1\text{H}\}$ NMR (CDCl_3 , δ (ppm)): 193.7, 193.9;

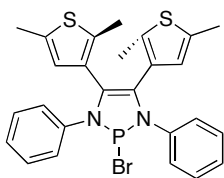
FT-IR (ranked intensity (cm^{-1})): 628(15), 689(1), 732(9), 754(2), 829(4), 865(14), 908(13), 1029(8), 1140(7), 1265(5), 1437(10), 1484(3), 1543(12), 1590(6), 2914(11);

FT-Raman (cm^{-1} (ranked intensity)): 421(1), 763(3), 1509(2), 2061(4), 2076(5), 2185(6), 2362(7);

HRMS: ($\text{C}_{26}\text{H}_{24}\text{N}_2\text{S}_2\text{P}_1^+$) Calcd (found) 459.1113 (459.1131);

Elemental Analysis (%) calc for $\text{C}_{26}\text{H}_{24}\text{I}_3\text{N}_2\text{PS}_2$: C 37.16, H 2.88, N 3.33, S 7.63; found 37.04, H 2.90, N 3.21, S 7.70

Compound 5.6.



Phosphorus tribromide (0.22 mL, 2.33 mmol) was added to a 10 mL CH₂Cl₂ solution of compound **5.2** (1.00 g, 2.33 mmol) and cyclohexene (1.41 mL, 13.9 mmol) and stirred for 12 h at rt. The orange solution was concentrated yielding a yellow solid, which was washed with *n*-pentane (3 x 5 mL) yielding the desired product as a light yellow powder.

Yield: 92 % (1.13 g, 2.1 mmol);

m.p.: 180 - 183 °C;

¹H NMR (CDCl₃, δ (ppm)): 7.28 (m, 10H, aryl), 6.11 (s, 2H, thienyl), 2.18 (s, 3H, CH₃), 2.16 (s, 3H, CH₃), 1.95 (s, 6H, CH₃);

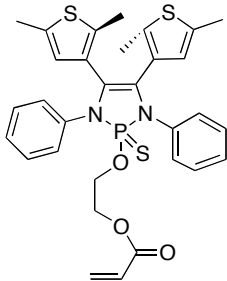
¹³C NMR (-20 °C) (CDCl₃, δ (ppm)): 138.3, 137.4, 136.8, 136.0, 135.8, 129.4, 129.0, 127.6, 127.4, 126.4, 126.3, 126.0, 125.6, 125.0, 124.9, 15.3, 15.1, 14.1, 14.0;

³¹P{¹H} NMR (CDCl₃, δ (ppm)): 163.0, 162.0;

FT-IR (ranked intensity (cm⁻¹)): 536(8), 623(3), 665(11), 865(12), 900(5), 922(4), 972(10), 1073(7), 1154(15), 1221(14), 1353(6), 1453(13), 2858(2), 2916(9), 3048(1);

Elemental Analysis (%) calc for C₂₆H₂₄BrN₂PS₂: C 57.88, H 4.48, N 5.19, S 11.89; found C 57.50, H 4.64, N 5.13, S 11.76.

Compound 5.7.



Hydroxyethylacrylate (0.21 mL, 1.85 mmol) and NEt₃ (0.39 mL, 2.77 mmol) was added to a 10 mL THF solution of compound **5.6** (1.00 g, 1.85 mmol) and a white solid precipitated from the reaction mixture immediately. The reaction was stirred for 3 h at rt. Upon completion the NEt₃HBr salt was centrifuged off and the solution was concentrated yielding a white solid. The product was then taken up in 10 mL of CH₂Cl₂ and charged with S₈ (0.06 g, 0.23 mmol). The reaction stirred for 12 h at rt. in the dark and upon completion the resulting yellow solution was concentrated yielding an off white solid.

Yield: 65 % (1.20 g, 1.91 mmol);

m.p.: 68 - 70 °C;

^1H NMR (CDCl₃, δ (ppm)): 7.11 (m, 10H, aryl), 6.34 (dd, 1H, $^3J_{\text{HH}} = 17.3$, $^2J_{\text{HH}} = 1.4$), 6.02 (m, 3H), 5.77 (dd, 1H, $^3J_{\text{HH}} = 10.4$, $^2J_{\text{HH}} = 1.4$), 4.10 (m, 4H, CH₂), 2.11 (s, 6H, CH₃), 1.80 (s, 6H, CH₃);

^{13}C NMR (CDCl₃, δ (ppm)): 165.8, 137.2, 135.6, 135.1, 131.3, 128.5, 127.9, 127.2, 126.5, 126.0, 121.0, 66.5 ($^3J_{\text{PC}} = 7.7$), 63.3 ($^2J_{\text{PC}} = 8.0$), 15.1, 13.9;

$^{31}\text{P}\{^1\text{H}\}$ (CDCl₃, δ (ppm)): 68.0;

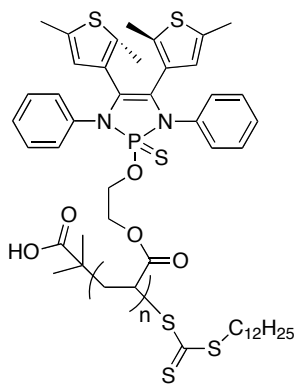
FT-IR (ranked intensity (cm⁻¹)): 494(9), 583(11), 694(3), 775(5), 862(10), 1026(7), 1185(13), 1274(2), 1342(15), 1407(12), 1489(4), 1595(6), 1636(14), 1727(1), 2915(8);

FT-Raman (ranked intensity (cm⁻¹)): 197(11), 696(6), 998(4), 1121(7), 1195(8), 1216(5), 1479(3), 1549(2), 1591(1), 2913(9), 3055(10);

HRMS: (C₃₁H₃₁N₂NaO₃PS₃) Calcd (found) 629.1132 (629.1154);

Elemental Analysis (%) calc for C₃₁H₃₁N₂O₃PS₃: C 61.36, H 5.15, N 4.62, S 15.85; found C 59.19, H 5.15, N 4.38, S 15.95.

Compound 5.8.



A 2 mL benzene solution of compound **5.7** (0.46 g, 0.73 mmol), RAFT reagent, **5.9** (16.00 mg, 0.04 mmol) and AIBN (2.51 mg, 0.01 mmol) was deoxygenated by bubbling N₂ for 20 min. The reaction mixture was heated to 80 °C for 8 h. Upon completion the polymer was precipitated by the dropwise addition of the reaction mixture to a 50 mL solution of hexanes and was repeated three times until all the monomer was washed away.

Yield: 48 % (0.22 g, 0.35 mmol);

T_g: 79.7°C;

^1H NMR (CDCl₃, δ (ppm)): 7.11 (br. m, 10 H, aryl), 6.04 (br. s, 2H, thienyl), 4.06 (br. s, 2H, alkyl), 3.88 (br. s, 2H, alkyl), 1.82 (br. s, 6H, CH₃);

$^{13}\text{C}\{^1\text{H}\}$ NMR (CDCl₃, δ (ppm)): 137.1, 135.6, 135.2, 128.6, 127.2, 126.6, 126.1, 121.0, 45.9, 31.9, 29.6, 22.7, 15.1, 14.0, 8.6;

$^{31}\text{P}\{^1\text{H}\}$ (CDCl₃, δ (ppm)): 68.1;

FT-IR (ranked intensity (cm⁻¹)): 669(14), 695(5), 776(7), 864(10), 969(11), 1028(3), 1148(8), 1223(15), 1277(1), 1346(16), 1451(12), 1491(4), 1596(6), 1737(2), 2981(9).

5.4 References

- (1) Feringa, B. L., Ed. *Molecular Switches*; Wiley-VCH: Weinheim, Germany, 1990.
- (2) Irie, M. *Chem. Rev.* **2000**, *100*, 1685-1716.
- (3) Examples of DTE containing transition metals: a) Roberts, M. N.; Carling, C.-J.; Nagle, J. K.; Branda, N. R.; Wolf, M. O. *J. Am. Chem. Soc.* **2009**, *131*, 16644-16645; b) Hasegawa, Y.; Nakagawa, T.; Kawai, T. *Coord. Chem. Rev.*, *254*, 2643-2651; c) Zhong, Y.-W.; Vila, N.; Henderson, J. C.; Abruna, H. D. *Inorg. Chem.* **2009**, *48*, 991-999; d) Wong, H.-L.; Tao, C.-H.; Zhu, N.; Yam, V. W.-W. *Inorg. Chem.* **2011**, *50*, 471-481; e) Roberts, M. N.; Nagle, J. K.; Majewski, M. B.; Finden, J. G.; Branda, N. R.; Wolf, M. O. *Inorg. Chem.* **2009**, *50*, 4956-4966; f) Fraysse, S.; Coudret, C.; Launay, J.-P. *Eur. J. Inorg. Chem.* **2000**, 1581-1590; g) Yam, V. W.-W.; Lee, J. K.-W.; Ko, C.-C.; Zhu, N. *J. Am. Chem. Soc.* **2009**, *131*, 912-913; h) Chan, J. C.-H.; Lam, W. H.; Wong, H.-L.; Zhu, N.; Wong, W.-T.; Yam, V. W.-W. *J. Am. Chem. Soc.* **2011**, *133*, 12690-12705; i) Lee, P. H.-M.; Ko, C.-C.; Zhu, N.; Yam, V. W.-W. *J. Am. Chem. Soc.* **2007**, *129*, 6058-6059.
- (4) Gudat, D. *Accounts of Chemical Research* **2010**, *43*, 1307-1316.
- (5) Asay, M.; Jones, C.; Driess, M. *Chemical Reviews* **2011**, *111*, 354-396.
- (6) Van, K. G.; Vrieze, K. *Adv. Organomet. Chem.* **1982**, *21*, 151-239.
- (7) Poon, C.-T.; Lam, W. H.; Wong, H.-L.; Yam, V. W.-W. *J. Am. Chem. Soc.* **2010**, *132*, 13992-13993.
- (8) Poon, C.-T.; Lam, W. H.; Yam, V. W.-W. *J. Am. Chem. Soc.* **2011**, *133*, 19622-19625.
- (9) Wong, H.-L.; Wong, W.-T.; Yam, V. W.-W. *Org. Lett.* **2012**, *14*, 1862-1865.
- (10) Yam, V. W.-W.; Lee, J. K.-W.; Ko, C.-C.; Zhu, N. *J. Am. Chem. Soc.* **2009**, *131*, 912-913.
- (11) Lemieux, V.; Spantulescu, M. D.; Baldrige, K. K.; Branda, N. R. *Angew. Chem. Int. Ed.* **2008**, *47*, 5034-5037.
- (12) Sud, D.; McDonald, R.; Branda, N. R. *Inorg. Chem.* **2005**, *44*, 5960-5962.

- (13) Neilson, B. M.; Lynch, V. M.; Bielawski, C. W. *Angew. Chem. Int. Ed.* **2011**, *50*, 10322 - 10326.
- (14) Neilson, B. M.; Bielawski, C. W. *J. Am. Chem. Soc.* **2012**, *134*, 12693-12699.
- (15) A similar procedure was used for the synthesis of compounds **3** and **4**. Segawa, Y.; Suzuki, Y.; Yamashita, M.; Nozaki, K. *J. Am. Chem. Soc.* **2008**, *130*, 16069-16079.
- (16) Reeske, G.; Hoberg, C. R.; Hill, N. J.; Cowley, A. H. *J. Am. Chem. Soc.* **2006**, *128*, 2800-2801.
- (17) Dube, J. W.; Farrar, G. J.; Norton, E. L.; Szekely, K. L. S.; Cooper, B. F. T.; Macdonald, C. L. B. *Organometallics* **2009**, *28*, 4377-4384.
- (18) Taniguchi, H.; Shinpo, A.; Okazaki, T.; Matsui, F.; Irie, M. *Nippon Kagaku Kaishi* **1992**, *1992*, 1138-1140.
- (19) Irie, M.; Lifka, T.; Uchida, K.; Kobatake, S.; Shindo, Y. *Chem. Commun.* **1999**, 747-750.

Chapter 6

6 Conclusions and future work

6.1 Conclusions

This thesis discusses (i) the synthesis of three new *N,N'*-chelating ligands containing thiophene, (ii) their coordination to main group elements and (iii) their resulting photophysical properties. The results outlined in the previous chapters highlight the need for new ligands that combine both the photophysical properties of thiophene with the reactivity of p-block atoms as an alternative way of tuning the photophysical properties in π conjugated molecules. This work represents an ongoing theme in the field of main group chemistry; the incorporation of reactive main group elements with organic conjugated architectures for specific functional applications.

Ligands containing a *N,N'*-chelating frameworks have been used extensively for the coordination of elements spanning the periodic table. I saw this as an opportunity to combine the desirable polymerizable and photophysical properties of thiophene with the chemical versatility and inherent electronic properties of main group atoms. The first ligand synthesized *N,N'*-(thiophene-3,4-diyl(bimethylene)) suffered from poor selectivity because of flexible diamine arms. The substitution on nitrogen (R = Mes or Dipp) dictated the resulting stoichiometric outcome of amine:chlorophosphine in the product. When R = Mes, only the acyclic bis(aminodichlorophosphine), **2.6**, was isolated, however when R = Dipp a mixture of the desired cyclic diaminochlorophosphine (**2.8**) and the undesired acyclic bis(aminodichlorophosphine) (**2.7**) were isolated in a 4:1 ratio respectively. Separation of the two substitution products was not possible because of similar solubilities. Slowing the addition of PCl_3 and changing the solvent polarity from THF to toluene allowed for the exclusive synthesis of the cyclic aminochlorophosphine. The synthesis of the subsequent phosphonium cation, (**2.9**) was successful using SiMe_3OTf as a halide-abstracting agent. This ligand system did not contain any extended conjugation and no significant change in the UV-visible absorption spectra was observed upon the addition of phosphorus.

A second ligand consisting of a benzo[1,2-b:5,6-b']dithiophene backbone with a rigid *N,N'*-chelating pocket was used to support pnictenium cations (Pn = P, As and Sb). The NHPn (Pn = P or As) were stable as the free pnictenium cations, however the stibonium cation required base stabilization. The NHPn (Pn = P and As) were also able to act as cationic ligands to Pt. The geometry at the phosphonium was trigonal planar, and is consistent with both σ donation from the phosphorus atom and π -backdonation from the metal center. The geometry at the arsenium, however, is pyramidal and is consistent with a stereochemically active lone pair and consists primarily of metal to pnictenium π -backdonation. All of the chloropnictines and pnictenium cations had similar UV-visible absorption spectra with the photophysical properties dominated by the benzo[1,2-b:5,6-b']dithiophene. The metal complexes were the exception; the Pt-NHP was a deep red ($\lambda_{\text{max}} = 466 \text{ nm}$) whereas the arsenic analogue was dark purple ($\lambda_{\text{max}} = 576 \text{ nm}$).

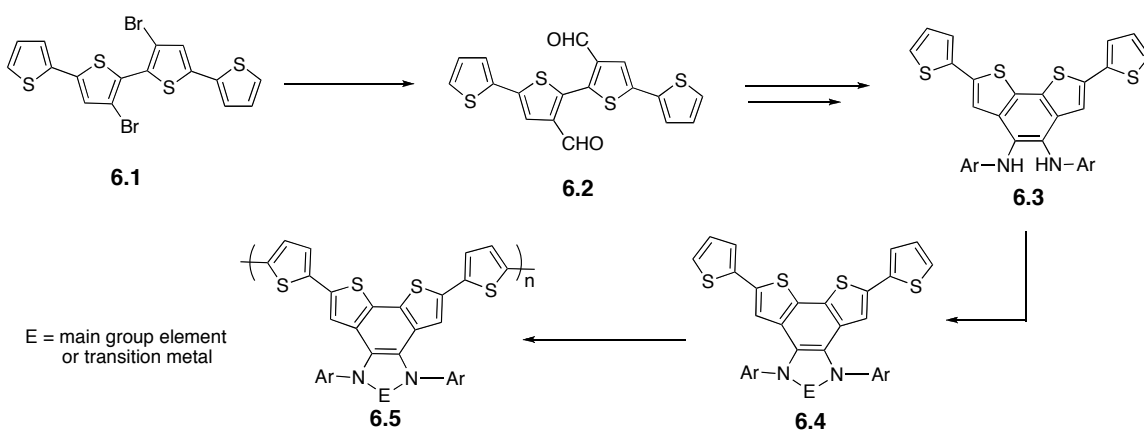
The benzo[1,2-b:5,6-b']dithiophene core was also used to stabilize a NHC which is isovalent but the electronic inverse to the analogous NHPns. The imidazolium salt was synthesized in high yields, however the free carbene could not be isolated and only the dimer was observed. The synthesis of a (NHC)AgCl salt and the successful transfer of the NHC onto rhodium forming the (NHC)Rh(CO)₂Cl complex from the (NHC)Rh(COD)Cl precursor was achieved. The donor strength of our NHC was measured and was found to be a stronger base than the 5-membered NHCs but weaker than the 6-membered and acyclic NHCs. Attempts to oxidatively polymerize our NHC was unsuccessful and only decomposition was observed.

A diazabutadiene with adjacent 2,5-dimethyl(thienyl) rings was synthesized and its coordination chemistry and photochromic reactivity was investigated. The phosphonium cation and bromophosphine were synthesized from a redox reaction between the α -diimine (**5.2**) with PI₃ or PBr₃ and cyclohexene respectively. The boron analogue (**5.4**) was synthesized from the lithium reduction of the α -diimine (**5.2**) and subsequent reaction with BCl₂Ph or BBr₃. The DTE containing halogens did not display any photochromic activity. Fortunately the *N,N'*-DTE phenylborane complex and the phosphorane, functionalized with a polymerizable acrylate group did exhibit reversible ring-closing/-opening reactivity. The acrylate functionalized phosphorane was also able

to undergo RAFT polymerization yielding a DTE side functionalized polymer which retained reversible photochromic activity with high cyclability. The resulting photophysical properties of the ring-closed isomer was dependant on the heteroatom present in the *N, N'*-chelating pocket and there was a 50 nm bathochromic shift between the ring-closed phosphorus derivative ($\lambda_{\text{max}} = 448 \text{ nm}$) and boron ($\lambda_{\text{max}} = 500 \text{ nm}$), along with the boron DTE displaying varying fluorescence in the ring open ($\lambda_{\text{max}} = 378 \text{ nm}$) versus ring closed ($\lambda_{\text{max}} = 578 \text{ nm}$) states.

6.2 Future work

Future work in this area includes extending the number of thiophene rings in the benzo[1,2-b:5,6-b']dithiophene core from two to four. This would lower the HOMO/LUMO band gap, increase flexibility and facilitate the oxidative electropolymerization of both the free ligand and the resulting main group or transition metal complexes. Increasing the number of thiophene rings can be accomplished by the synthesis of 3,3'-dibromo-2,2':5',2'':5'',2''':5'''-quaterthiophene (**6.1**), transformation to the aldehyde (**6.2**) and then onward synthesis to the diamine (**6.3**, Scheme 6.1). From there both main group elements and transition metals (**6.4**) can be inserted and their ability to undergo electropolymerization examined (**6.5**).



Scheme 6.1: Synthesis of thiophene polymers containing either main group or transition metal elements.

Future endeavors with the α -diimine, compound **5.2** include the addition of lanthanide metals. Lanthanide metals in the +2 oxidation state can readily undergo a one-electron oxidation, which is ideal for our redox active α -diimine. Lanthanide (III) complexes also have characteristic narrow emission bands and long emission lifetimes making these complexes ideal for photoswitchable probes for bioimaging (**6.4**). A second project would include the reduction of the diimine and subsequent addition of iodomethane yielding the air stable diamine (**6.5**) with the required ethene in the backbone. This would allow for the introduction of a wide range of both transition metals and main group elements into the DTE framework through simple donor-acceptor chemistry (Figure 6.2).

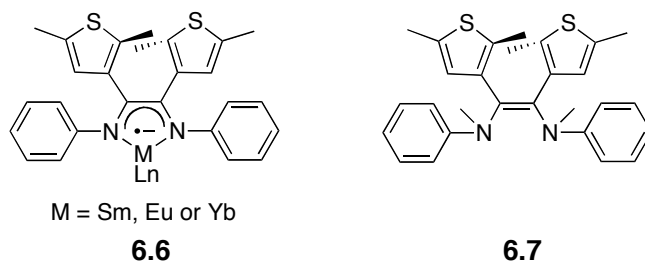
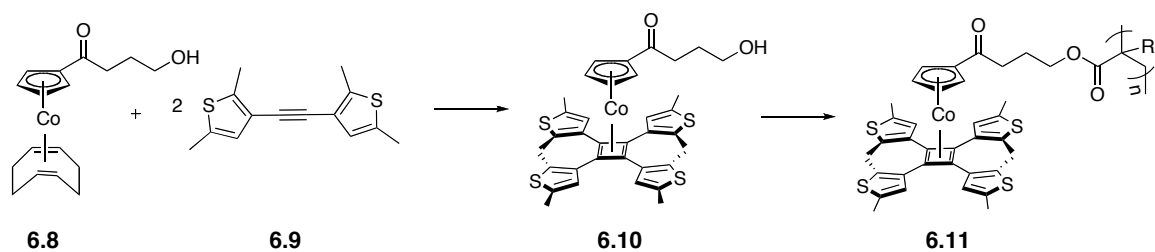
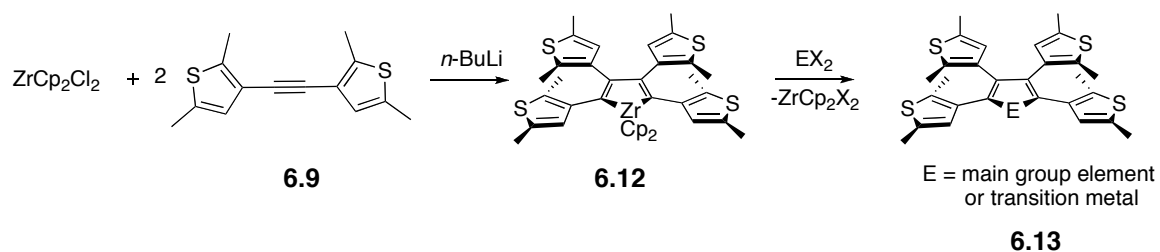


Figure 6.1: DTE lanthanide complexes (**6.6**) and a DTE diamine (**6.7**).

In addition, recent work in the Ragogna lab has focused on Co(I) side chain functionalized polymers containing pendant CoCp(C₄R₄) units.¹ The incorporation of DTEs into the cyclobutadiene ring on the Co(I) monomer would generate a photochromic Co(I) species that could be easily incorporated into a polymers and retain the optical switching properties of DTE systems. This could be accomplished through the dimerization of bis(2,5-dimethyl-3-thienyl)acetylene (**6.9**) with compound **6.8** to generate the cyclobutadiene ring followed by further functionalization with a polymerizable group (**6.11**, Scheme 6.2). The dimerization of the bis(2,5-dimethyl-3-thienyl)acetylene (**6.9**) could further find utility, as this acetylene can also dimerize in the presence of *n*-BuLi and ZrCp₂Cl₂ forming compound **6.12**. One could easily switch out the ZrCp₂ for a variety of main group or transition metal elements through simple salt metathesis chemistry and alter the photochromic properties the resulting compound (**6.13**, Scheme 6.3).



Scheme 6.2: Synthesis of CpCoCb side chain functionalized polymers with photochromic DTEs (6.11).



Scheme 6.3: Dimerization of compound 6.9 using $ZrCp_2Cl_2$ and the exchange of $ZrCp_2$ with either main group elements or transition metals.

6.3 References

- (1) Chadha, P.; Ragogna, P. J. *Chem. Commun.* **2011**, 47, 5301-53

Appendices

Appendix 1: General considerations

A.1 General experimental considerations

The synthesis of compounds **2.6 - 2.9**, **3.4 - 3.12**, **4.3 - 4.5** and **5.3 - 5.8** were performed in an inert atmosphere in a nitrogen filled MBraun Labmaster dp glovebox or using standard Schlenk techniques. Reagents were obtained from commercial sources. Triethylamine and n-methylmorpholine was distilled from CaH₂, phosphorus(III) chloride and arsenic(III) chloride were distilled prior to use, while all other reagents were used without further purification. All solvents were dried using an MBraun controlled atmospheres solvent purification system and stored in Straus flasks under an N₂ atmosphere or over 4 Å molecular sieves in the glovebox (3 Å for acetonitrile). Chloroform-d was dried over CaH₂, distilled prior to use, and stored in the glovebox over 4 Å molecular sieves. Synthesis of 2,2'-bithiophene,¹ 3,3',5,5'-tetrabromo-2,2'-bithiophene,¹ 3,3'-dibromo-2,2'-bithiophene¹ and 2,2'-bithiophene-3,3'-biscarboxaldehyde,² 3-Acetyl-2,5-dimethylthiophene,³ 2-(2,5-Dimethyl-3-thienyl)-2-oxoacetaldehyde,³ 1,2-Bis(2,5-dimethyl-3-thienyl)-2-hydroxy-1-ethanone³ and 1,2-Bis(2,5-dimethyl-3-thienyl)ethandione³ were synthesized following literature procedures.

All ¹H, ¹¹B{¹H}, ¹³C{¹H}, ¹⁹F{¹H} and ³¹P{¹H} data were collected on a 400 MHz Varian Inova spectrometer (399.762 MHz for ¹H, 128.27 MHz for ¹¹B, 100.52 MHz for ¹³C, 376.15 for ¹⁹F and 161.825 MHz for ³¹P). Spectra were recorded at room temperature, unless otherwise indicated, in CDCl₃ using the residual protons of the deuterated solvent for reference and are listed in ppm, coupling constants (*J*) are listed in Hz. Phosphorus, boron and fluorine NMR spectra were recorded unlocked relative to an external standard (85% H₃PO₄, δ_P = 0.0; BF₃•OEt₂, δ_B = 0.00; CF₃C₆H₅, δ_F = -63.9).

FT-IR spectra were collected on samples as KBr pellets using a Bruker Tensor 27 spectrometer, with a resolution of 4 cm⁻¹. Samples for FT-Raman spectroscopy were

packed in capillary tubes and flame-sealed. Data was collected using a Bruker RFS 100/S spectrometer, with a resolution of 4 cm^{-1} .

UV-visible absorption spectra were recorded over a range of 200 - 700 nm using a Varian Cary 150 spectrometer and a hand held UV-vis lamp at 254 nm was used as the light source for the ring-closing reaction and a 100 W mercury lamp was used as the visible light source for the ring-opening reactions placed above a quartz cuvette. Emission spectra were recorded on a Fluorolog (QM-7/2005) instrument with a slit width of 0.6 nm in pentane. SpinWorks 3.1 software was used to determine the rate constant for the activation energy between parallel and anti-parallel conformations and Fulgide Abercrome 540⁴ was used as the standard to determine the quantum efficiencies in Chapter 5.

Melting (m.p.) and decomposition (d.p.) points were recorded in flame sealed capillary tubes using a Gallenkamp Variable Heater. High resolution mass spectrometry (HRMS) was collected using a Finnigan MAT 8200 instrument. Elemental analyses (C, H, N, S) were performed by Laboratoire d'Analyse Élémentaire de l'Université de Montréal, Montréal, QC, Canada.

A1.2 General crystallography considerations

Single crystal X-ray diffraction data were collected on a Nonius Kappa-CCD area detector or a Bruker Apex II-CCD detector using Mo-K α radiation ($\lambda = 0.71073\text{ \AA}$) and at a temperature of 150(2) K. Suitable single crystals were selected under Paratone-N oil, mounted on MiTeGen micromounts or nylon loops then immediately placed in a cold stream of N₂ on the diffractometer. Structures were solved by direct methods and refined using full matrix least squares on F^2 using the SHELXTL suite of software.⁵ Hydrogen atoms positions were calculated.

A1.3 References

- (1) Letizia, J. A.; Salata, M. R.; Tribout, C. M.; Facchetti, A.; Ratner, M. A.; Marks, J. *Am. Chem. Soc.* **2008**, 130, (30), 9679-9694.
- (2) Boersma, A. D.; Goff, H. M., *Inorg. Chem.* **1982**, 21, 581-586.

- (3) Darcy, P. J.; Heller, H. G.; Strydom, P. J.; Wittal, J. J. *Chem. Soc. Perkin I*, **1981**, 202-205.
- (4) Ivanov, S. N.; Lichitskii, B. V.; Dudinov, A. A.; Martynkin, A. Y.; Krayushkin, M. M. *Chem. Heterocycl. Compd.* **2001**, 37, 85-90.
- (5) Sheldrick, G. M. *Acta Cryst. A* **2008**, 64, 112.

Appendix 2: Copyright permission

A2.1: American Chemical Society's policy on theses and dissertation

This is regarding request for permission to include **your** paper(s) or portions of text from **your** paper(s) in your thesis. Permission is now automatically granted; please pay special attention to the **implications** paragraph below. The Copyright Subcommittee of the Joint Board/Council Committees on Publications approved the following:

Copyright permission for published and submitted material from theses and dissertations

ACS extends blanket permission to students to include in their theses and dissertations their own articles, or portions thereof, that have been published in ACS journals or submitted to ACS journals for publication, provided that the ACS copyright credit line is noted on the appropriate page(s).

Publishing **implications** of electronic publication of theses and dissertation material

Students and their mentors should be aware that posting of theses and dissertation material on the Web prior to submission of material from that thesis or dissertation to an ACS journal may affect publication in that journal. Whether Web posting is considered prior publication may be evaluated on a case-by-case basis by the journal's editor. If an ACS journal editor considers Web posting to be "prior publication", the paper will not be accepted for publication in that journal. If you intend to submit your unpublished paper to ACS for publication, check with the appropriate editor prior to posting your manuscript electronically.

Reuse/Republication of the Entire Work in Theses or Collections: Authors may reuse all or part of the Submitted, Accepted or Published Work in a thesis or dissertation that the author writes and is required to submit to satisfy the criteria of degree-granting institutions. Such reuse is permitted subject to the ACS' "Ethical Guidelines to Publication of Chemical Research" (<http://pubs.acs.org/page/policy/ethics/index.html>); the author should secure written confirmation (via letter or email) from the respective ACS journal editor(s) to avoid potential conflicts with journal prior publication*/embargo policies. Appropriate citation of the Published Work must be made. If the thesis or dissertation to be published is in electronic format, a direct link to the Published Work must also be included using the ACS Articles on Request author-directed link – see <http://pubs.acs.org/page/policy/articlesonrequest/index.html>

* Prior publication policies of ACS journals are posted on the ACS website at <http://pubs.acs.org/page/policy/prior/index.html>

If your paper has **not** yet been published by ACS, please print the following credit line on the first page of your article: "Reproduced (or 'Reproduced in part') with permission from [JOURNAL NAME], in press (or 'submitted for publication'). Unpublished work copyright [CURRENT YEAR] American Chemical Society." Include appropriate information.

If your paper has already been published by ACS and you want to include the text or portions of the text in your thesis/dissertation, please print the ACS copyright credit line on the first page of your article: "Reproduced (or 'Reproduced in part') with permission from [FULL REFERENCE CITATION.] Copyright [YEAR] American Chemical Society." Include appropriate information.

Submission to a Dissertation Distributor: If you plan to submit your thesis to UMI or to another dissertation distributor, you should not include the unpublished ACS paper in your thesis if the thesis will be disseminated electronically, until ACS has published your paper. After publication of the paper by ACS, you may release the entire thesis (**not the**

individual ACS article by itself) for electronic dissemination through the distributor; ACS's copyright credit line should be printed on the first page of the ACS paper.

A.2.3: National Research Council of Canada Rights Retained by Journal Authors

As of 2009, copyright in all articles in NRC Research Press journals remains with the authors. All articles published previously are copyright Canadian Science Publishing (which operates as NRC Research Press) or its licensors (also see our Copyright information). Under the terms of the license granted to NRC Research Press, authors retain the following rights:

1. To post a copy of their submitted manuscript (pre-print) on their own Web site, an institutional repository, or their funding body's designated archive.
2. To post a copy of their accepted manuscript (post-print) on their own Web site, an institutional repository, or their funding body's designated archive. Authors who archive or self-archive accepted articles must provide a hyperlink from the manuscript to the Journal's Web site.
3. They and any academic institution where they work at the time may reproduce their manuscript for the purpose of course teaching.
4. To reuse all or part of their manuscript in other works created by them for noncommercial purposes, provided the original publication in an NRC Research Press journal is acknowledged through a note or citation. These authors' rights ensure that NRC Research Press journals are compliant with open access policies of top international granting bodies, including the Canadian Institutes of Health Research, US National Institutes of Health, the Wellcome Trust, the UK Medical Research Council, the Institut national de la santé et de la recherche médicale in France, and others. The above rights do not extend to copying or reproduction of the full article for commercial purposes. Authorization to do so may be obtained by clicking on the "Reprints and Permissions" link in the Article Tools Box of the article in question or under license by Access©. The Article Tool Box is accessible through the full-text article or abstract page. In support of authors who wish or need to sponsor open access to their published research articles, NRC Research Press also offers an OpenArticle option.

This information can be found at:

<http://www.nrcresearchpress.com/page/authors/information/rights>

Appendix 3: Supplementary information

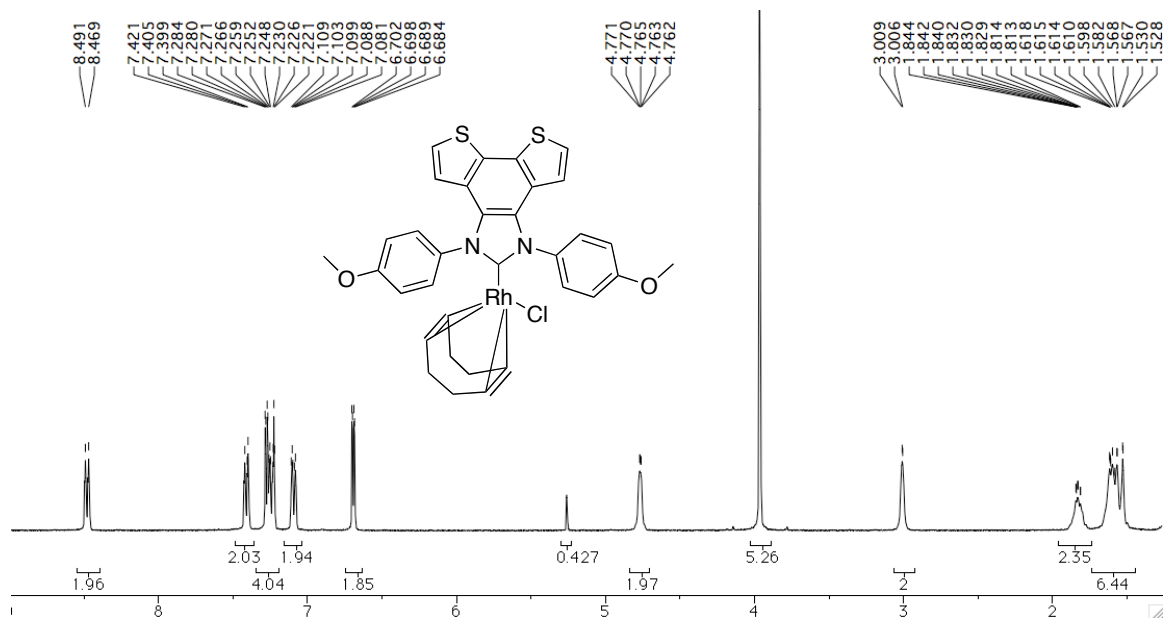


Figure A. 1: ^1H NMR spectrum of Compound 4.7.

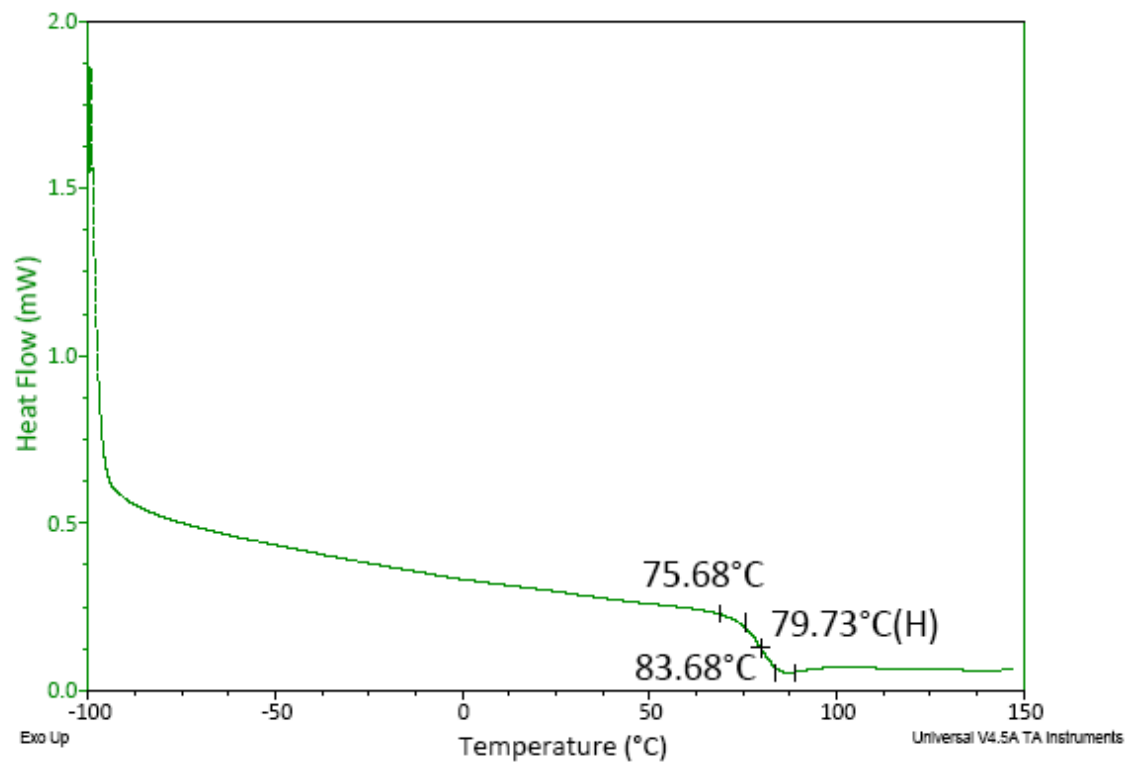


Figure A. 2: TGA of polymer 5.8.

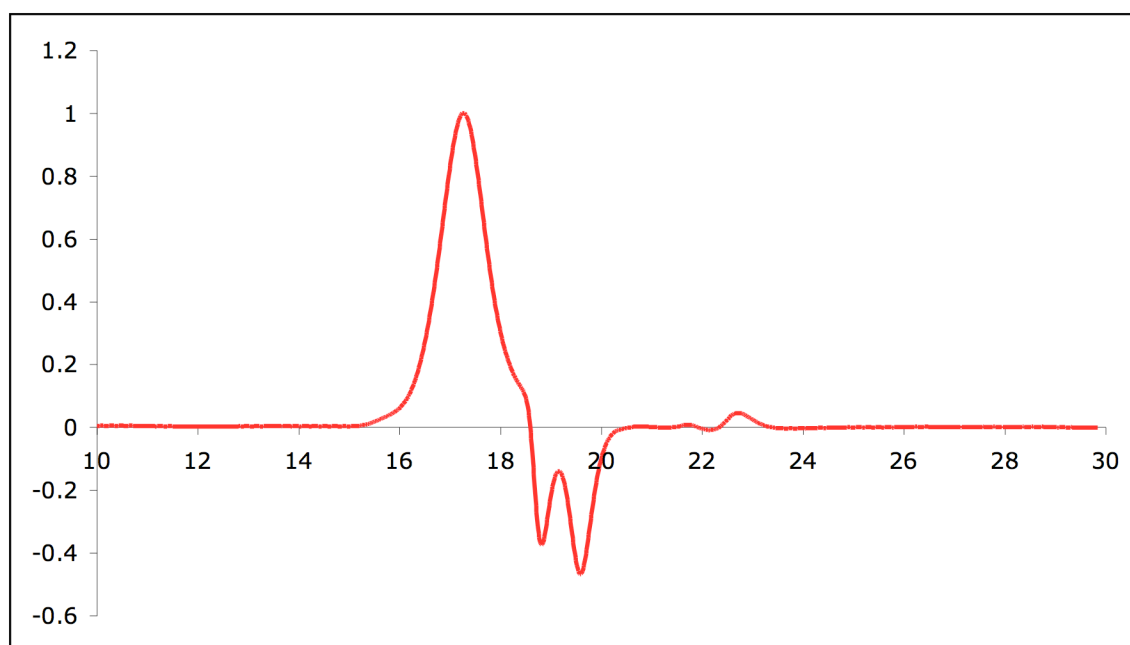


Figure A. 3: GPC trace of polymer 5.8.

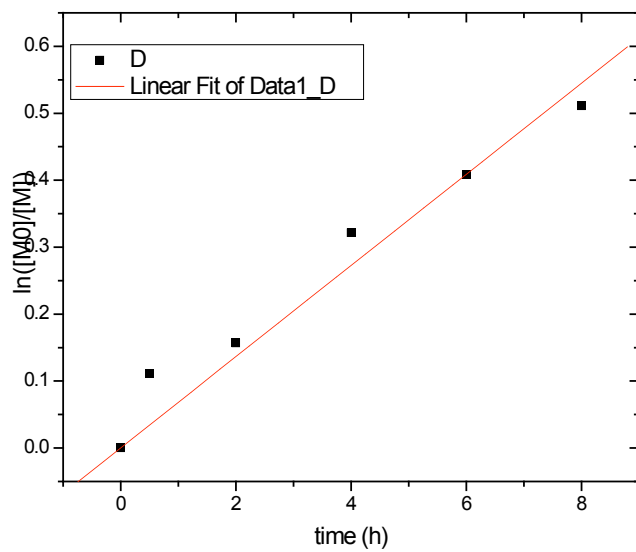


Figure A. 4: A linear plot of the amount of polymer/monomer vs. time for compound 5.8.

Curriculum Vitae

- Name:** Jacquelyn T. Price
- Post-secondary Education and Degrees:** University of Western Ontario
London, Ontario, Canada
2002-2006, BSc.
- The University of Western Ontario
London, Ontario, Canada
2006-2008, MSc.
- The University of Western Ontario
London, Ontario, Canada
2009-2013, Ph.D.
- Honours and Awards:** Ontario Graduate Scholarships in Science and Technology
2007-2008
- Natural Sciences and Engineering Research Council Postgraduate
Scholarship
2010-2013
- Western Graduate Research Scholarship
2010-2013
- Related Work Experience** Teaching Assistant
The University of Western Ontario
2006-2012
- Publications:**
11. "A versatile dithienylethene functionalized Ph-DAB ligand: From photoswitchable main group molecules to photochromic polymers" Jacquelyn T. Price and Paul J. Ragona. *Chem. Eur. J.*, **2013**, DOI: 10.1002/chem.201301086.
 10. "Phosphenium cation in a seven membered ring supported by thiophene" Jacquelyn T. Price, Nathan D. Jones and Paul J. Ragona, *Can. J. Chem.*, **2013**, DOI: 10.1139/cjc-2013-0015

9. "Synthesis, Structure, Electrochemistry, and Electrochemiluminescence of Thienyltriazoles" Kalen N. Swanick; Jacquelyn T. Price; Nathan D. Jones; Zhifeng Ding, *J. Org. Chem.*, **2012**, 77(13), pp 5646.
8. "An N-Heterocyclic carbene containing a bithiophene backbone: Synthesis and coordination chemistry" Jacquelyn T. Price, Nathan D. Jones, and Paul J. Ragoana, *Inorg. Chem.*, **2012**; 51(12), pp 6776.
7. "Group 15 Pnictenium Cations Supported by a Conjugated Bithiophene Backbone" Jacquelyn T. Price, Melanie Lui, Nathan D. Jones, and Paul J. Ragoana, *Inorg. Chem.*, **2011**, 50 (24), pp 12810.
6. "Electrogenerated chemiluminescence of triazole-modified deoxycytidine analogues in *N,N*-dimethylformamide" Kalen N. Swanick, David W. Dodd, Jacquelyn T. Price, Allison L. Brazeau, Nathan D. Jones, Robert H. E. Hudson and Zhifeng Ding, *Phys. Chem. Chem. Phys.* **2011**, 13, pp 17405.
5. "Blue fluorescent deoxycytidine analogues: convergent synthesis, solid-state and electronic structure, and solvatochromism" David W. Dodd, Kalen N. Swanick, Jacquelyn T. Price, Allison L. Brazeau, M. J. Ferguson, Nathan D. Jones and Robert H. E. Hudson, *Org. Biomol. Chem.* **2010**, 8, pp 663.
4. "C2- and C3-symmetric Meta-Substituted Thienyl Benzenes: A Comparative Synthetic, Structural and Computational Study" Angelica L. P. Cornacchio, Jacquelyn T. Price, Michael C. Jennings, Robert McDonald., Victor Staroverov, Nathan D. Jones, *J. Org. Chem.* **2009**, 74(2), pp 530.
3. "A Cation-Captured Palladium(0) Anion: Synthesis, Structure, and Bonding of [PdBr(PPh₃)₂]⁻ Ligated by an N-Heterocyclic Phosphenium Cation" Christine A. Caputo, Allison L. Brazeau, Zachery Hynes, Jacquelyn T. Price, Heikki M. Tuononen and Nathan D. Jones, *Organometallics* **2009**, 28, pp 5261.
2. "Modular synthesis of chiral and achiral C,N-chelated Pd(II)-pyridinylidenes" Elizabeth T. J. Strong, Jacquelyn T. Price, Nathan D. Jones, *Dalton Trans.*, **2009**, 42, pp 9123.
1. "N-Heterocyclic phosphenium cations: syntheses and cycloaddition reactions" Christine A. Caputo, Jacquelyn T. Price, Michael C. Jennings, Robert McDonald, Nathan D. Jones, *Dalton Trans.* **2008**, 26, pp 3461.

Conferences

8. "Dithienylethenes containing diazabutadiene functionality and their main group derivatives" Jacquelyn T. Price and Paul Ragoana; International Symposium on Inorganic Ring Systems, Victoria, British Columbia. July 29, **2012**. (oral)

7. "Group 15 cations coordinated by thiophene containing ligands" Jacquelyn T. Price, Melanie Liu, Nathan D. Jones and Paul J. Ragona; 93rd Canadian Chemistry Conference, Montreal, Quebec. June 5th, **2011**. (oral)
6. "Pnictenium cations supported by a novel conjugated bithiophene framework" Jacquelyn T. Price, Melanie Liu, Nathan D. Jones and Paul J. Ragona; Inorganic Discussion Weekend, Windsor Ontario. November 5th, **2010** (oral)
5. "New Thiophene Analogues of Bis(imino)acenaphthene and their N-Heterocyclic Carbene and Phosphenium Cation Complexes" Jacquelyn T. Price, Nathan D. Jones and Paul J. Ragona; 93rd Canadian Chemistry Conference, Toronto, Ontario. May 29, **2010**. (poster)
4. "New Thiophene Substituted N-Heterocyclic Phosphenium Cations" Jacquelyn T. Price, Nathan D. Jones and Paul J. Ragona; 93rd Canadian Chemistry Conference, Toronto, Ontario May 29, **2010**. (poster)
3. "Electrogenerated chemiluminescence of new thiophene containing compounds" Jacquelyn T. Price, Yanhua Chan, Rober Mcdonald, Zhifeng Ding, Nathan D. Jones; 91st Canadian Chemistry Conference, Edmonton, Alberta. May 28th, **2008**. (oral)
2. "Electrogenerated chemiluminescence of new thiophene containing compounds" Jacquelyn T. Price, Yanhua Chan, Rober Mcdonald, Zhifeng Ding, Nathan D. Jones Quebec Ontario Minisymposium in Synthetic and Biological Chemistry, Toronto, Ontario. October 12, **2008**. (poster)
1. "Towards New N-Heterocyclic Carbene Ligands" Jacquelyn T. Price, Nathan D. Jones. The 34th Southern Ontario Undergraduate Student Chemistry Conference, York University, Toronto, Ontario. March 18th, **2006**. (oral)